Estimating the Effects of Pavement Condition on Vehicle Operating Costs

DETAILS

77 pages | 8.5 x 11 | PAPERBACK
ISBN 978-0-309-25821-0 | DOI 10.17226/22808

AUTHORS

Chatti, Karim; and Zaabar, Imen

NATIONAL COOPERATIVE HIGHWAY RESEARCH PROGRAM

NCHRP REPORT 720

Estimating the Effects of Pavement Condition on Vehicle Operating Costs

Karim Chatti
Imen Zaabar
MICHIGAN STATE UNIVERSITY
East Lansing, MI

Subscriber Categories
Energy • Finance • Pavements

Research sponsored by the American Association of State Highway and Transportation Officials
in cooperation with the Federal Highway Administration

TRANSPORTATION RESEARCH BOARD

WASHINGTON, D.C.
2012
www.TRB.org

NATIONAL COOPERATIVE HIGHWAY RESEARCH PROGRAM

Systematic, well-designed research provides the most effective approach to the solution of many problems facing highway administrators and engineers. Often, highway problems are of local interest and can best be studied by highway departments individually or in cooperation with their state universities and others. However, the accelerating growth of highway transportation develops increasingly complex problems of wide interest to highway authorities. These problems are best studied through a coordinated program of cooperative research.

In recognition of these needs, the highway administrators of the American Association of State Highway and Transportation Officials initiated in 1962 an objective national highway research program employing modern scientific techniques. This program is supported on a continuing basis by funds from participating member states of the Association and it receives the full cooperation and support of the Federal Highway Administration, United States Department of Transportation.

The Transportation Research Board of the National Academies was requested by the Association to administer the research program because of the Board's recognized objectivity and understanding of modern research practices. The Board is uniquely suited for this purpose as it maintains an extensive committee structure from which authorities on any highway transportation subject may be drawn; it possesses avenues of communications and cooperation with federal, state and local governmental agencies, universities, and industry; its relationship to the National Research Council is an insurance of objectivity; it maintains a full-time research correlation staff of specialists in highway transportation matters to bring the findings of research directly to those who are in a position to use them.

The program is developed on the basis of research needs identified by chief administrators of the highway and transportation departments and by committees of AASHTO. Each year, specific areas of research needs to be included in the program are proposed to the National Research Council and the Board by the American Association of State Highway and Transportation Officials. Research projects to fulfill these needs are defined by the Board, and qualified research agencies are selected from those that have submitted proposals. Administration and surveillance of research contracts are the responsibilities of the National Research Council and the Transportation Research Board.

The needs for highway research are many, and the National Cooperative Highway Research Program can make significant contributions to the solution of highway transportation problems of mutual concern to many responsible groups. The program, however, is intended to complement rather than to substitute for or duplicate other highway research programs.

NCHRP REPORT 720

Project 1-45
ISSN 0077-5614
ISBN 978-0-309-25821-0
Library of Congress Control Number 2012939367

COPYRIGHT INFORMATION

NOTICE

The project that is the subject of this report was a part of the National Cooperative Highway Research Program, conducted by the Transportation Research Board with the approval of the Governing Board of the National Research Council.

The members of the technical panel selected to monitor this project and to review this report were chosen for their special competencies and with regard for appropriate balance. The report was reviewed by the technical panel and accepted for publication according to procedures established and overseen by the Transportation Research Board and approved by the Governing Board of the National Research Council.

The opinions and conclusions expressed or implied in this report are those of the researchers who performed the research and are not necessarily those of the Transportation Research Board, the National Research Council, or the program sponsors.

The Transportation Research Board of the National Academies, the National Research Council, and the sponsors of the National Cooperative Highway Research Program do not endorse products or manufacturers. Trade or manufacturers' names appear herein solely because they are considered essential to the object of the report.

Published reports of the

NATIONAL COOPERATIVE HIGHWAY RESEARCH PROGRAM

are available from:

Transportation Research Board
Business Office
500 Fifth Street, NW
Washington, DC 20001

and can be ordered through the Internet at:

http://www.national-academies.org/trb/bookstore

Printed in the United States of America

THE NATIONAL ACADEMIES

Advisers to the Nation on Science, Engineering, and Medicine

The **National Academy of Sciences** is a private, nonprofit, self-perpetuating society of distinguished scholars engaged in scientific and engineering research, dedicated to the furtherance of science and technology and to their use for the general welfare. On the authority of the charter granted to it by the Congress in 1863, the Academy has a mandate that requires it to advise the federal government on scientific and technical matters. Dr. Ralph J. Cicerone is president of the National Academy of Sciences.

The **National Academy of Engineering** was established in 1964, under the charter of the National Academy of Sciences, as a parallel organization of outstanding engineers. It is autonomous in its administration and in the selection of its members, sharing with the National Academy of Sciences the responsibility for advising the federal government. The National Academy of Engineering also sponsors engineering programs aimed at meeting national needs, encourages education and research, and recognizes the superior achievements of engineers. Dr. Charles M. Vest is president of the National Academy of Engineering.

The **Institute of Medicine** was established in 1970 by the National Academy of Sciences to secure the services of eminent members of appropriate professions in the examination of policy matters pertaining to the health of the public. The Institute acts under the responsibility given to the National Academy of Sciences by its congressional charter to be an adviser to the federal government and, on its own initiative, to identify issues of medical care, research, and education. Dr. Harvey V. Fineberg is president of the Institute of Medicine.

The **National Research Council** was organized by the National Academy of Sciences in 1916 to associate the broad community of science and technology with the Academy's purposes of furthering knowledge and advising the federal government. Functioning in accordance with general policies determined by the Academy, the Council has become the principal operating agency of both the National Academy of Sciences and the National Academy of Engineering in providing services to the government, the public, and the scientific and engineering communities. The Council is administered jointly by both Academies and the Institute of Medicine. Dr. Ralph J. Cicerone and Dr. Charles M. Vest are chair and vice chair, respectively, of the National Research Council.

The **Transportation Research Board** is one of six major divisions of the National Research Council. The mission of the Transportation Research Board is to provide leadership in transportation innovation and progress through research and information exchange, conducted within a setting that is objective, interdisciplinary, and multimodal. The Board's varied activities annually engage about 7,000 engineers, scientists, and other transportation researchers and practitioners from the public and private sectors and academia, all of whom contribute their expertise in the public interest. The program is supported by state transportation departments, federal agencies including the component administrations of the U.S. Department of Transportation, and other organizations and individuals interested in the development of transportation. **www.TRB.org**

www.national-academies.org

COOPERATIVE RESEARCH PROGRAMS

AUTHOR ACKNOWLEDGMENTS

The research reported herein was performed under NCHRP Project 1-45 by the Department of Civil and Environmental Engineering at Michigan State University (MSU).

Dr. Karim Chatti, Professor of Civil Engineering at MSU, is the principal investigator. The other author of this report is Dr. Imen Zaabar, Research Associate at MSU. Dr Tom Papagiannakis, University of Texas at San Antonio, also helped in editing this final report.

The work was done under the general supervision of Dr. Chatti. The identification, the evaluation, and the calibration/validation of the vehicle operating cost models were done by Dr. Imen Zaabar. Dr. Jorje Prozzi and Mrs. Jolanda Prozzi, University of Texas at Austin, assisted with the repair and maintenance cost data collection effort. The information regarding applicability of the model to the emerging technologies was provided by Dr. Oliver Page, University of Michigan Transportation Research Institute.

The authors also would like to thank the technical support staff from the Texas Department of Transportation (DOT) for providing the repair and maintenance data of their fleet and the technical support from Michigan DOT for providing repair and maintenance data of their fleet and conducting pavement condition testing, coordinated by Mr. Tom Hynes. The authors also acknowledge the help received by several MSU postdoctoral, graduate, and undergraduate students in conducting the field tests.

FOREWORD

By Amir N. Hanna
Staff Officer
Transportation Research Board

This report presents models for estimating the effects of pavement condition on vehicle operating costs. These models address fuel consumption, tire wear, and repair and maintenance costs and are presented as computational software on the accompanying CD-ROM to facilitate use. The material contained in the report should be of immediate interest to state pavement, construction, and maintenance engineers; vehicle fleet managers; and those involved in pavement-investment decision processes and financial aspects of highway transportation.

Vehicle operating costs are part of the costs that highway agencies must consider when evaluating pavement-investment strategies. For conventional vehicles, these costs are related to fuel and oil consumption, tire wear, repair and maintenance, and depreciation; emerging vehicle technologies may involve other cost items. These costs depend on the vehicle class and are influenced by vehicle technology, pavement-surface type, pavement condition, roadway geometrics, environment, speed of operation, and other factors. A large body of research is available on the effects of pavement condition on vehicle operating costs and on models used to estimate these effects. Much of this information and many of the models were developed on the basis of data generated more than 30 years ago in other countries for vehicle fleets that vary substantially from those used currently in the United States and for roadways that differ from those built in the United States. However, some relevant information was collected in the United States in recent years that could help in refining these models or developing models that would better apply to current and future US conditions.

Inadequate models for estimating the effects of pavement condition on vehicle operating costs make it difficult to conduct a rational economic analysis. Research was needed to review available information and to develop models applicable to traffic and environmental conditions encountered in the United States. Such models will provide highway agencies with the tools necessary for considering vehicle operating costs in evaluating pavement-investment strategies and identifying options that yield economic and other benefits.

Under NCHRP Project 1-45, "Models for Estimating the Effects of Pavement Condition on Vehicle Operating Costs," Michigan State University worked with the objective of recommending models for estimating the effects of pavement condition on vehicle operating costs that reflect current vehicle technology in the United States. To accomplish this objective, the researchers identified the factors affecting vehicle operating costs, reviewed available models for estimating these costs, and identified those models that could be refined and made applicable to current US conditions. The research also included a field investigation of fuel consumption and tire wear, and the collection and review of data on the repair and maintenance of state departments of transportation vehicle fleets. Using this information,

the researchers calibrated available fuel consumption and tire wear models and developed improved repair and maintenance models. These models are presented as computational software on the accompanying CD-ROM to facilitate use.

Appendixes A through D contained in the research agency's final report provide further elaboration on the work performed in this project. These appendixes are not published herein, but they are available online at http://www.trb.org/Main/Blurbs/166904.aspx. These appendixes are titled as follows:

- Appendix A: Fuel Consumption Models,
- Appendix B: Tire Wear Models,
- Appendix C: Repair and Maintenance Models, and
- Appendix D: An Overview of Emerging Technologies.

CONTENTS

ix Acronyms

xi Notations

1 **Chapter 1** Introduction
1 Background
1 Description of the Problem
1 Project Objective and Scope
1 Research Approach
2 Report Organization

3 **Chapter 2** Vehicle Operating Cost Models
3 Overview of Existing VOC Models
5 Evaluation of the Existing Models
6 Empirical and Mechanistic VOC Models
7 Selection of Appropriate VOC Models

8 **Chapter 3** Fuel Consumption Model
8 HDM 4 Fuel Consumption Model
8 Field Trials and Data Collection
11 Testing of the Accuracy and Precision of Test Equipment
12 Field Trials
15 Calibration of the HDM 4 Model
15 Calibration of the HDM 4 Engine Speed Model
18 Calibration of HDM 4 Fuel Consumption Model
19 Effect of Roughness and Texture on Fuel Consumption
21 Roughness
23 Texture
23 Summary

27 **Chapter 4** Tire Wear Model
27 HDM 4 Tire Wear Model
27 Data Collection
27 Articulated Truck Tire Wear: NCAT Test Track Data
28 Passenger Cars: Field Trials
30 Calibration of the HDM 4 Tire Wear Model
36 Effect of Roughness on Tire Wear
36 Summary

40 **Chapter 5** Repair and Maintenance Costs Model
40 Repair and Maintenance Models
40 HDM 4 Model
40 TRDF Study
41 Collection and Assessment of Data Applicability

43 Updating Results of TRDF Study
44 Mechanistic–Empirical Approach
44 Artificial Generation of Road Surface Profiles
45 Dynamic Vehicle Simulation
46 Vehicle Fatigue Damage Analysis
46 Suspension Failure Threshold
48 Mechanistic versus Empirical Approach
49 Effect of Roughness on Repair and Maintenance Costs
49 Summary

51 **Chapter 6** Applicability to Emerging Technologies
51 New Engine and Alternative Fuel Technology
52 Vehicle Design
53 Automatic Gear Shift for Heavy Trucks
53 New Tire Technology
53 Summary

55 **Chapter 7** Summary and Suggested Research
55 Summary
55 Fuel Consumption
56 Tire Wear
56 Repair and Maintenance
58 Applicability to Emerging Technologies
59 Suggested Research

60 References

62 **Attachment** User Guide for Vehicle Operating Cost Model

76 **Appendixes**

Note: Many of the photographs, figures, and tables in this report have been converted from color to grayscale for printing. The electronic version of the report (posted on the Web at www.trb.org) retains the color versions.

ACRONYMS

AAA	American Automobile Association
AASHTO	American Association of State Highways and Transportation Officials
ACC	adaptive cruise control
AMT	automated manual transmission
BTS	Bureau of Transportation Statistics
CCS	cruise control systems
CNG	compressed natural gas
COBA	Cost Benefit Analysis Program of the United Kingdom
CRRI	Central Road Research Institute in India
CVT	continuously variable transmissions
DOT	Department of Transportation
ECU	engine control unit
EMD	electric motor drive/assist
EPA	Environmental Protection Agency
ETSAP	Energy Technology System Analysis Program
EV	electric vehicle
FC	fuel consumption
FE	fuel economy
FHWA	Federal Highway Administration
FFV	flex fuel vehicles
GAO	Government Accountability Office
GDI	gasoline direct injection
GPS	global positioning systems
HCCI	homogeneous charge compression ignition
HDM	Highway Development and Management System
HERS	Highway Economic Requirements
HEV	hybrid electric vehicle
HIAP	Highway Investment Analysis Package
HPP	highway performance predictor
HPMS	highway performance monitoring system
HUBAM	Highway User Benefit Assessment Model of Canada
HV	hydrogen vehicle
ICE	internal combustion engine
IFC	instantaneous fuel consumption
IRI	international roughness index
ISG	integrated starter/generator systems
ITS	intelligent transportation systems

LCPC	Laboratoire Central des Ponts et Chaussées
LF	left front
LR	left rear
MDOT	Michigan Department of Transportation
MIT	Massachusetts Institute of Technology
MPD	mean profile depth
MTD	mean texture depth
NHTSA	National Highway Traffic Safety Administration
NITRR	National Institute for Transport and Road Research
NZVOC	New Zealand vehicle operating cost
OBD	on board diagnostic
OEM	original equipment manufacturer
PHEV	plug-in hybrid electric vehicle
PIARC	Permanent International Association of Road Congresses
PMIS	pavement management information system
PTI	Pennsylvania Transportation Institute
R&D	research and development
R&M	repair and maintenance
RBS	regenerative braking systems
RPM	revolution per minute
RR	right rear
SUV	sports utility vehicle
TPMS	tire pressure monitors systems
TRB	Transportation Research Board
TRDF	Texas Research and Development Foundation
TRIB	Tire Retread and Repair Information Bureau
TRRL	Transport and Road Research Laboratory
VCR	variable compression ratio
VETO	Swedish National Road and Transport Research Institute VOC model
VKT	vehicle kilometers traveled
VMT	vehicle miles traveled
VOC	vehicle operating costs
VVL	variable value lift systems
VVT	variable valve timing systems

NOTATIONS

AF	Frontal Area (m^2)
beng	Speed dependent engine drag parameter (dimensionless)
ceng	Speed independent engine drag parameter (dimensionless)
C_{0tc}	Tread wear rate constant (dm^3/1000 km)
C_{tcte}	Tread wear coefficient (dm^3/MNm)
CD	Drag Coefficient (dimensionless)
CDmult	CD multiplier (dimensionless)
Cs	Tire stiffness (kN/rad)
CR1	Rolling resistance tire factor (dimensionless)
CR2	Rolling resistance surface factor (dimensionless)
Ct	Cost per tire ($/tire)
CFT	Circumferential force on the tire (N)
CTCON	Incremental change of tire consumption related to congestion (dimensionless)
CONFAC	Congestion modification factor (dimensionless)
DEF	Benkelman Beam rebound deflection (mm)
dFUEL	Incremental change of fuel consumption related to congestion (dimensionless)
EALC	Accessory load constant (KW)
ECFLC	Cooling fan constant (dimensionless)
ehp	Proportionate decrease in efficiency at high output power (dimensionless)
e	Superelevation (radians)
E_{SLIP}	Slip energy, (lb-mi; 1 lb-mi = 7,159 N.m)
EQNT	Number of equivalent new tires consumed per 1000 km (1/1000 km)
FCLIM	Climatic factor (dimensionless)
FC	Fuel consumption (mL/s)
Fa	Aerodynamic forces (N)
Fg	Gradient forces (N)
Fc	Curvature forces (N)
Fr	Rolling resistance forces (N)
Fi	Inertial forces (N)
GR	Gradient (radians)
g	Gravity (m/s^2)
IFC	Instantaneous fuel consumption (mL/s)
K0	Calibration factor reflecting pavement properties (dimensionless)
KCS	Calibration factor (dimensionless)
Kcr2	Calibration factor (dimensionless)

K_{tr}	Road roughness coefficient (dimensionless)
K_u	Road texture coefficient (dimensionless)
L_t	Life of tire (km)
LFT	Lateral force on the tire (N)
M	Vehicle mass (kg)
MODFAC	Tire life modification factor (dimensionless)
N_t	Number of tires
N_w	Number of wheels (dimensionless)
NFT	Normal force on the tire (N)
P_{tot}	Total power requirement (kW)
P_{eng}	Power required to run the engine and overcome internal engine friction (kW)
P_{max}	Rated power or the maximum power (kW)
P_{out}	Total output power of the engine required to provide tractive force and run the accessories (kW)
P_{tr}	Power required to overcome traction forces (kW)
P_{accs}	Power required for engine accessories (e.g., fan belt, alternator etc.) (kW)
P_{accs_a0}	Ratio of engine and accessories drag to rated engine power when traveling at 100 km/h (dimensionless)
PctPeng	Percentage of the engine and accessories power used by the engine (Default = 80%)
RPM	Engine speed (rotation per minute)
RPM100	Engine speed at 100 km/h (rev/min)
RPMIdle	Idle engine speed (rev/min)
R	Curvature radius (m)
RREC	Ratio of the cost of retreads to new tires (dimensionless)
RTWR	Life of a retreaded tire relative to a new tire
S_{WE}	Slip energy-volume wear coefficient (lb-mi/in^3)
T	Engine torque (N-m)
TRPM	*Load governed maximum engine speed (rotation per minute)*
Tdsp	Texture depth using sand patch method (mm)
TWT	Total change in tread wear (dm^3/1000 km)
TE	Tire energy (MNm/1000 km)
TYREFAC	Tire type modification factor (dimensionless)
V_{WR}	Volume of worn tread rubber (in^3; 1 in = 25.4 mm)
VOL	Tire volume (dm^3)
VEHFAC	Vehicle specific modification factor (dimensionless)
α	Fuel consumption at Idling (mL/s)
αst	Steady state fuel consumption (mL/s)
β	Fuel efficiency factor (mL/kW/s) or (mL/KJ)
βst	Steady state fuel efficiency parameter (mL/KJm/s)
β_2	Acceleration fuel efficiency parameter (mL/KJm/s^2)
β_b	Base fuel efficiency parameter (mL/KJm/s)
ΔTWT	Change in tread wear (mm)
λ	Tire slip coefficient (dimensionless)
μ	Coefficient of friction (dimensionless)
υ	Vehicle velocity (m/s)
ξ	Fuel-to-power efficiency factor (mL/KW/s)
ξ_b	Base fuel-to-power efficiency depends on the technology type (gasoline versus diesel) (mL/kW/s)
ρ	Mass density of the air (Kg/m3)

CHAPTER 1

Introduction

Background

Understanding the costs of highway construction, highway maintenance, and vehicle operation is essential to sound planning and management of highway investments, especially under increasing infrastructure demands and limited budgetary resources. While the infrastructure costs borne by road agencies are substantial, the cost borne by the road users are even greater. Therefore, vehicle operating costs (VOCs) should be considered by highway agencies when evaluating pavement investment strategies. For conventional vehicles, these costs are related to fuel and oil consumption, tire wear, repair and maintenance, and depreciation. However, emerging vehicle technologies may involve other cost items. These costs depend on the vehicle class and are influenced by vehicle technology, pavement-surface type, pavement condition, roadway geometrics, environment, speed of operation, and other factors.

A large body of research is available on the effects of pavement condition on vehicle operating costs and on models used to estimate these effects. Much of this information and many of the models were developed on the basis of data generated some 30 years ago in other countries for vehicle fleets that differ substantially from those used currently in the United States and for roadways that differ from those built in the United States. However, information relevant to operating costs of heavy trucks was recently collected in the United States. This information could be used to refine these models or develop models that would better apply to current and future US conditions. Nevertheless, information on the effects of pavement condition on the operating costs of light vehicles (automobiles and pickup trucks) is not readily available.

Description of the Problem

There are models of vehicle operating costs (and other road user costs) that are a function of road design characteristics, level of congestion, and work zone characteristics. However, unavailability of reliable models for estimating the effects of pavement condition on vehicle operating costs make conducting a comprehensive analysis of highway investment difficult. Therefore, there is a need to develop models applicable to current vehicle technology and to traffic and environmental conditions encountered in the United States. Such models will provide highway agencies with the tools necessary for considering vehicle operating costs in evaluating pavement investment strategies and identifying options that yield economic and other benefits. In this case, benefits include reductions in vehicle operating costs to meet the requirements related to more performance-based analyses of highway needs and justification of expenditures. NCHRP Project 1-45 was initiated to address these needs.

Project Objective and Scope

The objective of this research was to develop models for estimating the effects of pavement condition on vehicle operating costs. These models were to reflect current vehicle technologies in the United States.

The work performed for the research project included the collection and review of relevant literature, current practices, and data information relative to estimating the effects of pavement condition on vehicle operating costs (i.e., fuel consumption, tire wear, and repair and maintenance costs). The research also identified and evaluated current VOC models and recommended models that consider paved surfaces and traffic and environmental conditions encountered in the United States and address the full range of vehicle types. However, the research does not include the effects of pavement conditions on changes in travel time, nor does it consider the safety-related, environmental, or other implications of pavement conditions.

Research Approach

In this study, a large amount of data and information was collected, reviewed, and analyzed to identify the most relevant VOC models. This process focused on research that had

identified factors affecting vehicle operating costs including pavement conditions. The most relevant reports to this study were those dealing with the relationship between pavement conditions and vehicle operating costs. A detailed investigation involving field surveys to collect pavement condition data and field trials to collect fuel consumption and tire wear data was conducted. These data were used to calibrate and validate fuel and tire wear models and estimate the effects of pavement conditions on these VOC components. The research also involved the collection of repair and maintenance data of vehicle fleets from two departments of transportation (Michigan and Texas). The fleet data were used to develop repair and maintenance models. The end products of this research study are improved fuel consumption, tire wear, and repair and maintenance costs models that consider the paved surface conditions encountered in the United States and address the full range of vehicle types.

Report Organization

The report is divided into seven chapters. Chapter 1 is the introduction. Chapter 2 describes and evaluates existing VOC models. Chapter 3 discusses the calibration and validation of the selected fuel consumption model. Chapter 4 presents the results for the tire wear model. Chapter 5 discusses the development of the repair and maintenance costs model. Chapter 6 investigates the applicability of the improved models to emerging technologies. Chapter 7 summarizes the results of the study including the improved models and model parameters. An attachment to the report presents the user guide for the new VOC models and examples of analysis at the project and network levels using the results from this study.

Four appendixes to the report are available on the TRB website (http://www.trb.org/Main/Blurbs/166904.aspx). Appendixes A and B present the details of existing fuel and tire consumption models, respectively, and the collected data. Appendix C discusses the details of the repair and maintenance costs, the data collected from Texas and Michigan Departments of Transportation, and the results of the model development. Appendix D presents a summary of information on the emerging technologies and their effect on vehicle operating costs.

CHAPTER 2

Vehicle Operating Cost Models

This chapter summarizes the findings from the review of published literature on the relationship between pavement conditions and vehicle operating costs. The review included Federal Highway Administration (FHWA) and National Cooperative Highway Research Program (NCHRP) reports, and other relevant domestic and foreign reports and publications.

Road user costs represent a portion of the transportation cost. These costs include vehicle operating costs, travel time delay, safety, comfort and convenience, and environmental impacts. Figure 2-1 presents the different components of road user costs (Bennett and Greenwood, 2003b).

Vehicle operating costs are the costs associated with owning, operating, and maintaining a vehicle and include fuel consumption, oil and lubrication, tire wear, repair and maintenance, depreciation, and license and insurance. VOC components modeled include fuel and oil consumption, repair and maintenance costs, tire wear, and vehicle depreciation. Each of these cost components are typically modeled separately and summed to obtain overall vehicle operating costs. Common to many of these relationships is a road roughness factor used to describe the condition of the road. One such roughness measure is the international roughness index (IRI) developed as part of the World Bank Highway Development and Management System (HDM) standards studies (Sayers et al., 1986).

Road roughness is a broad term describing the range of irregularities from surface texture through road unevenness. To better characterize the influence of road roughness on vehicle operating costs, the total texture spectrum was subdivided into the four categories defined in Figure 2-2 (Sandberg and Ejsmont, 2002).

This categorization of roughness allowed a better evaluation of the surface factors influencing fuel consumption. As with fuel consumption, road roughness influences repair and maintenance costs, tire replacement, and the market value of vehicles. Barnes and Langworthy (2004) estimated vehicle operating costs using data from various sources. Figure 2-3 shows the reported costs of fuel, tire replacement, and repair and maintenance expressed as a percentage of total operating expenses. Fuel cost is shown to be the primary cost component followed by maintenance and repair costs, and tire wear.

Overview of Existing VOC Models

Based on the literature review, the major models that have been developed in various countries were identified. The most relevant models include:

- The World Bank's HDM 3 and HDM 4 VOC models (Bennett and Greenwood, 2003a, 2003b);
- Texas Research and Development Foundation (TRDF) VOC model (Zaniewski et al., 1982);
- MicroBENCOST VOC model (McFarland et al., 1993);
- Saskatchewan VOC models (Berthelot et al., 1996);
- British COBA VOC module (British Department of Transportation, 1993);
- Swedish VETO model (Hammarström and Karlsson, 1991);
- Australian NIMPAC VOC module (National Association of Australian State Road Authorities, 1978);
- ARFCOM model of fuel consumption (Biggs, 1988);
- New Zealand NZVOC (Bennett, 1989); and
- South African VOC models (du Plessis, 1989).

Most of the present VOC models have benefited from the World Bank's HDM research to some extent. Figures 2-4 and 2-5 outline the chronological development of these models. As shown in Figure 2-4, the basis of HDM research dates back to a study by de Weille (1966) for the World Bank, which led to the development of the Highway Cost Model (Becker, 1972) and subsequently to the most recent HDM 4 module.

Figure 2-5 highlights the VOC research conducted in the United States, which was primarily initiated by Winfrey (1969)

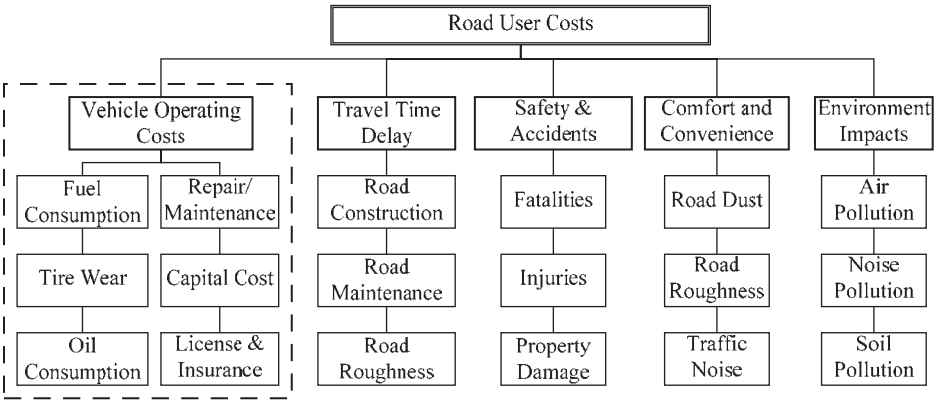

Source: adapted from Bennett and Greenwood (2003b)

Figure 2-1. Components of road user costs.

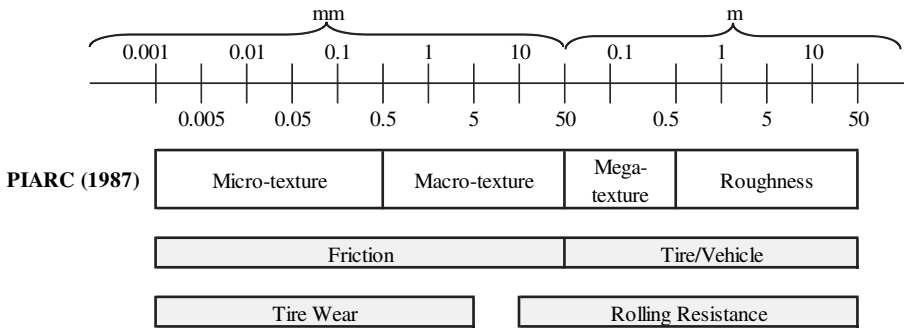

1 mm = 0.04 in, 1 m = 3.3 ft.
PIARC: Permanent International Association of Road Congresses
Source: adapted from Henry (2000) and Sandberg and Ejsmont (2002)

Figure 2-2. Ranges in terms of texture wavelength and their influence on pavement–tire interactions.

followed by Claffey (1971). These initial efforts laid the foundation for an assembly of VOC data and estimation models in the American Association of State Highway and Transportation Officials (AASHTO) Red Book by 1977. In 1982, Zaniewski et al. (1982) developed new VOC models as part of the TRDF study.

The TRDF models considered vehicle technology at that time and the effect of pavement roughness on vehicle operating costs addressed in the Brazil HDM study (Chesher and Harrison, 1987). These models were incorporated into the MicroBENCOST VOC models, which was intended to replace the AASHTO Red Book models. It should be noted that IRI was not an accepted roughness index at that time.

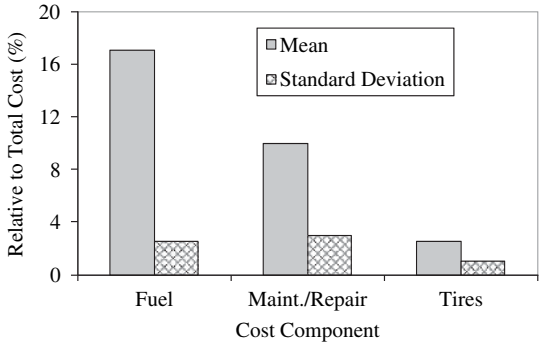

Source: after Barnes and Langworthy (2004)

Figure 2-3. Relative vehicle operating costs for trucks.

More recently, a user-friendly model for personal computers, Vehicle/Highway Performance Predictor (HPP), was developed for highway designers, planners, and strategists to estimate fuel consumption and exhaust emissions related to modes of vehicle operations on highways of various configurations and traffic controls (Klaubert, 2001). This model simulates vehicle operations by evaluating the vehicle external loads or propulsive demands determined by longitudinal and lateral accelerations, positive and negative road grades, rolling resistance, and aerodynamic drag for various transmission gears.

Table 2-1 summarizes the essential features of the existing VOC models; Appendixes A, B, and C present the detailed equations and relationships of these VOC models. In summary, most of the recent available VOC models were developed in countries other than the United States. Most of the existing models are derived from previous models as a means

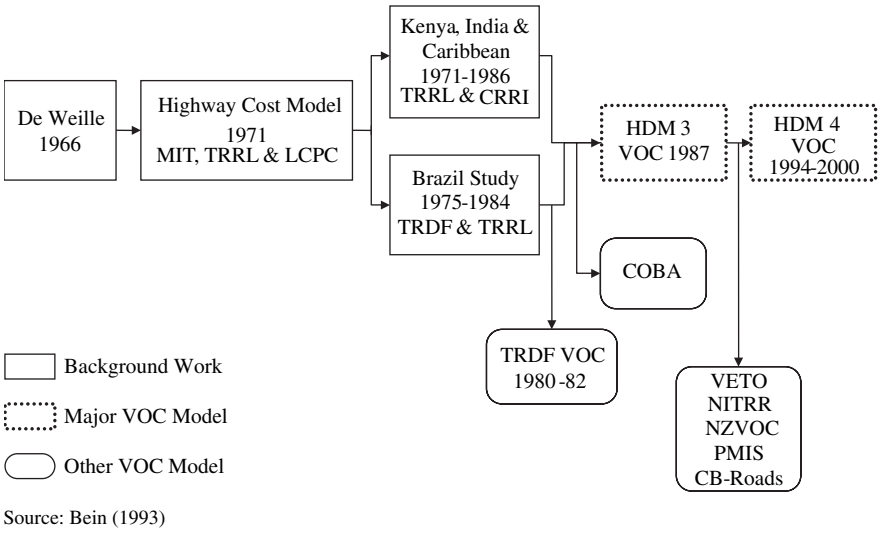

Figure 2-4. World Bank VOC models development.

for improving them. The most recent VOC model found in the literature is HDM 4 (Bennett and Greenwood, 2003b).

Evaluation of the Existing Models

This section summarizes the findings of the evaluation of available models. More details are presented in Appendixes A (fuel consumption models), B (tire wear models), and C (repair and maintenance models). The model evaluation and selection were based on the practicality and statistical soundness of the model.

The practicality evaluation of the models considered the following factors:

(1) Ease of use,
(2) Availability of appropriate input data,
(3) Ability of the model to incorporate pavement-surface conditions as currently being measured, and
(4) Reasonableness and applicability to US conditions.

The statistical soundness evaluation of the models considered the theoretical validity and accuracy of the models. In this regard the following factors were assessed:

(1) Data reliability,
(2) Original sample size,
(3) Model assumptions,
(4) Model formulation,
(5) Estimation techniques,
(6) Goodness-of-fit of the model,
(7) Estimated standard error of the predictions, and
(8) Statistics of the parameters.

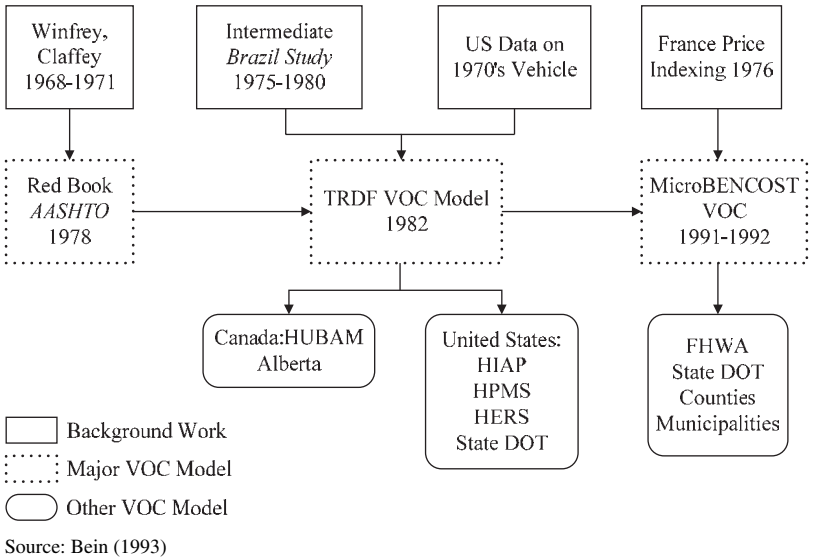

Figure 2-5. VOC models development in the United States.

Table 2-1. Categories of VOC models (empirical versus mechanistic).

Feature	VOC Models						
	HDM 3	COBA9	VETO	NIMPAC	ARFCOM	TRDF, MicroBENCOST	HDM 4
Empirical	✓	✓	–	✓	–	✓	–
Mechanistic	✓	–	✓	–	✓	–	✓
Level of Aggregation							
Simulation	–	–	✓	–	✓	–	✓
Project Level	✓	✓	✓	✓	✓	✓	✓
Network Level	✓	✓	–	✓	✓	–	✓
Vehicle Operation							
Uniform Speed	✓	✓	✓	✓	✓	✓	✓
Curves	✓	–	✓	✓	✓	✓	✓
Speed Change	–	–	✓	✓	✓	✓	✓
Idling	–	–	✓	✓	✓	✓	✓
Typical Vehicles							
Default	✓	✓	✓	✓	✓	✓	✓
User Specified	✓	–	✓	–	✓	–	✓
Modern Truck	✓	–	✓	✓	✓	–	✓
Road–Related Variables							
Gradient	✓	✓	✓	✓	✓	✓	✓
Curvature	✓	✓	✓	✓	✓	✓	✓
Superelevation	✓	–	✓	–	✓	–	✓
Roughness	✓		✓	✓	✓	✓	✓
Pavement Type	✓	–	✓	✓	✓	–	✓
Texture	–	–	✓	–	✓	–	✓
Snow, Water	–	–	✓	–	✓	–	✓
Wind, Temperature	–	–	✓	–	✓	–	✓
Absolute Elevation	✓		✓	–	✓	–	✓
VOC Components							
Fuel, Oil, Tires, Repair/Maintenance, Depreciation	✓	✓	✓	✓	✓	✓	✓
Interest	✓		✓	✓	–	–	✓
Cargo Damage	–	–	✓	–	–	–	–
Overhead	✓	✓	✓	–	–	–	–
Fleet Stock	–	✓	✓	–	–	–	–
Exhaust Emissions	–	–	✓	–	–	–	✓

Empirical and Mechanistic VOC Models

VOC models can be categorized as empirical and mechanistic models. Mechanistic models are theoretically formulated so that they encompass the main physical parameters according to basic laws of physics/mechanics. Empirical models rely more on "blind" mathematical correlations between different parameters to produce a model whose applicability can be limited by the specific data used in its development. In light of the relative strengths and weaknesses of both modeling approaches, a hybrid mechanistic–empirical approach is often used.

The development of empirical models is data-intensive and requires frequent updating and re-calibration to account for the changes in prices, and vehicle and road parameters. Also, most of the empirical models make use of classical regression assumptions (i.e., normality, independence, constant variance). However, many of the response variables (i.e., vehicle operating costs) do not follow these classical assumptions. These models would produce appropriate results when the input data are within the ranges used for developing the models but could produce erroneous results if the input data were outside these ranges. Nevertheless, these models have the advantage of requiring less input data and therefore are more suitable for those applications where limited data are available.

Mechanistic–empirical models are based on mathematical representations of the mechanical relationship between vehicle and road conditions. The accuracy of these formulations depends on the validity of the theoretical assumptions and the calibration process. The calibration of these models is generally less data-intensive than for empirical models. This type of model is capable of predicting the cost for a wide variety of scenarios, where the appropriate input data are available. However, extensive input data are often necessary to obtain reliable results. To address the data issues, analytical approaches—such as making valid assumptions in the absence of full data, using default values, using composite or weighted values, and conducting scenarios and sensitivity analysis—were used.

Table 2-2. Assessment of VOC models.

Model	Forces Opposing Motion[1]	Internal Vehicle Forces[2]	Engine Speed[2]	Excess Fuel due to Acceleration[2]	Transferability[2]
HDM 3	✓		✓		
South African	✓			✓	✓
ARFCOM	✓	✓	✓	✓	✓

[1] Suitable when considering the effect of pavement conditions
[2] Suitable when considering the effect of emerging vehicle technologies

Selection of Appropriate VOC Models

Fuel Consumption Models

The major mechanistic–empirical fuel consumption models are the HDM 3, the South African model, and the Australian model (ARFCOM) that was adapted in the HDM 4 study. The assessment of these models considered their appropriateness to model the key characteristics (i.e., forces opposing motion, internal vehicle forces, engine speed effect, driving in acceleration mode and transferability to different vehicles). Table 2-2 summarizes the results of the assessment. It can be seen that only the ARFCOM model satisfies all the listed requirements.

The assessment of the models also considered the validity of the assumptions used in their formulation. The following issues were identified:

- The South African model assumes that the fuel efficiency of the vehicle is independent from the driving mode. However, a number of studies that were conducted in the early 1980s in Australia to model fuel consumption found that the fuel efficiency increases in the acceleration case (Biggs, 1987) and that it is a function of tractive and engine power.
- The HDM 3 model adopted a constant engine speed. However, it is known that the engine speed is a function of the vehicle speed and the driving mode.
- The ARFCOM model predicts the fuel consumption as a function of the input (engine) and output power. However, the determination of the parameter values for the engine drag equation had low coefficients of determination and high standard errors (Biggs, 1988). Also, two different equations in the engine speed model were formulated: one for a vehicle in top gear, the other for a vehicle in less than top gear. However, these equations lead to a discontinuous relationship between vehicle speed and engine speed when the vehicle shifts into top gear. Such discontinuities lead to inconsistent fuel consumption predictions and should therefore be avoided (Biggs, 1988).

The World Bank updated the ARFCOM fuel consumption module in the HDM 4 model (Bennett and Greenwood, 2003b). Therefore, the HDM 4 model was selected for calibration and field tests were conducted to collect fuel consumption data for calibration and validation purposes.

Tire Wear Models

The only mechanistic–empirical tire wear models are included in HDM 3 and HDM 4. The HDM 3 model adopted the slip energy concept to calculate the changes in tread wear. The HDM 4 model has been extended from the HDM 3 model to include horizontal curvature force and traffic interaction effects. The theoretical formulation of the HDM 4 tire wear model is based on the same assumptions as the fuel consumption model. Therefore, the model was selected for calibration using field test data for passenger cars and the data provided by the National Center for Asphalt Technology (NCAT) for trucks.

Repair and Maintenance Models

All the repair and maintenance models are empirical, except for the Swedish VETO model. The empirical models that were developed in other countries (such as the World Bank's HDM 3 and HDM 4 models, the Saskatchewan models, and the South African model) could not be applied to US conditions, because these models were developed using data from different vehicle fleets (i.e., different vehicle characteristics and different technologies), different pavement conditions, as well as different labor and parts costs. The effect of pavement conditions on repair and maintenance costs predicted by the (mechanistic) VETO model are far higher than the change in parts cost predicted using empirical models. Therefore, it was decided to update the results from the latest study in the United States (Zaniewski et al., 1982), which is the only model that could be applied for the United States, and to develop a new mechanistic–empirical repair and maintenance model. This was done using the data obtained from Michigan and Texas Departments of Transportation.

CHAPTER 3

Fuel Consumption Model

The most recent VOC model found in the literature review is the HDM 4. It incorporates a mechanistic–empirical model of fuel consumption. This chapter describes the calibration of the HDM 4 fuel consumption model using data from instrumentation on board vehicles driven on roads of known condition.

HDM 4 Fuel Consumption Model

The general form of the HDM 4 fuel consumption model is expressed conceptually by Equation 3.1 (Bennett and Greenwood, 2003b).

$$IFC = f(P_{tr},\ P_{accs} + P_{eng}) = \frac{1000}{\upsilon} * (\max(\alpha, \xi * Ptot * (1 + dFuel))) \quad (3.1)$$

where:

IFC = Instantaneous fuel consumption (mL/km)
υ = Vehicle speed (m/s)
P_{tr} = Power required to overcome traction forces (kW)
P_{accs} = Power required for engine accessories (e.g., fan belt, alternator etc.) (kW)
P_{eng} = Power required to overcome internal engine friction (kW)
α = Fuel consumption at idling (mL/s)
ξ = Fuel-to-power efficiency factor (mL/kW/s)

$$= \xi_b \left(1 + ehp \frac{(P_{tot} - P_{eng})}{P_{\max}}\right)$$

ξ_b = Base fuel-to-power efficiency (depends on the technology type: gasoline versus diesel)
P_{max} = Rated engine power (kW)
ehp = Proportionate decrease in efficiency at high output power (dimensionless)
$Ptot$ = Total power (kW)
$dFuel$ = Excess fuel conception due to congestion as a percentage

The engine efficiency decreases at high levels of output power, resulting in an increase in the fuel efficiency factor ξ. The total power required is divided into tractive power, and engine drag and vehicle accessories power. The total requirement can be calculated by two alternative methods depending on whether the tractive power is positive or negative as shown in Table 3-1. Table 3-2 shows parameters for the engine speed model that feeds into the engine and accessories power equation. The tractive power is a function of the aerodynamic, gradient, curvature, rolling resistance, and inertial forces. The aerodynamic forces are expressed as a function of the air density and the aerodynamic vehicle characteristics, and are given in Table 3-3. The gradient forces are a function of vehicle mass, gradient, and gravity. The curvature forces are computed using the slip energy method. Table 3-4 shows parameters for the tire stiffness model. The rolling resistance forces are a function of vehicle characteristics, pavement conditions, and climate. Table 3-5 shows parameters for the rolling resistance model for asphalt and concrete pavements. The inertial forces are a function of the vehicle mass, speed, and acceleration. Table 3-6 shows the parameters for the effective mass ratio model.

Field Trials and Data Collection

The main objective of the field trials was to validate and calibrate the HDM 4 fuel consumption model. During the field trials, the following data related to vehicle engine parameters, pavement surface characteristics, and environmental factors were collected:

- Engine/vehicle parameters
  - Mass air flow rate (g/s)
  - Air-to-fuel ratio
  - Fuel rate (L/h)
  - Engine rotation (rev/min)
  - Fuel temperature (°C)

Table 3-1. HDM 4 fuel consumption model.

Name	Description	Unit
Total power (P_{tot})	$P_{tot} = \frac{P_{tr}}{edt} + P_{accs} + P_{eng}$ for $P_{tr} \geq 0$, uphill/level $P_{tot} = edtP_{tr} + P_{accs} + P_{eng}$ for $P_{tr} < 0$, downhill	kW
edt	Drive-train efficiency factor	factor
Engine and accessories power ($P_{engaccs} = P_{eng} + P_{accs}$)	$Pengaccs = KPea * P\max * (Paccs\_a1 + (Paccs\_a0 - Paccs\_a1) * \frac{RPM - RPMIdle}{RPM100 - RPMIdle}$	kW
KPea	Calibration factor	
*P*max	Rated engine power	kW
*Paccs_a*1	$Paccs\_a1 = \frac{-b + \sqrt{b^2 - 4*a*c}}{2*a}$ $a = \xi_b * ehp * KPea^2 * P\max * \frac{100 - PctPeng}{100}$ $b = \xi_b * KPea * P\max$ $c = -\alpha$	factor
ξ_b	Base fuel-to-power efficiency (depends on the technology type: gasoline versus diesel)	mL/kW/s
ehp	Proportionate decrease in efficiency at high output power	dimensionless
α	Fuel consumption at idling	mL/s
*Paccs_a*0	Ratio of engine and accessories drag to rated engine power when traveling at 100 km/h	dimensionless
PctPeng	Percentage of the engine and accessories power used by the engine (Default = 80%)	%
Engine speed (*RPM*)	$RPM = a0 + a1 * SP + a2 * SP^2 + a3 * SP^3$ $SP = \max(20, \upsilon)$	rev/min
υ	Vehicle speed	m/s
*a*0 to *a*3	Model parameter (Table 3-2)	dimensionless
RPM100	Engine speed at 100 km/h	rev/min
RPMIdle	Idle engine speed	rev/min
Tractive power (P_{tr})	$P_{tr} = \frac{\upsilon(Fa + Fg + Fc + Fr + Fi)}{1000}$	kW
Fa	Aerodynamic forces	N
Fg	Gradient forces	N
Fc	Curvature forces	N
Fr	Rolling resistance forces	N
Fi	Inertial forces	N

Table 3-2. Engine speed model parameters for the HDM 4 model.

Vehicle Type	Engine Speed			
	*a*0	*a*1	*a*2	*a*3
Motorcycle	−162	298.86	−4.6723	−0.0026
Small car	1910	−12.311	0.2228	−0.0003
Medium car	1910	−12.311	0.2228	−0.0003
Large car	1910	−12.311	0.2228	−0.0003
Light delivery car	1910	−12.311	0.2228	−0.0003
Light goods vehicle	2035	−20.036	0.356	−0.0009
Four−wheel drive	2035	−20.036	0.356	−0.0009
Light truck	2035	−20.036	0.356	−0.0009
Medium truck	1926	−32.352	0.7403	−0.0027
Heavy truck	1905	−12.988	0.2494	−0.0004
Articulated truck	1900	−10.178	0.1521	0.00004
Mini bus	1910	−12.311	0.2228	−0.0003
Light bus	2035	−20.036	0.356	−0.0009
Medium bus	1926	−32.352	0.7403	−0.0027
Heavy bus	1926	−32.352	0.7403	−0.0027
Coach	1926	−32.352	0.7403	−0.0027

Source: Bennett and Greenwood (2003b)

  - Calculated power (kW)
  - Calculated efficiency (%)
  - Vehicle speed (km/h)
- Environmental variables
  - Ambient temperature (°C)
  - Maximum relative humidity (%)
  - Minimum relative humidity (%)
  - Wind speed (km/h)
- Pavement surface characteristics
  - Roughness (IRI)
  - Grade (%)
  - Texture depth (mm)
  - Pavement type

Since the goal of the study was to estimate the effect of roughness on fuel consumption, the repeatability and accuracy

Table 3-3. HDM 4 tractive forces model.

Name	Description	Unit
Aerodynamic forces (*Fa*)	$Fa = 0.5 * \rho * CDmult * CD * AF * \upsilon^2$	N
CD	Drag coefficient	dimensionless
CDmult	CD multiplier	dimensionless
AF	Frontal area	m^2
ρ	Mass density of the air	kg/m^3
υ	Vehicle speed	m/s
Gradient forces (*Fg*)	$Fg = M * GR * g$	N
M	Vehicle weight	kg
GR	Gradient	radians
g	Gravity	m/s^2
Curvature forces (*Fc*)	$Fc = \max\left(0, \frac{\left(\frac{M*\upsilon^2}{R} - M*g*e\right)^2}{Nw*Cs} * 10^{-3}\right)$	N
R	curvature radius	m
Superelevation (e)	$e = \max(0, 0.45 - 0.68 * Ln(R))$	m/m
Nw	Number of wheels	dimensionless
Tire stiffness (Cs)	$Cs = KCS * \left[a0 + a1 * \frac{M}{Nw} + a2 * \left(\frac{M}{Nw}\right)^2\right]$	kN/rad
KCS	Calibration factor	factor
$a0$ to $a2$	Model parameter (Table 3-4)	dimensionless
Rolling resistance (F_r)	$Fr = CR2 * FCLIM * (b11 * Nw + CR1 * (b12 * M + b13 * \upsilon^2))$	N
$CR1$	Rolling resistance tire factor	factor
Rolling resistance parameters ($b11$, $b12$, $b13$)	$b11 = 37 * Dw$; $b12 = \begin{cases} 0.067/Dw & old\ \ tires \\ 0.064/Dw & latest\ \ tires \end{cases}$; $b12 = 0.012 * Nw/Dw^2$	factor
Rolling resistance surface factor ($CR2$)	$CR2 = Kcr2[a0 + a1 * Tdsp + a2 * IRI + a3 * DEF]$	dimensionless
$Kcr2$	Calibration factor	factor
$a0$ to $a3$	Model coefficient (Table 3-5)	dimensionless
$Tdsp$	Texture depth using sand patch method	mm
IRI	International roughness index	m/km
DEF	Benkelman Beam rebound deflection	mm
Climatic factor ($FCLIM$)	$FCLIM = 1 + 0.003 * PCTDS + 0.002 * PCTDW$	factor
$PCTDS$	Percentage driving on snow	
$PCTDW$	Percentage driving on wet surface	
Inertial forces (F_i)	$Fi = M * \left(a0 + a1 * \arctan\left(\frac{a2}{\upsilon^3}\right)\right) * a$	N
$a0$ to $a2$	Model parameter (Table 3-6)	dimensionless

Table 3-4. Tire stiffness (Cs) model parameters for the HDM 4 model.

	≤ 2500 kg		> 2500 kg	
Coefficient	Bias	Radial	Bias	Radial
$a0$	30	43	8.8	0
$a1$	0	0	0.088	0.0913
$a2$	0	0	−0.0000225	−0.0000114
KCS	1	1	1	1

Source: Bennett and Greenwood (2003b)

Table 3-5. Parameters for rolling resistance (*CR*2) model in the HDM 4 model for asphalt and concrete pavements.

Surface Type	≤ 2500 kg				> 2500 kg			
	$a0$	$a1$	$a2$	$a3$	$a0$	$a1$	$a2$	$a3$
Asphalt	0.5	0.02	0.1	0	0.57	0.04	0.04	1.34
Concrete	0.5	0.02	0.1	0	0.57	0.04	0.04	0

Source: Bennett and Greenwood (2003b)

Table 3-6. Effective mass ratio model parameters for the uncalibrated HDM 4 model.

Vehicle Type	Effect Mass Ratio Model Coefficients		
	*a*0	*a*1	*a*2
Motorcycle	1.1	0	0
Small car	1.14	1.01	399
Medium car	1.05	0.213	1260.7
Large car	1.05	0.213	1260.7
Light delivery car	1.1	0.891	244.2
Light goods vehicle	1.1	0.891	244.2
Four-wheel drive	1.1	0.891	244.2
Light truck	1.04	0.83	12.4
Medium truck	1.04	0.83	12.4
Heavy truck	1.07	1.91	10.1
Articulated truck	1.07	1.91	10.1
Mini bus	1.1	0.891	244.2
Light bus	1.1	0.891	244.2
Medium bus	1.04	0.83	12.4
Heavy bus	1.04	0.83	12.4
Coach	1.04	0.83	12.4

Source: Bennett and Greenwood (2003b)

of the measurements are considered a key criterion for data interpretation. Therefore, preliminary tests were conducted to validate the accuracy and repeatability of the equipment that were used during field tests. The data acquisition system was able to access and log data from the vehicle's engine control unit (ECU) via an on-board diagnostic (OBD) connector.

Testing of the Accuracy and Precision of Test Equipment

Repeatability/Precision

Two different tests were conducted at two different locations (Flint and Lansing areas in Michigan) using two different vehicles (a 2008 Mercury Sable and a 2008 Chevy Impala) to measure the repeatability of the instrument. During both tests, the outdoor conditions for the identified sections were measured using a portable weather station. The tire pressure during the runs was maintained at 207 kPa (30 psi).

The first section was a loop of 32 km or 20 mi (I-69E, I-496N and I-75S). The start and end points of each run were marked by distinct flags and road markers. The data acquisition system was connected to the vehicle during the test. Five runs were made on the pavement: three runs (Runs 1 through 3) at a speed of 105 km/h (65 mph) and two runs (Runs 4 and 5) at a speed of 96 km/h (60 mph). Cruise control was engaged to reduce the acceleration and deceleration cycles.

The results of the repeatability test are summarized in terms of correlations in Tables 3-7 and 3-8. The correlation between Runs 1 through 3 was almost perfect ($\rho \approx 0.98$ and 0.02% error). Also, Runs 4 and 5 were highly correlated ($\rho \approx 0.9$ and 0.05% error).

Table 3-7. Correlations for Runs 1 through 3.

		Run 1	Run 2	Run 3
Run 1	Pearson Correlation	1.00	0.99**	0.98**
	Sig. (2-tailed)		0.00	0.00
	N	638	633	638
Run 2	Pearson Correlation	0.99**	1.00	0.97**
	Sig. (2-tailed)	0.00		0.00
	N	633	633	633
Run 3	Pearson Correlation	0.98**	0.97**	1.00
	Sig. (2-tailed)	0.00	0.00	
	N	638	633	638

** Correlation is significant at the 0.01 level (2-tailed).

Table 3-8. Correlations for Runs 4 and 5.

		Run 4	Run 5
Run 4	Pearson Correlation	1.00	0.91**
	Sig. (2-tailed)		0.00
	N	747	745
Run 5	Pearson Correlation	0.91**	1.00
	Sig. (2-tailed)	0.00	
	N	745	745

** Correlation is significant at the 0.01 level (2-tailed).

The second section selected was a 14 km (8.8 mi) stretch along I-69 (E and W). The speed for the runs was 105 km/h (65 mph). The start and end points of each run were also marked by distinct flags and road markers. Two runs were made on this section. The repeatability test results are summarized in terms of correlations in Table 3-9. The correlation between Runs 1 and 2 was also almost perfect ($\rho \approx 0.92$ and 0.02% error).

Based on these results, it was concluded that the instrument was reliable enough to determine the changes in fuel consumption due to minor changes of surface conditions.

Table 3-9. Correlations for Runs 1 and 2.

		Run 1	Run 2
Run 1	Pearson Correlation	1.00	0.924**
	Sig. (2-tailed)		0.00
	N	4733	4733
Run 2	Pearson Correlation	0.924**	1.00
	Sig. (2-tailed)	0.00	
	N	4733	4733

** Correlation is significant at the 0.01 level (2-tailed).

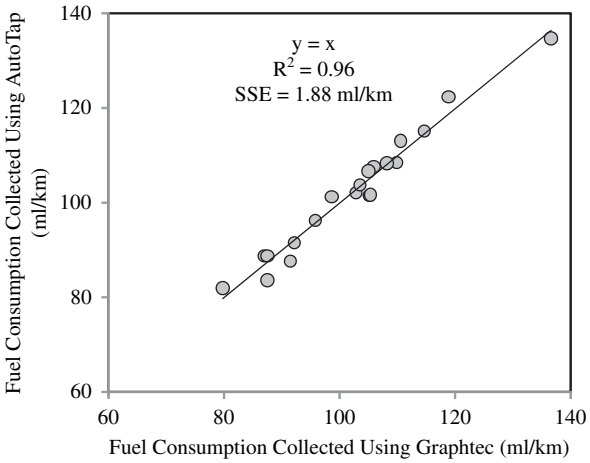

Figure 3-1. Comparison between data collected using AutoTap and Graphtec.

Data Acquisition System Accuracy/Calibration

The calibration of the data acquisition system was conducted by comparing the OBD fuel consumption data to direct fuel meter measurements. The fuel measurement tests were conducted using a fuel meter. An instrumented van was driven under the same environmental, operating, and pavement conditions using both data acquisitions systems for 20 s at highway speed. Figure 3-1 summarizes the data collected using both data acquisition systems (Graphtec fuel meter and OBD AutoTap).

Table 3-10 summarizes the results of the paired *t*-test that was conducted. A paired samples *t*-test failed to reveal a statistically reliable difference between the mean fuel consumption measured using Graphtec (mean = 102.38 mL/km, standard deviation = 13.09 mL/km) and AutoTap (mean = 102.24 mL/km, standard deviation = 13.08 mL/km), t(19) = 0.34, p = 0.74, α = 0.05. The maximum difference is 2.56%. Previous studies indicated that a pavement surface with an IRI range of 1 to 5 m/km contributes to a change in fuel consumption of 3% to 5%. Therefore, this level of error was judged as acceptable.

Field Trials

Five different locations near Lansing, Michigan, were selected for field trials to reflect a wide range of pavement conditions (i.e., roughness, gradient, texture, and pavement type). Table 3-11 shows the field test matrix. Both asphalt and concrete pavements were included; IRI values for the test sections ranged from 0.8 to 8.5 m/km (51 to 539 in./mi); mean profile depth (MPD) values ranged from 0.2 to 2.7 mm (0.01 to 0.1 in.); grade ranged from –3.4% to 3.1%; and five speeds were considered. The tests were conducted during both winter wet and summer dry conditions. The actual weather conditions (temperature and wind speed), summarized in Table 3-12, were recorded using a portable weather station. Tests were repeated when changes of more than 3°C (5°F) in ambient temperature were recorded. The pavement and weather test

Table 3-10. Paired samples *t*-test results.

	Paired Differences					t	df	Significance
	Mean (mL/km)	Standard Deviation (mL/km)	Standard Error Mean	95% Confidence Interval of the Difference (mL/km) Lower	Upper			
FC_Graphtec–FC_AutoTap	0.14	1.88	0.42	−0.74	1.02	0.34	19	0.74

FC: Fuel Consumption

Table 3-11. Field test matrix.

Day	Road	Start	End	Pavement Type AC	Pavement Type PCC	Length (km)	IRI range (m/km)	MPD (mm)	Grade (%)	Speed limit (km/h)	Operating Speed (km/h) 56	72	88	96	112
1	Creyts Rd	Lansing Rd	Millett Hwy	X		1.5	1.28–8.5	0.2–2.0	(−1.6) – 0.7	72	✓	✓			
1	Creyts Rd	Millett Hwy	Mount Hope	X		1.6	1.7–7		(−0.5) – 2.3	72	✓	✓			
2	Waverly Rd	Willow Hwy	Tecumseh River Rd	X		0.8	3.5–6	0.2–1.0	(−3.1) – 1.9	72	✓	✓			
2	Waverly Rd	Tecumseh River Rd	Delta River Dr	X		0.8	3.25–6		(−0.27) – 3.1	72	✓	✓			
2	I-69E	Airport Rd	Francis Rd		X	7.6	0.8–3.8	0.3–0.8	(−0.9) – 1.4	112			✓	✓	✓
2	I-69W	Francis Rd	Airport Rd		X	7.6	1.1–3.1	0.2–1.3	(−1.4) – 0.9	112			✓	✓	✓
2	M-99S	Holt Hwy	Columbia Hwy		X	6.4	0.8–4.8	0.2–2.7	(−3.4) – 2.1	88	✓	✓	✓		
2	M-99S	Bishop Rd	Holt Hwy		X	3.6			(−2.5) – 1.8	88	✓	✓	✓		
2	M-99N	Columbia Hwy	Holt Hwy	X		6.4	0.5–4.1	0.2–1.9	(−3.2) – 3.1	88	✓	✓	✓		
2	M-99N	Dimondale Rd	Waverly Rd		X	0.8			(−0.9) – 2.5	88	✓	✓	✓		
2	M-99N	Waverly Rd	Bishop Rd		X	2.1			(−1.8) – 1.4	88	✓	✓	✓		

Note: All tests were repeated.
1 km = 0.63 mi; 1 mm = 0.04 in.; 1 m/km = 63.4 in./mi; 1 km/h = 0.63 mph.

Table 3-12. Recorded weather conditions.

Variables	Winter		Summer		
	11/24/2008	11/25/2008	06/05/2009	06/06/2009	06/07/2009
Ambient temperature (°C)	0–2	1–3	28.9–29.2	27.2–28.3	22.5–25.2
Wind speed (m/s)	1.7–2.4	0.4–1	2.1 – 2.9	1.4–2.4	1.7–2.4

conditions were considered typical of those encountered in the United States.

The pavement conditions data (raw profile and texture depth) were collected by the Michigan Department of Transportation using a Rapid Travel Profilometer (ASTM E950-98) and a Road Surface Analyzer (ASTM E1845-09).

In addition, slope data surveys were collected using a high-precision global positioning system (GPS). The sampling rate was every 1 s at highway speed (i.e., every 30.5 m or 100 ft). The average error of the measurement was 12.7 mm per 0.5 km (0.5 in. per 0.3 mi), i.e., 0.003% (about twice the error of the total station).

Six different vehicles that represent typical vehicles in the United States—medium car, sport utility vehicle (SUV), van, light truck (gas and diesel), and articulated truck (Figure 3-2)—were used. Table 3-13 lists the characteristics of the

(a) Medium Car

(b) SUV

(c) Van

(d) Light Truck

(e) Articulated Truck

Figure 3-2. Vehicles used in field trials.

Table 3-13. Characteristics of the vehicles used in the field trials.

Characteristics	Vehicle Class				
	Medium Car	SUV	Van	Light Truck	Heavy Truck
Make	Mitsubishi	Chevrolet	Ford	GMC	International
Model	Galant	Tahoe	E350	W4500	9200 6x4
Year	2008	2009	2008	2006	2005
Drag coefficient	0.4	0.5	0.5	0.6	0.8
Frontal area (m^2)	1.9	2.9	2.9	4.2	9
Tare weight (t)	1.46	2.5	2.54	3.7	13.6
Maximum allowable load (t)	–	–	–	2.9	22.7
GVW (t)	–	–	–	6.6	36.3
Weight of the load (t)	–	–	–	2.8	21.3
Gas type	Gas	Gas	Gas	Gas/Diesel	Diesel
Tire diameter (m)	0.38	0.4	0.4	0.4	0.57
Tire pressure in kPa (psi)	242 (35)	269 (39)	297 (43)	393 (57)	759 (110)
Tire type	radial	radial	radial	radial	bias
Cargo length (m)	–	–	–	4.88	15.85
Other	–	4WD	15 seats	–	Flat bed

vehicles used in field trials. Tests for trucks were conducted using loaded (Figure 3-3) and unloaded (Figure 3-2e) trucks. The light truck was loaded with two concrete blocks weighing a total of 2.82 metric tons (6,210 lb), in accordance with the recommended payload. Both blocks were tightly secured to the truck bed. The trailer of the heavy truck was loaded with steel sheets (21.32 metric tons or 47,000 lb) also tightly secured to the trailer. The gross vehicle weight (GVW) was about 36.3 metric tons (80,000 lb), which is the maximum GVW allowed in the United States.

(a) Loading of Light Truck

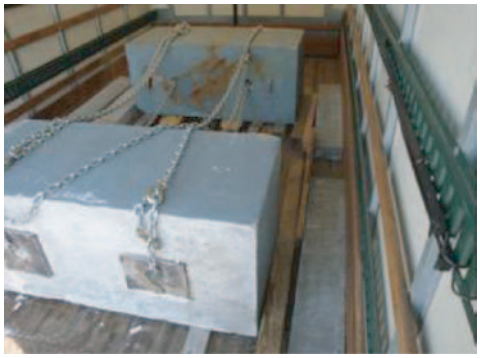

(b) Loaded Light Truck

(c) Loading of Heavy Truck

(d) Loaded Heavy Truck

Figure 3-3. Truck loading conditions.

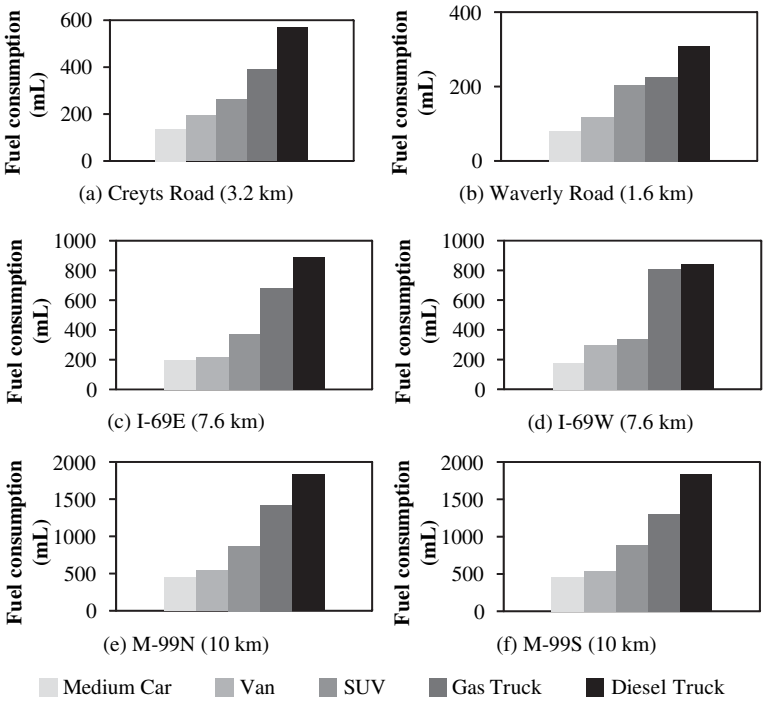

Figure 3-4. Examples of collected data.

Each vehicle had a data logger (scanner) connected to the OBD connector and the vehicle was driven at different speeds on cruise control to reduce the acceleration and deceleration cycles. Multiple and repeated runs were performed. In order to understand the effect of cruise control on the collected data, all the tests were conducted at constant speed with and without cruise control. The start and end points of data logging were marked by distinct flags and road markers.

Figure 3-4 shows example data collected during runs at 56 km/h (35 mph) except for section I-69 east and west where the speed was 88 km/h (55 mph).

Calibration of the HDM 4 Model

The data acquisition system collects the mass airflow rate (MAF) in grams per second and the air-to-fuel ratio. Equation 3.2 is used to convert these data to instantaneous fuel consumption in terms of milliliters per kilometer.

$$IFC = \frac{1000 * MAF}{\upsilon * 14.7 * \rho_g} \tag{3.2}$$

where:

IFC = Instantaneous fuel consumption (mL/km)
υ = Vehicle speed (m/s)
MAF = Mass air flow (g/s)
14.7 = Air-to-fuel ratio
ρ_g = Density of gasoline (g/mL) = 0.74

The predicted and measured engine speeds are plotted in Figure 3-5 for the medium car, van, SUV, light truck, and articulated truck. The plots show that the HDM 4 model overpredicts the engine speed of the vehicle; it will therefore overpredict the engine and accessories power and overestimate the fuel consumption. Consequently, when calibrating the fuel consumption model, the tractive power (i.e., the effect of pavement conditions) will be underestimated. Therefore, the HDM 4 engine speed model had to be calibrated first, before calibrating the fuel consumption model.

Calibration of the HDM 4 Engine Speed Model

The engine speed model expressed in terms of revolutions per minute (rpm) was calibrated for all vehicle classes using the data collected during the field tests. Vehicles were classified into categories listed in Table 3-14. Figure 3-5 show the results of the calibration for both winter and summer field test data. Note that the HDM 4 engine speed model has a discontinuity at idle speed. It was observed that the engine speed model calibrated using winter data could be used to predict the engine speed in the summer for all vehicle classes except for the light truck because the engine of the light truck used in the winter tests misfired. Therefore, only summer test data were used to calibrate the HDM 4 engine speed model for the light truck.

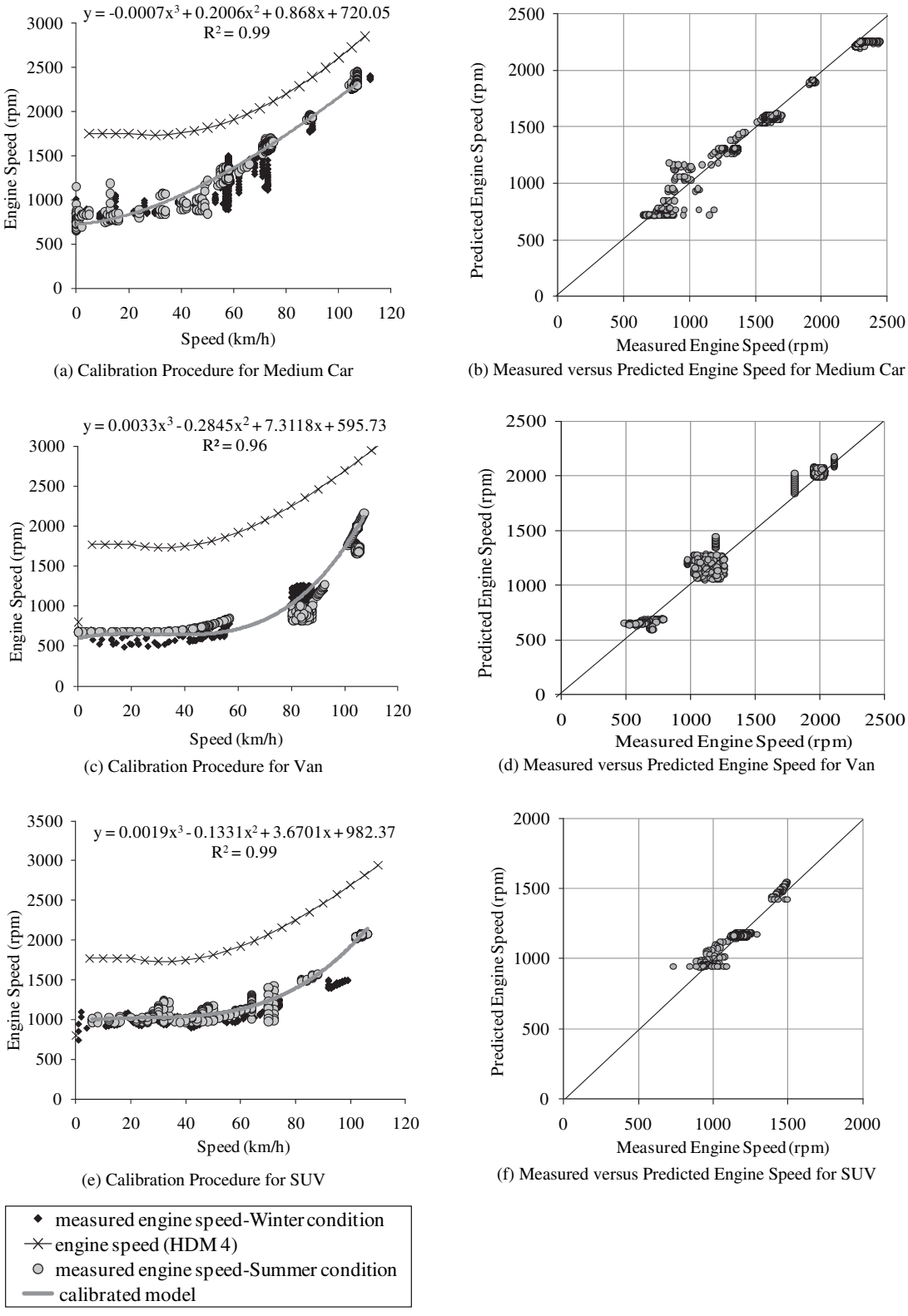

Figure 3-5. Calibration of HDM 4 engine speed model for all vehicle classes.

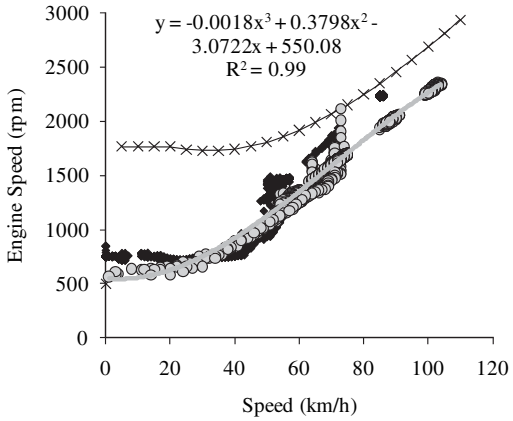

(g) Calibration Procedure for Light Truck

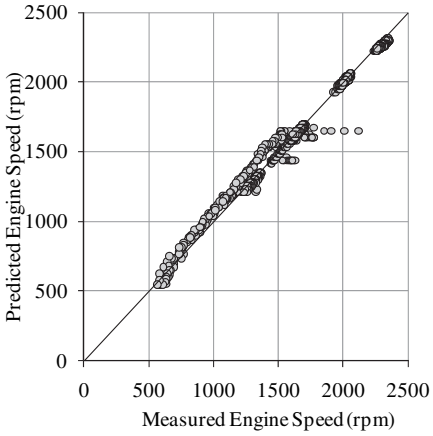

(h) Measured Versus Predicted Engine Speed for Light Truck

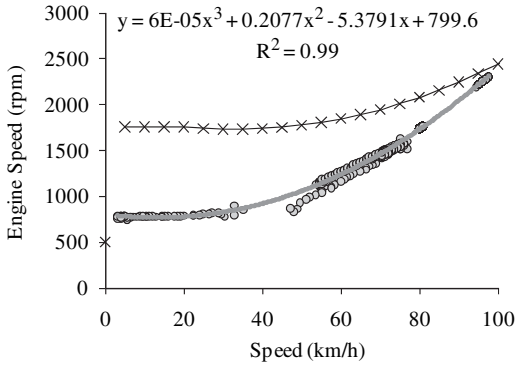

(i) Calibration Procedure for Articulated Truck

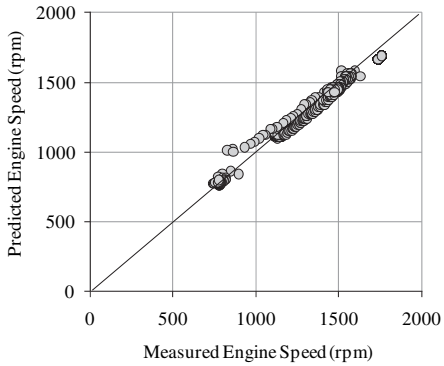

(j) Measured Versus Predicted Engine Speed for Articulated Truck

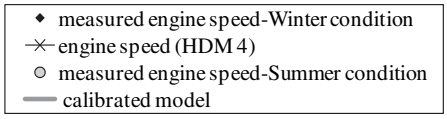

Figure 3-5. (Continued).

Table 3-14. Vehicle classification used in the engine speed model calibration.

Categories	Vehicle Classes	Vehicle Used
Passenger car	• Small car • Medium car • Large car • Mini bus	• Medium car
Light commercial vehicle	• Light delivery vehicle • Light goods vehicle	• Van
Four-wheel drive	• Four-wheel drive	• SUV
Light truck	• Light truck • Light bus	• Light truck
Heavy truck	• Medium truck • Heavy truck • Articulated truck • Medium bus • Heavy bus • Coach	• Articulated truck

Table 3-15. Estimated coefficients for engine speed model.

Vehicle Class	Engine Speed Coefficients							
	Winter Condition				Summer Condition			
	*a*0	*a*1	*a*2	*a*3	*a*0	*a*1	*a*2	*a*3
Small car	823.78	−4.6585	0.2702	−0.0012	720.05	0.868	0.2006	−0.0007
Medium car	823.78	−4.6585	0.2702	−0.0012	720.05	0.868	0.2006	−0.0007
Large car	823.78	−4.6585	0.2702	−0.0012	720.05	0.868	0.2006	−0.0007
Light delivery car	595.73	7.311	−0.2845	0.0033	671.98	6.7795	−0.3018	0.0062
Four-wheel drive	943.51	−0.0861	−0.0069	0.0007	982.37	3.6701	−0.1331	0.0019
Light truck	797.01	−25.028	0.9112	−0.0049	550.08	−3.0722	0.3798	−0.0018
Mini bus	823.78	−4.6585	0.2702	−0.0012	720.05	0.868	0.2006	−0.0007
Light bus	797.01	−25.028	0.9112	−0.0049	550.08	−3.0722	0.3798	−0.0018
Medium truck	–	–	–	–	799.6	−5.3791	0.2077	0.00006
Heavy truck	–	–	–	–	799.6	−5.3791	0.2077	0.00006
Articulated truck	–	–	–	–	799.6	−5.3791	0.2077	0.00006
Medium bus	–	–	–	–	799.6	−5.3791	0.2077	0.00006
Heavy bus	–	–	–	–	799.6	−5.3791	0.2077	0.00006
Coach	–	–	–	–	799.6	−5.3791	0.2077	0.00006

Table 3-15 lists the engine speed model coefficients for winter and summer conditions. These coefficients were used for the calibration of the HDM 4 fuel consumption model. Table 3-16 lists the recommended coefficients for the HDM 4 engine speed model.

Calibration of HDM 4 Fuel Consumption Model

The HDM 4 fuel consumption model provides the following two coefficients for calibration (Bennett and Greenwood, 2003a):

- *Kcr*2, which modifies the tractive power;
- *KPea,* which modifies the accessories and engine power.

The calibration procedure determines the coefficients required to minimize the sum of squared errors (i.e., sum of squared differences between the observed field values and those predicted using HDM 4 model). The methodology used is according to the HDM 4 calibration guide (Bennett and Greenwood, 2003a) and is summarized as follows:

1. A random value is assigned to *Kcr*2, and then the value of *KPea* yielding the lower least squared value is determined.
2. This process is continued iteratively until the lowest sum of the squared errors (SSE) is obtained.

Table 3-16. Recommended coefficients for engine speed model.

Vehicle Class	Engine Speed Coefficients			
	*a*0	*a*1	*a*2	*a*3
Small car	720.05	0.868	0.2006	−0.0007
Medium car	720.05	0.868	0.2006	−0.0007
Large car	720.05	0.868	0.2006	−0.0007
Light delivery car	595.73	7.311	−0.2845	0.0033
Light goods vehicle	595.73	7.311	−0.2845	0.0033
Four-wheel drive	982.37	3.6701	−0.1331	0.0019
Light truck	550.08	−3.0722	0.3798	−0.0018
Mini bus	720.05	0.868	0.2006	−0.0007
Light bus	550.08	−3.0722	0.3798	−0.0018
Medium truck	799.6	−5.3791	0.2077	0.00006
Heavy truck	799.6	−5.3791	0.2077	0.00006
Articulated truck	799.6	−5.3791	0.2077	0.00006
Medium bus	799.6	−5.3791	0.2077	0.00006
Heavy bus	799.6	−5.3791	0.2077	0.00006
Coach	799.6	−5.3791	0.2077	0.00006

The data collected during the field tests were used to calibrate the HDM 4 fuel consumption model. It was observed that, for light vehicles (medium car, SUV, and van), the fuel consumption with and without cruise control were comparable. On the other hand, there was a noticeable difference between the fuel consumption of heavier vehicles (light and articulated trucks) with and without cruise control. This is illustrated in Figure 3-6 which shows the measured and predicted fuel consumption with cruise control for van and light truck. The figure shows that, with the cruise control engaged, low consumption was underestimated, and the high consumption was overestimated for the light truck but not for the van. Figure 3-7, which shows measured versus predicted fuel consumption for the articulated truck with and without cruise control engagement, confirms that the HDM 4 predictions agree only with the measure-

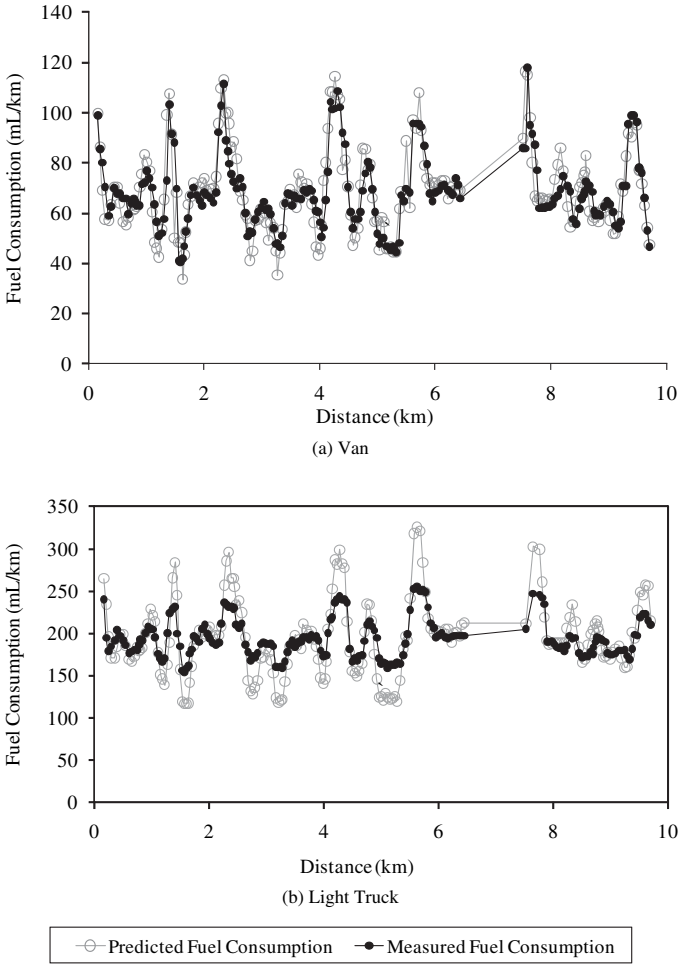

Figure 3-6. Predicted and measured fuel consumption (with cruise control) versus distance.

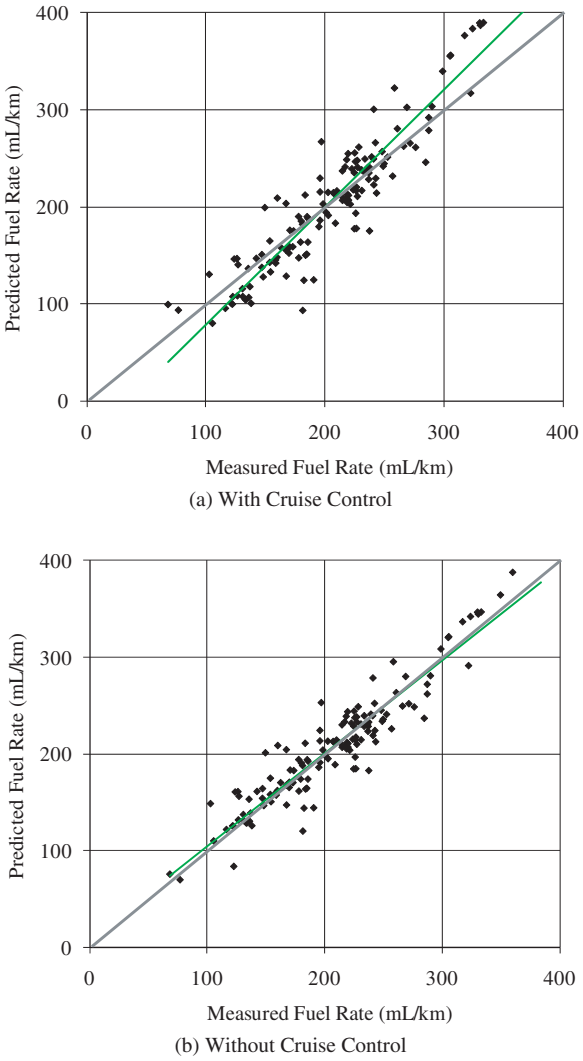

Figure 3-7. Measured versus estimated fuel consumption for heavy truck.

ments without cruise control for the heavier vehicles. The HDM 4 overpredicts fuel consumption in the high range (above 200 mL/km) and underpredicts fuel consumption in the low range (less than 200 mL/km). The reason can be explained as follows: During testing, when the vehicle was driven over a steep positive slope, the cruise control disengaged and the vehicle speed decreased resulting in a decrease in fuel consumption. However, for a vehicle driven over a steep negative slope, the HDM 4 model yields negative tractive power, indicating that the vehicle requires no traction force from the engine, and predicts lower fuel consumption. This did not occur during the tests; instead the speed increased.

For some vehicles, it was difficult to maintain constant speed without cruise control especially when the roads are very rough. For calibration purposes, data collected during the tests with cruise control were used for light vehicles; the data collected during tests without cruise control were used for light and heavy trucks. Figure 3-8 shows the results after calibration of the HDM 4 fuel consumption model for all vehicle classes. Table 3-17 lists the calibration coefficients and the corresponding errors. Statistical analysis showed that there is no difference between the observed and the estimated fuel consumption at 95 percent confidence level.

Effect of Roughness and Texture on Fuel Consumption

To verify that the calibrated HDM 4 model is able to correctly predict the effects of pavement conditions on fuel consumption, a more detailed analysis was conducted. The analysis assumes that there is no interaction between the effects of roughness and surface texture and that, in most cases, PCC and AC pavements exhibit similar trends in how fuel consumption increases with greater pavement roughness.

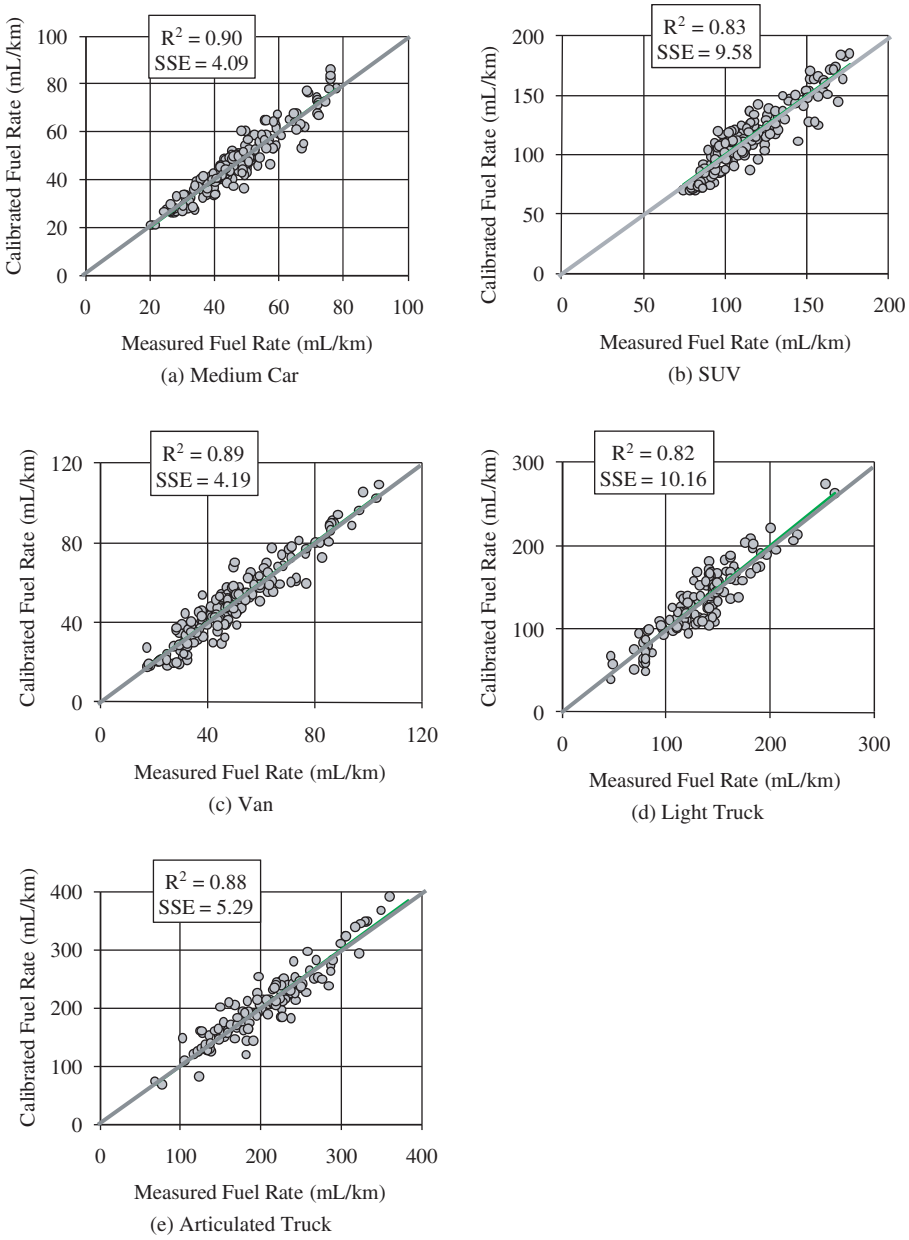

Figure 3-8. Measured versus estimated fuel consumption using HDM 4 model.

Table 3-17. Calibration coefficients and statistical performance.

Vehicle Class	*Kcr*2	*KPea*	SSE (mL/km)	Number of Data Points Considered
Medium car	0.5	0.25	4.09	456
SUV	0.58	0.56	9.58	250
Light truck	0.99	0.61	10.16	356
Van	0.67	0.49	4.19	352
Articulated truck	1.1	0.35	5.29	456

The effects of roughness and texture on fuel consumption were estimated using a detailed analysis that induced the following operations:

1. **Range discretization:** The grade data were divided into equal ranges. A width of the discretization interval of 0.1% was selected (based on the sensitivity of fuel consumption to the grade).
2. **Analysis of covariance (ANCOVA):** The grade was treated as a fixed factor, IRI and texture as covariate variables, and the fuel consumption as the dependent variable. The groups that have at least 3 points were selected for use in this analysis. A 95% confidence level is generally suitable

Table 3-18. Analysis of covariance results for all vehicles.

Vehicle Class	Speed (km/h)	Summer					Winter				
		Significance (p-value)*				Number of Data Points	Significance (p-value)*				Number of Data Points
		IRI	MPD	Grade	Lack of Fit		IRI	MPD	Grade	Lack of Fit	
Medium car	56	0.00	0.54	0.00	0.77	136	0.00	0.81	0.00	0.61	136
	72	0.00	0.22	0.00	0.78	146	0.00	0.13	0.00	0.56	146
	88	0.00	0.90	0.00	0.75	136	0.00	0.84	0.00	0.78	136
Van	56	0.00	0.35	0.00	0.96	136	0.00	0.83	0.00	0.79	136
	72	0.00	0.38	0.00	0.68	146	0.00	0.21	0.00	0.97	146
	88	0.00	0.29	0.00	0.77	136	0.00	0.22	0.00	0.78	136
SUV	56	0.00	0.20	0.00	0.75	136	0.00	0.61	0.00	0.86	136
	72	0.00	0.40	0.00	0.86	146	0.00	0.83	0.00	0.91	146
	88	0.00	0.70	0.00	0.71	136	0.00	0.35	0.00	0.88	136
Light truck	56	0.00	0.50	0.00	0.79	136	0.00	0.96	0.00	0.75	136
	72	0.00	0.60	0.00	0.75	146	0.00	0.40	0.00	0.86	146
	88	0.00	0.10	0.00	0.77	136	0.00	0.72	0.00	0.71	136
Articulated truck	56	0.00	0.03	0.00	0.79	137	No tests were conducted in winter.				
	72	0.00	0.06	0.00	0.97	146					
	88	0.00	0.07	0.00	0.78	137					

*If higher than 5%, the mean difference is considered statistically not significant.

for scientific research. Lower confidence levels would lead to perhaps too many variables that are statistically significant and greater confidence would require more data to generate intervals of usable lengths.

First, separate analyses were conducted for summer and winter conditions and for asphalt and concrete pavement sections. The results in terms of the effect of roughness and texture were similar for both pavement types. Therefore, the data from all pavement sections were combined.

3. **Linear regression analysis:** A linear function was fitted to the data within each group of grade.

The quality of fit analysis for all vehicle classes is presented in Table 3-18. The lack of fit test showed that the selected models fit the data very well (p-value is more than 0.05). The results from the analysis showed that the effect of roughness is statistically significant for all vehicle classes. On the other hand, the effect of surface texture was only statistically significant for the articulated truck at low speed (56 km/h or 35 mph), although the p-value is close to 0.05 for higher speed.

Roughness

Table 3-18 shows that the effect of roughness is statistically significant (p-value is less than 0.05). Therefore, focus was also placed on the accuracy of the calibrated model to predict the effect of roughness. Figure 3-9 shows the change in fuel consumption (from the baseline condition of IRI = 1 m/km) as a function of IRI using the current and calibrated HDM 4 models and regression from the measured field test data. Figure 3-9a shows that the current HDM 4 underpredicts the effect of roughness on fuel consumption. Figure 3-9b shows that the calibrated HDM 4 model predicts the effect of roughness on fuel consumption reasonably well.

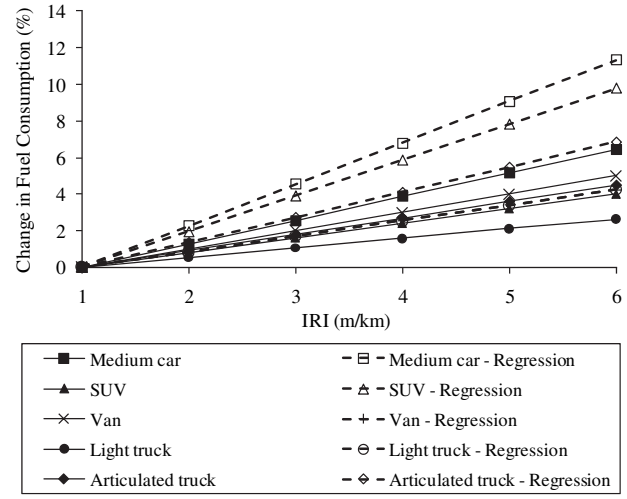

(a) Current HDM 4 model

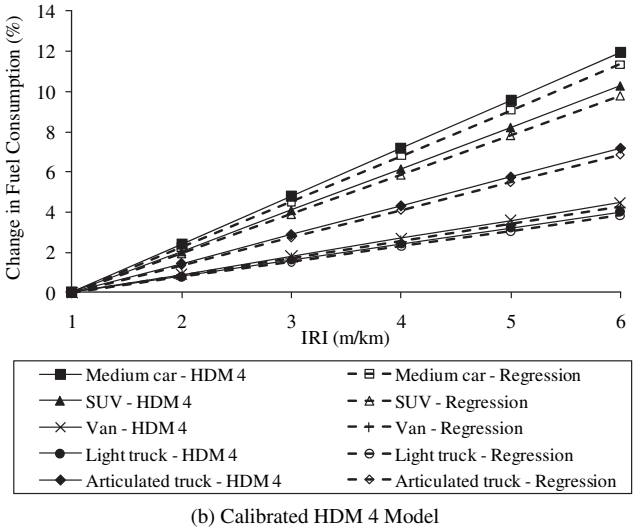

(b) Calibrated HDM 4 Model

1 m/km = 63.4 in./mi

Figure 3-9. Effect of roughness on fuel consumption at 88 km/h (55 mph).

The sensitivity analyses for the current and calibrated models (Figures 3-9a and 3-9b, respectively) at 88 km/h (55 mph) show the following increase in fuel consumption as a result of increasing IRI from 1 to 3 m/km at 30°C (86°F) when the MPD is 1 mm (0.04 in.) and grade is 0%:

- For medium car: 2.6% and 4.8% for the current and calibrated models, respectively.
- For SUV: 0.8% and 4.1% for the current and calibrated models, respectively.
- For van: 0.8% and 1.8% for the current and calibrated models, respectively.
- For light truck: 0.5% and 1.6% for the current and calibrated models, respectively.
- For articulated truck: 0.9% and 2.9% for the current and calibrated models, respectively.

Figure 3-10 shows the effect of roughness on fuel consumption for all vehicle classes at different speeds at 17°C (62.6°F) when the MPD is 1 mm (0.04 in.) and grade is 0%.

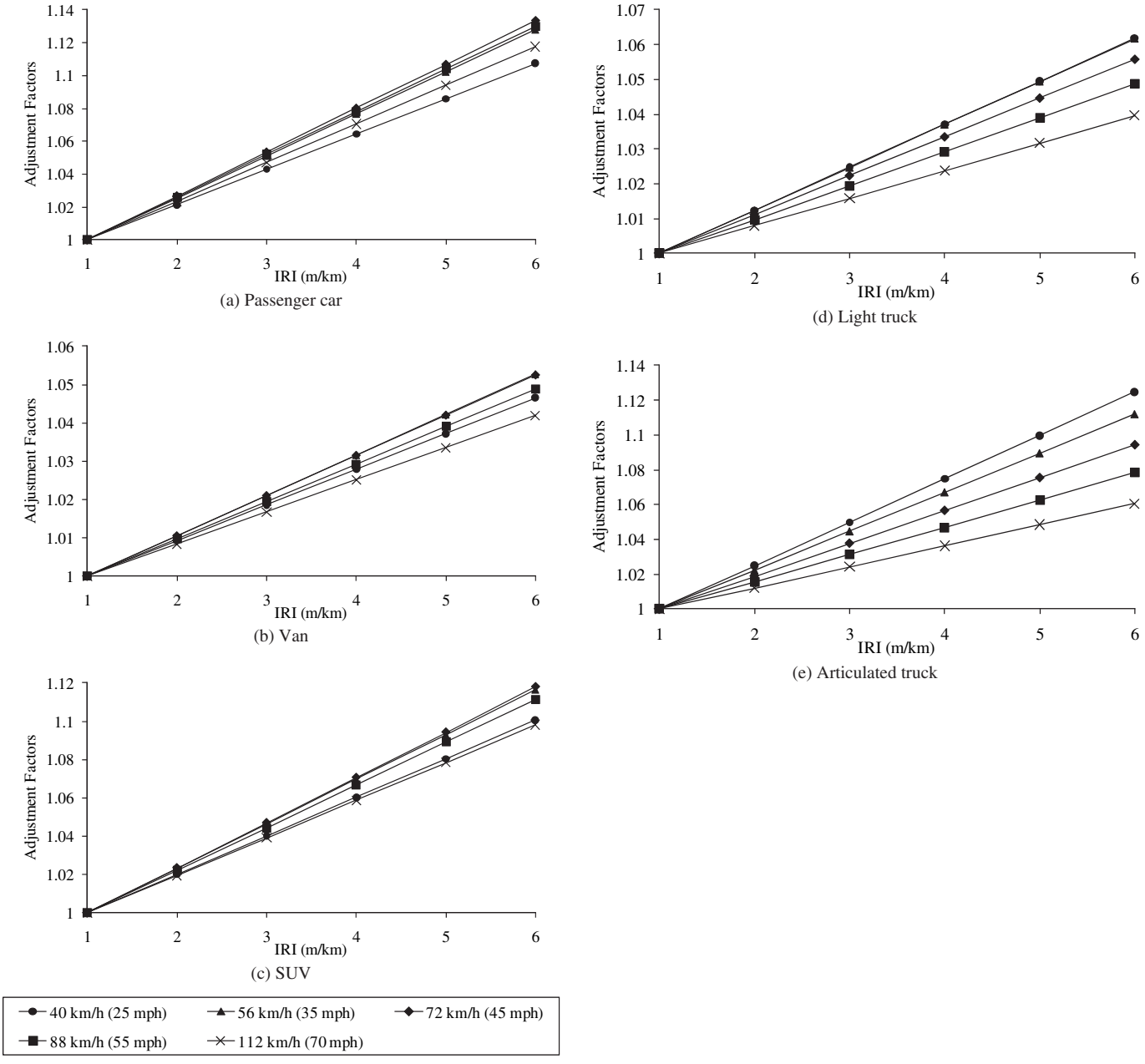

1 m/km = 63.4 in./mi.

Figure 3-10. Effect of roughness on fuel consumption estimated using calibrated HDM 4.

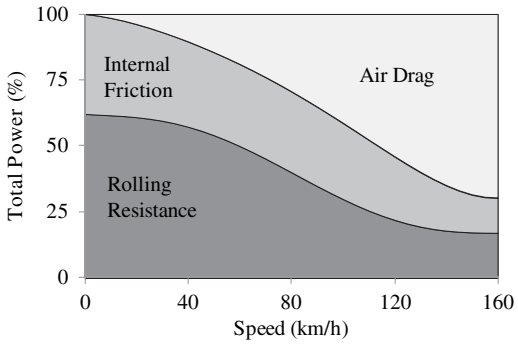

Source: adapted from Michelin (2003)

Figure 3-11. Energy distribution in a passenger car versus speed.

Texture

According to Sandberg (1990), road surface texture has a higher effect on rolling resistance at higher speeds. However, the analysis of covariance showed that the effect of texture on fuel consumption is statistically not significant at higher speeds. An explanation for these observations is that, at higher speeds, air drag becomes the largely predominant factor in fuel consumption such that the increase in rolling resistance due to texture will be masked by the increase in air drag. Figure 3-11 shows the mechanical power available by the engine as a function of the vehicle speed (no climbing, no acceleration) for passenger cars. At a constant speed of 100 km/h on a horizontal road, air drag represents 60% of energy loss while rolling resistance accounts for 25% and internal friction (drive line loss) for 15%. For a heavy truck operating at 80 km/h, approximately 12% of the fuel consumption is accounted for by the rolling resistance losses in the tires, which accounts for approximately 30% of the available mechanical power from the engine. Figure 3-12 shows the change in fuel consumption (from the baseline condition of MPD = 0.5 mm) as a function of texture using the calibrated HDM 4 model and regression. The results were generated for a vehicle speed of 56 and 88 km/h (35 and 55 mph) at 30°C (86°F) when IRI is 1 m/km (63.4 in./mi) and grade is 0%. The figure shows that the calibrated HDM 4 model predicts the effect of texture on fuel consumption reasonably well.

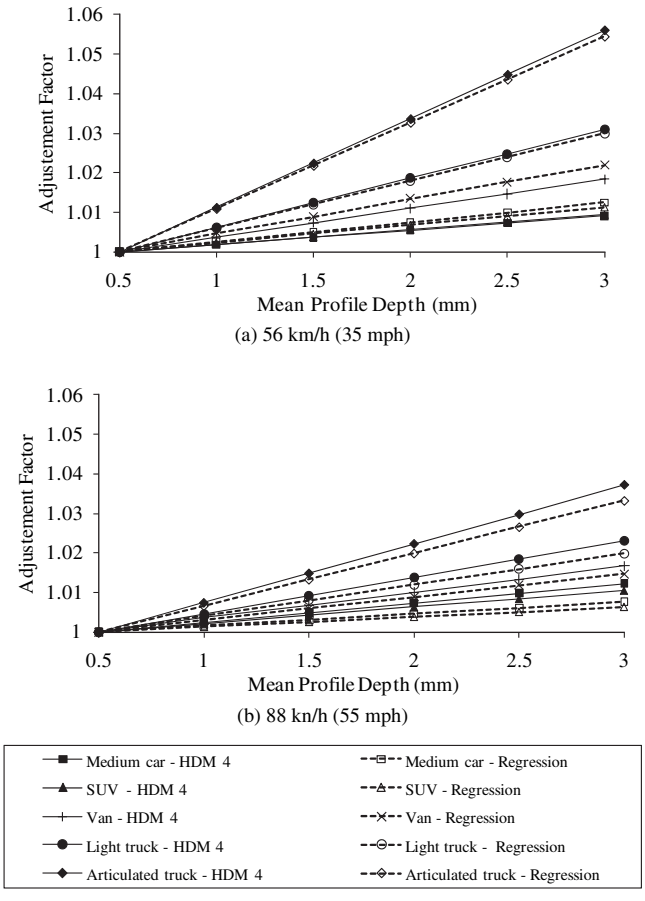

1 mm = 0.04 in.

Figure 3-12. Effect of surface texture on fuel consumption.

Summary

The analysis presented in this chapter shows that the HDM 4 fuel consumption model, after appropriate calibration, adequately predicts the fuel consumption of five different vehicle classes under different operating, weather, and pavement conditions. Also, because the key characteristics of representative vehicles used in the current HDM 4 model vary substantially from those used in the United States, the current model (i.e., without calibration) predicted lower fuel consumption than actually consumed. Table 3-19 summarizes the predictions using the current and the calibrated HDM 4 model.

The analysis of covariance of the data collected during the field test showed that the effect of surface texture is statistically significant at 95 percent confidence interval only for heavier trucks and at low speed. An explanation of this observation is that, at higher speeds, air drag becomes the largely predominant factor in fuel consumption. The increase in rolling resistance (i.e., fuel consumption) due to texture is masked by the increase in air drag due to speed.

The calibrated HDM 4 fuel consumption model is listed in Tables 3-20 through 3-25.

Table 3-19. Effect of roughness on fuel consumption.

Speed	Vehicle Class	Calibrated HDM 4 model						Current HDM 4 model					
		Base (mL/km)	Adjustment factors from the base value					Base (mL/km)	Adjustment factors from the base value				
		IRI (m/km)						IRI (m/km)					
		1	2	3	4	5	6	1	2	3	4	5	6
56 km/h (35 mph)	Medium car	70.14	1.03	1.05	1.08	1.10	1.13	81.83	1.01	1.03	1.04	1.05	1.06
	Van	76.99	1.01	1.02	1.03	1.04	1.05	94.8	1.01	1.02	1.03	1.04	1.05
	SUV	78.69	1.02	1.05	1.07	1.09	1.12	96	1.01	1.02	1.02	1.03	1.04
	Light truck	124.21	1.01	1.02	1.04	1.05	1.06	159.1	1.01	1.01	1.02	1.02	1.03
	Articulated truck	273.41	1.02	1.04	1.07	1.09	1.11	425	1.01	1.02	1.03	1.04	1.04
88 km/h (55 mph)	Medium car	83.38	1.03	1.05	1.08	1.10	1.13	76.60	1.01	1.03	1.04	1.05	1.06
	Van	96.98	1.01	1.02	1.03	1.04	1.05	98.04	1.01	1.02	1.03	1.04	1.05
	SUV	101.29	1.02	1.04	1.07	1.09	1.11	103.12	1.01	1.02	1.02	1.03	1.04
	Light truck	180.18	1.01	1.02	1.03	1.04	1.05	187.06	1.01	1.01	1.02	1.02	1.03
	Articulated truck	447.31	1.02	1.03	1.05	1.06	1.08	420.09	1.01	1.02	1.03	1.04	1.04
112 km/h (70 mph)	Medium car	107.85	1.02	1.05	1.07	1.09	1.12	87.64	1.01	1.03	1.04	1.05	1.06
	Van	128.96	1.01	1.02	1.03	1.03	1.04	115	1.01	1.02	1.03	1.04	1.05
	SUV	140.49	1.02	1.04	1.06	1.08	1.10	124	1.01	1.02	1.02	1.03	1.04
	Light truck	251.41	1.01	1.02	1.02	1.03	1.04	250.5	1.01	1.01	1.02	1.02	1.03
	Articulated truck	656.11	1.01	1.02	1.04	1.05	1.06	584.7	1.01	1.02	1.03	1.04	1.04

$$\text{mpg} = \frac{2352}{\text{mL/km}}$$

Table 3-20. Calibrated HDM 4 fuel consumption model.

Name	Description	Unit
Fuel Consumption (FC)	$FC = \frac{1000}{\upsilon} * \left(\max\left(\alpha, \xi * Ptot * (1 + dFuel)\right)\right)$	mL/km
υ	Vehicle speed	m/s
α	Fuel consumption at idling (Table 3-22)	mL/s
Engine efficiency (ξ)	$= \xi_b \left(1 + ehp \frac{\left(P_{tot} - P_{eng}\right)}{P\max}\right)$	mL/kW/s
ξ_b	Engine efficiency (depends on the technology type: gasoline versus diesel) (Table 3-22)	mL/kW/s
Pmax	Rated engine power (Table 3-22)	kW
ehp	Engine horsepower (Table 3-22)	hp
$dFuel$	Excess fuel consumption due to congestion as a ratio (default = 0)	dimensionless
P_{eng}	Power required to overcome internal engine friction (80 percent of the engine and accessories power)	kW
Engine and accessories power ($P_{engaccs} = P_{eng} + P_{accs}$)	$P_{engaccs} = KPea * P\max * (Paccs\_a1 + (Paccs\_a0 - Paccs\_a1) * \frac{RPM - RMPIdle}{RPM100 - RPMIdle})$	kW
$KPea$	Calibration factor (Table 3-23)	dimensionless
$Paccs\_a1$	$Paccs\_a1 = \frac{-b + \sqrt{b^2 - 4 * a * c}}{2 * a}$ $\begin{cases} a = \xi_b * ehp * kPea^2 * P\max * \frac{100 - PctPeng}{100} \\ b = \xi_b * kPea * P\max \\ c = -\alpha \end{cases}$	
$Paccs\_a0$	Ratio of engine and accessories drag to rated engine power when traveling at 100 km/h (Table 3-23)	dimensionless
$PctPeng$	Percentage of the engine and accessories power used by the engine (Default = 80%)	%
Engine speed (RPM)	$RPM = a0 + a1 * SP + a2 * SP^2 + a3 * SP^3$ $SP = \max(20, v)$	rev/min
$a0$ to $a3$	Model parameter (Table 3-22)	
$RPM100$	Engine speed at 100 km/h	rev/min
$RPMIdle$	Idle engine speed (Table 3-22)	rev/min
Total power (P_{tot})	$P_{tot} = \frac{P_{tr}}{edt} + P_{accs} + P_{eng}$ for $P_{tr} \geq 0$, uphill/level $P_{tot} = edtP_{tr} + P_{accs} + P_{eng}$ for $P_{tr} < 0$, downhill	kW
edt	Drive-train efficiency factor (Table 3-22)	dimensionless
Tractive power (P_{tr})	$P_{tr} = \frac{\upsilon * \left(Fa + Fg + Fc + Fr + Fi\right)}{1000}$	kW

Table 3-21. Calibrated HDM 4 tractive forces model.

Name	Description	Unit
Aerodynamic forces (*Fa*)	$Fa = 0.5 * \rho * CD * AF * \upsilon^2$	N
CD	Drag coefficient (Table 3-23)	dimensionless
AF	Frontal area (Table 3-23)	m^2
ρ	Mass density of the air (Default = 1.2)	kg/m^3
υ	Vehicle speed	m/s
Gradient forces (*Fg*)	$Fg = M * GR * g$	N
M	Vehicle weight (Table 3-23)	kg
GR	Gradient	radians
g	Gravity (Default = 9.81)	m/s^2
Curvature forces (*Fc*)	$Fc = \max\left(0, \frac{\left(\frac{M*\upsilon^2}{R} - M*g*e\right)^2}{Nw*Cs} * 10^{-3}\right)$	N
R	curvature radius (Default=3000)	m
Superelevation (*e*)	$e = \max(0, 0.45 - 0.68 * Ln(R))$	m/m
Nw	Number of wheels (Table 3-23)	dimensionless
Tire stiffness (*Cs*)	$Cs = a0 + a1 * \frac{M}{Nw} + a2 * \left(\frac{M}{Nw}\right)^2$	kN/rad
*a*0 to *a*2	Model parameter (Table 3-24)	
Rolling resistance (F_r)	$Fr = CR2 * \left(b11 * Nw + CR1 * \left(b12 * M + b13 * \upsilon^2\right)\right)$	N
*CR*1	Rolling resistance tire factor (Table 3-25)	factor
Rolling resistance parameters (*b*11, *b*12, *b*13)	$\begin{cases} b11 = 37 * WD \\ b12 = 0.064 / WD \\ b13 = 0.012 * Nw / WD^2 \end{cases}$	parameters
WD	Wheel diameter (Table 3-23)	m
Rolling resistance surface factor (*CR*2)	$= Kcr2\left[a0 + a1 * Tdsp + a2 * IRI + a3 * DEF\right]$	factor
*Kcr*2	Calibration factor (Table 3-23)	factor
*a*0 to *a*3	Model coefficient (Table 3-23)	dimensionless
Texture depth using sand patch method (*Tdsp*)	$Tdsp = 1.02 * MPD + 0.28$	mm
MPD	Mean profile depth	mm
IRI	International roughness index	m/km
DEF	Benkelman Beam rebound deflection	mm
Inertial forces (F_i)	$Fi = M * \left(a0 + a1 * \arctan\left(\frac{a2}{\upsilon^3}\right)\right) * acc$	N
acc	Vehicle acceleration	m/s^2
*a*0 to *a*2	Model parameter (Table 3-23)	dimensionless

Table 3-22. Calibrated HDM 4 default values for engine and vehicle characteristics.

Vehicle Class	Fuel Type	Engine Speed (rpm) *a*0	*a*1	*a*2	*a*3	*RPMIdle*	α (mL/s)	ξ_b (mL/kW/s)	*ehp* (hp)	*P*max (kW)	edt	*Paccs_a*0	*PctPeng* (%)
Small car	P	720.05	0.868	0.2006	−0.0007	800	0.65	0.096	0.05	130	0.91	0.2	80
Medium car	P	720.05	0.868	0.2006	−0.0007	800	0.65	0.096	0.05	130	0.91	0.2	80
Large car	P	720.05	0.868	0.2006	−0.0007	800	0.65	0.096	0.05	130	0.91	0.2	80
Light delivery car	P	589.6	−0.5145	0.0168	0.0019	500	0.65	0.072	0.05	90	0.91	0.2	80
Light goods vehicle	P	589.6	−0.5145	0.0168	0.0019	500	0.65	0.072	0.05	90	0.91	0.2	80
Four-wheel drive	P	982.37	3.6701	−0.1331	0.0019	500	0.65	0.072	0.25	95	0.91	0.2	80
Light truck	P	550.08	−3.0722	0.3798	−0.0018	500	0.7	0.062	0.1	150	0.86	0.2	80
Medium truck	P	799.6	−5.3791	0.2077	0.00006	833.7	0.8	0.059	0.1	200	0.86	0.2	80
Heavy truck	D	799.6	−5.3791	0.2077	0.00006	833.7	0.9	0.059	0.1	350	0.86	0.2	80
Articulated truck	D	799.6	−5.3791	0.2077	0.00006	833.7	0.9	0.059	0.1	350	0.86	0.2	80
Mini bus	P	720.05	0.868	0.2006	−0.0007	500	0.48	0.096	0.25	55	0.9	0.2	80
Light bus	P	550.08	−3.0722	0.3798	−0.0018	589.6	0.48	0.062	0.1	100	0.86	0.2	80
Medium bus	D	799.6	−5.3791	0.2077	0.00006	833.7	0.7	0.059	0.1	200	0.86	0.2	80
Heavy bus	D	799.6	−5.3791	0.2077	0.00006	833.7	0.8	0.059	0.1	350	0.86	0.2	80
Coach	D	799.6	−5.3791	0.2077	0.00006	833.7	0.9	0.059	0.1	350	0.86	0.2	80

P = petroleum; D = diesel

Table 3-23. Calibrated HDM 4 default values for tire and vehicle characteristics.

Vehicle Class	Number of Axles	CD	AF (m^2)	*NW*	M (tons)	*WD* (m)	Tire Type	*CR*1	*b*11	*b*12	*b*13	Effect Mass Ratio Model Coefficients			*Kcr*2	*KPea*
												*a*0	*a*1	*a*2		
Small car	2	0.42	2.16	4	1.9	0.62	Radial	1	22.2	0.11	0.13	1.05	0.213	1260.7	0.5	0.25
Medium car	2	0.42	2.16	4	1.9	0.62	Radial	1	22.2	0.11	0.13	1.05	0.213	1260.7	0.5	0.25
Large car	2	0.42	2.16	4	1.9	0.62	Radial	1	22.2	0.11	0.13	1.05	0.213	1260.7	0.5	0.25
Light delivery car	2	0.5	2.9	4	2.54	0.7	Radial	1	25.9	0.09	0.10	1.1	0.891	244.2	0.67	0.49
Light goods vehicle	2	0.5	2.9	4	2.54	0.7	Radial	1	25.9	0.09	0.10	1.1	0.891	244.2	0.67	0.49
Four-wheel drive	2	0.5	2.8	4	2.5	0.7	Radial	1	25.9	0.09	0.10	1.1	0.891	244.2	0.58	0.56
Light truck	2	0.6	5	4	4.5	0.8	Radial	1	29.6	0.08	0.08	1.04	0.83	12.4	0.99	0.61
Medium truck	2	0.6	5	6	6.5	0.8	Bias	1.3	29.6	0.08	0.11	1.04	0.83	12.4	0.99	0.61
Heavy truck	3	0.7	8.5	10	13	1.05	Bias	1.3	38.85	0.06	0.11	1.07	1.91	10.1	1.1	0.35
Articulated truck	5	0.8	9	18	13.6	1.05	Bias	1.3	38.85	0.06	0.20	1.07	1.91	10.1	1.1	0.35
Mini bus	2	0.5	2.9	4	2.16	0.7	Radial	1	25.9	0.09	0.10	1.1	0.891	244.2	0.67	0.49
Light bus	2	0.5	4	4	2.5	0.8	Radial	1	29.6	0.08	0.08	1.1	0.891	244.2	0.99	0.61
Medium bus	2	0.6	5	6	4.5	1.05	Bias	1.3	38.85	0.06	0.07	1.04	0.83	12.4	0.99	0.61
Heavy bus	3	0.7	6.5	10	13	1.05	Bias	1.3	38.85	0.06	0.11	1.04	0.83	12.4	1.1	0.35
Coach	3	0.7	6.5	10	13.6	1.05	Bias	1.3	38.85	0.06	0.11	1.04	0.83	12.4	1.1	0.35

Table 3-24. Final parameters for tire stiffness (*Cs*) model.

Coefficient	≤ 2500 kg		> 2500 kg	
	Bias	Radial	Bias	Radial
*a*0	30	43	8.8	0
*a*1	0	0	0.088	0.0913
*a*2	0	0	–0.0000225	–0.0000114

Source: Bennett and Greenwood (2003b)

Table 3-25. Final parameters for rolling resistance coefficient (*CR*2) model.

Surface Type	≤ 2500 kg				> 2500 kg			
	*a*0	*a*1	*a*2	*a*3	*a*0	*a*1	*a*2	*a*3
Asphalt	0.5	0.02	0.1	0	0.57	0.04	0.04	1.34
Concrete	0.5	0.02	0.1	0	0.57	0.04	0.04	0

Source: Bennett and Greenwood (2003b)

CHAPTER 4

Tire Wear Model

This chapter describes the research approach used for developing the appropriate models to estimate the effects of pavement condition on tire wear. The most recent tire wear model found in the literature is the mechanistic–empirical model found in HDM 4 (Bennett and Greenwood, 2003b). This model was calibrated to US conditions using truck tire wear data collected from NCAT and from field trials conducted in this project for a passenger car.

HDM 4 Tire Wear Model

The general form of the tire consumption model is the following:

$$TC = \frac{NW * EQNT}{MODFAC} \quad (4.1)$$

where:

TC = Tire consumption per vehicle (%/km)
Nw = Number of wheels
$EQNT$ = Equivalent new tire (%/km)
$MODFAC$ = Tire life modification factor

Tables 4-1 through 4-3 summarize the HDM 4 tire wear model (Bennett and Greenwood, 2003b). Tire wear is a function of the normal, lateral, and circumferential forces applied on the tire. The latter include the aerodynamic, gradient, and rolling resistance forces. These forces are functions of vehicle characteristics, pavement conditions, and climate. Bennett and Greenwood (2003b) noted that, when testing the model, the values for C_{0tc} (tire wear rate constant) were found to be too low and resulted in an unreasonably high tire life. Therefore, an interim model was adopted for HDM 4. A constant was added to the EQNT equation in Table 4-1, which becomes as follows:

$$EQNT = \frac{1}{10} \times \left(\frac{TWT}{VOL} + 0.0027 \right) \quad (4.2)$$

where:

$EQNT$ = Equivalent new tire (%/km)
TWT = Total tire wear (dm³/1000 km)
VOL = Tire volume (dm³)

Data Collection

Articulated Truck Tire Wear: NCAT Test Track Data

Four tractor-trailer assemblies applied traffic to the NCAT track. Each tractor (13.6 metric tons or 30,000 lbs) towed three 2-axle trailers, each loaded to 18.2 metric tons (40,000 lbs) resulting in a GVW of 68 metric tons (150,000 lbs) (Brown et al., 2002). The truck configuration is shown in Figure 4-1; this configuration applies approximately 10 equivalent single-axle loads (ESALs) per pass. The tractor-trailer assemblies were driven at 72 km/h (45 mph) around the track for 18 hours a day, 6 days a week, for 2 years.

Figure 4-2 shows the NCAT track configuration. The track consists of two tangent sections connected by two spiral curves. The north–south straight sections on the NCAT track are precisely 0.8 km (2,600 ft long: 13 sections of 200 ft in each direction), connected with two spiral sections approximately 0.6 km (2,000 ft in length: 10 sections of 200 ft in each direction). The east curve profile travels down a –0.5% grade, while the west curve profile travels up a +0.5% grade. The maximum superelevation of both curves is 15%. The profiles of both the north and south straight sections are level with 2% normal cross slopes. Thus, of each duty cycle, about 60% is on level pavement (with 2% cross slope), 15% on up grade, and 15% on down grade (with 15% superelevation). Figures 4-3 and 4-4 show the pavement roughness and mean profile texture, respectively, provided by NCAT.

The data collected by NCAT showed that the average life of truck tires are 148,563 km (92,852 mi) for drive/trailer

Table 4-1. HDM 4 tire consumption model.

Name	Description	Unit
Number of equivalent new tires (*EQNT*)	$EQNT = \frac{TWT}{10 \times VOL}$	%/km
VOL	= Tire volume	dm^3
Total change in tread wear (*TWT*)	$TWT = C_{0tc} + C_{tcte} \times \frac{CFT^2 + LFT^2}{NFT}$ $TWT = C_{0tc} + C_{tcte} \times TE$	dm^3/1000 km
C_{0tc}	= Tread wear rate constant (Table 4-3)	dm^3/1000 km
C_{tcte}	= Tread wear coefficient (Table 4-3)	dm^3/MNm
The tire energy (*TE*)	$TE = \frac{CFT^2 + LFT^2}{NFT}$	MNm/1000 km
The circumferential force on the tire (*CFT*)	$CFT = \frac{(1+CTCON * dFUEL) * (Fa + Fr + Fg)}{NW}$	N
CTCON	= Incremental change of tire consumption related to congestion	ratio
dFUEL	= Incremental change of fuel consumption related to congestion	ratio
Fa	= Aerodynamic forces	N
Fr	= Rolling resistance forces	N
Fg	= Gradient forces	N
The lateral force on the tire (*LFT*)	$LFT = \frac{Fc}{NW}$	N
Fc	= Curvature forces	N
Nw	= Number of wheels	dimensionless
The normal force on the tire (*NFT*)	$NFT = \frac{M * g}{NW}$	N
M	= Vehicle mass	kg
g	= Gravity	m/s^2

tires and 75,906 km (47,442 mi) for steer tires. These data were converted to tire wear rates assuming standard truck tires with tread depth of 23.8 mm initially (0.94 in.), and that the tires were replaced when the tread depth was 3.2 mm or 0.13 in. (according to tire manufacturers recommendation). The cumulative distribution of tire wear for each tire type was calculated, as shown in Figure 4-5. The range of data (25th to 75th percentile) is taken as the useful range, as shown in Figure 4-6. These data reveal that the range in truck tire wear rates is 0.0006%/km to 0.0021%/km (0.0009%/mi to 0.0034%/mi).

Passenger Cars: Field Trials

To validate the HDM 4 tire wear model for passenger cars, field tests were conducted using vehicles driven over long distances. Two different roads (I-69 and M-99) from the sections used during the fuel consumption field tests were selected based on the variability level of their pavement conditions (i.e., roughness, gradient, texture, and pavement type). Information on passenger car tire life collected from tire manufacturers was used to estimate the minimum length of test sections sufficient to establish tire wear rates. Table 4-4 summarizes the conditions of the test sections. Five field tests were conducted on M-99 (Trials 1 through 5) and two tests were conducted on I-69 (Trials 1 and 2). Measurements were repeated for Trial 1 on I-69 (Measurements 1 through 3).

A 2008 Chevrolet Malibu (1.69 metric tons or 3,732 lb) with front-wheel drive and typical passenger car (radial) tires was used in the field tests (model P215/60R17). The tire pressure was kept at the manufacturer's recommended value (207 kPa or 30 psi). Tire wear was investigated in the left front (LF), the right rear (RR), and the left rear (LR) tires. The initial tread depths at time of testing were 7.14 mm (9/32 in.) for the LF tire, 5.55 mm (7/32 in.) for the RR tire, and 7.23 mm (9/32 in.) for the LR tire. Test tires were driven only on the test sections; replacements tires were used while driving between the laboratory (where the measurement apparatus is) and the test sections. For tire tread depth measurement, the tires were mounted on a tire balancer, which allowed the tires to freely rotate so that measurements could be made at multiple points around the tire circumferences. A laser-based data acquisition system with accuracy of 4 microns, which was attached to the balancer, was used to measure tread depth.

The vehicle's tire tread depth (TD_0) and pressure (P_0) were measured before the start of the tests and after the

Table 4-2. HDM 4 tractive forces model.

Name	Description	Unit
Aerodynamic forces (*Fa*)	$Fa = 0.5 * \rho * CDmult * CD * AF * \upsilon^2$	N
CD	Drag coefficient	dimensionless
CDmult	CD multiplier	dimensionless
AF	Frontal area	m^2
ρ	Mass density of the air	kg/m^3
υ	Vehicle speed	m/s
Gradient forces (*Fg*)	$Fg = M * GR * g$	N
M	Vehicle weight	kg
GR	Gradient	radians
g	Gravity	m/s^2
Curvature forces (*Fc*)	$Fc = \max\left(0, \frac{\left(\frac{M*\upsilon^2}{R} - M*g*e\right)^2}{Nw*Cs} * 10^{-3}\right)$	N
R	curvature radius	m
Superelevation (*e*)	$e = \max(0, 0.45 - 0.68 * Ln(R))$	m/m
Nw	Number of wheels	dimensionless
Tire stiffness (*Cs*)	$Cs = KCS * \left[a0 + a1 * \frac{M}{Nw} + a2 * \left(\frac{M}{Nw}\right)^2\right]$	kN/rad
KCS	Calibration factor	factor
*a*0 to *a*2	Model parameter (Table 3-28)	dimensionless
Rolling resistance (*Fr*)	$Fr = CR2 * FCLIM * \left(b11 * Nw + CR1 * \left(b12 * M + b13 * \upsilon^2\right)\right)$	N
*CR*1	Rolling resistance tire factor	factor
Rolling resistance parameters (*b*11, *b*12, *b*13)	$b11 = 37 * Dw$ $b12 = \begin{cases} 0.067/Dw & old\ \ tires \\ 0.064/Dw & latest\ \ tires \end{cases}$ $b12 = 0.012 * Nw / Dw^2$	factors
Dw	Diameter of wheel	
Rolling resistance surface factor (CR2)	$= Kcr2\left[a0 + a1 * Tdsp + a2 * IRI + a3 * DEF\right]$	factor
*Kcr*2	Calibration factor	factor
*a*0 to *a*3	Model coefficient (Table 3-28)	dimensionless
Tdsp	Texture depth using sand patch method	mm
IRI	International roughness index	m/km
DEF	Benkelman Beam rebound deflection	mm
Climatic factor (*FCLIM*)	$FCLIM = 1 + 0.003 * PCTDS + 0.002 * PCTDW$	dimensionless

vehicle was finished with the loops (TD_{final} and P_{final}). The tire wear was calculated as the difference between TD_0 and TD_{final}. Because the accuracy of the measurement is highly sensitive to tire pressure, it was ensured that P_0 and P_{final} were the same prior to computing the difference tread depth. The tread depth was measured in two different positions along the cross section of the tire as shown in Figure 4-7. For each position, the tread depth was also measured in 30 different cells along the longitudinal direction of the tire as shown in Figure 4-8.

Table 4-5 summarizes the data collected from tire manufacturers. Based on these data, a passenger car tire incurs 0.1 mm (0.004 in.) of tread wear after the vehicle is driven at constant speed for 1,040 km (650 mi). However, according to the Uniform Tire Quality Grading Standards (UTQGS), the vehicle should be driven for at least 2560 km (1,600 mi) to measure a reliable tire wear value. Based on the detailed statistical analysis conducted as part of this study (Appendix B), the selected distance travelled by the vehicle during the field tests was 4,000 km (2,500 mi).

The accumulated tire wear data for all trials were first normalized to 4,000 km (2,500 mi) for comparison purposes. The data for all cells were used to allow calculating the cumulative distribution of the tire wear across the

Table 4-3. Tread wear rate constants.

Vehicle type	C_{0tc} (dm^3/1000 km)	C_{tcte} (dm^3/MNm)
Motorcycle	0.00639	0.0005
Small car	0.02616	0.00204
Medium car	0.02616	0.00204
Large car	0.02616	0.00204
Light delivery car	0.024	0.00187
Light goods vehicle	0.024	0.00187
Four-wheel drive	0.024	0.00187
Light truck	0.024	0.00187
Medium truck	0.02585	0.00201
Heavy truck	0.03529	0.00275
Articulated truck	0.03988	0.00311
Mini bus	0.024	0.00187
Light bus	0.02173	0.00169
Medium bus	0.02663	0.00207
Heavy bus	0.03088	0.00241
Coach	0.03088	0.00241

Source: Bennett and Greenwood (2003b)

longitudinal direction, as shown in Figure 4-9. The data in the 25th to 75th percentile range were used to perform the calibration of the HDM 4 model; these data are shown in Figure 4-10.

Calibration of the HDM 4 Tire Wear Model

When the HDM 4 model was developed, it was calibrated using tire replacement data. Therefore, the following assumptions were made during the calibration:

- For passenger cars: The average wear rates of the front and rear tire were used for calculating overall tire wear rate, because tires are generally rotated every 6 months or so.
- For trucks: Only tire wear data for drive or trailer tires were used.

Source: NCAT (2010)

Figure 4-1. NCAT test track vehicle.

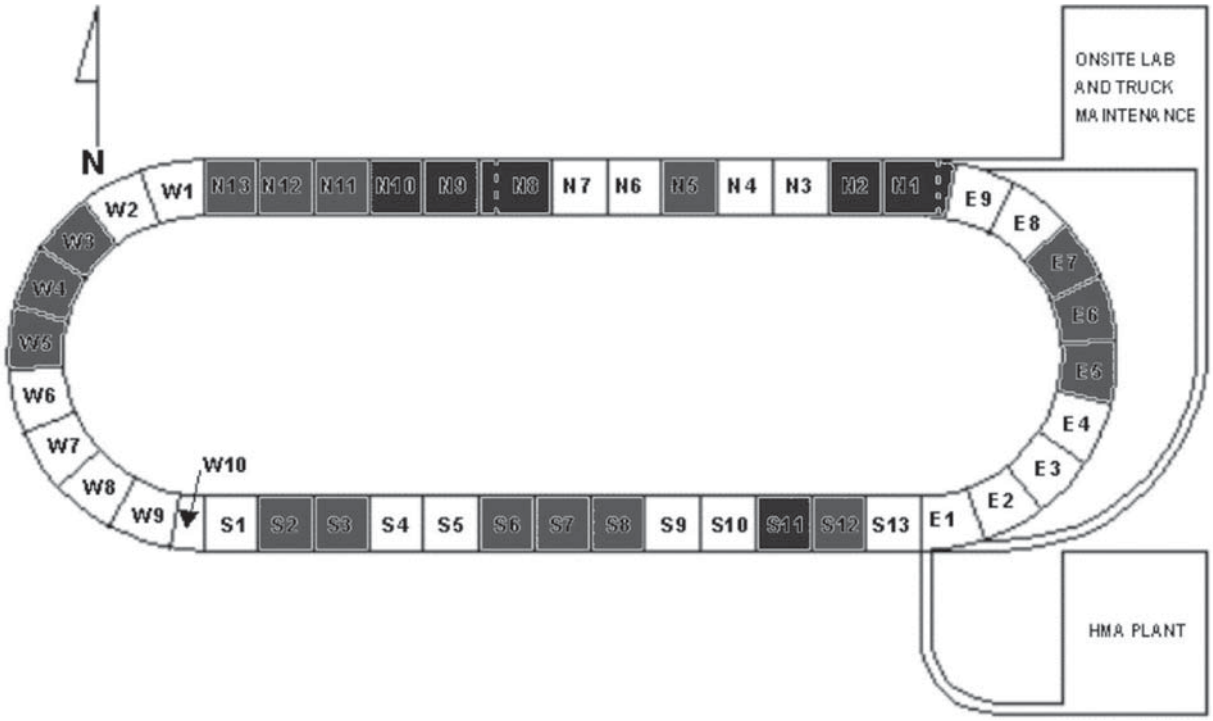

Source: NCAT (2010)

Figure 4-2. NCAT track layout and configuration.

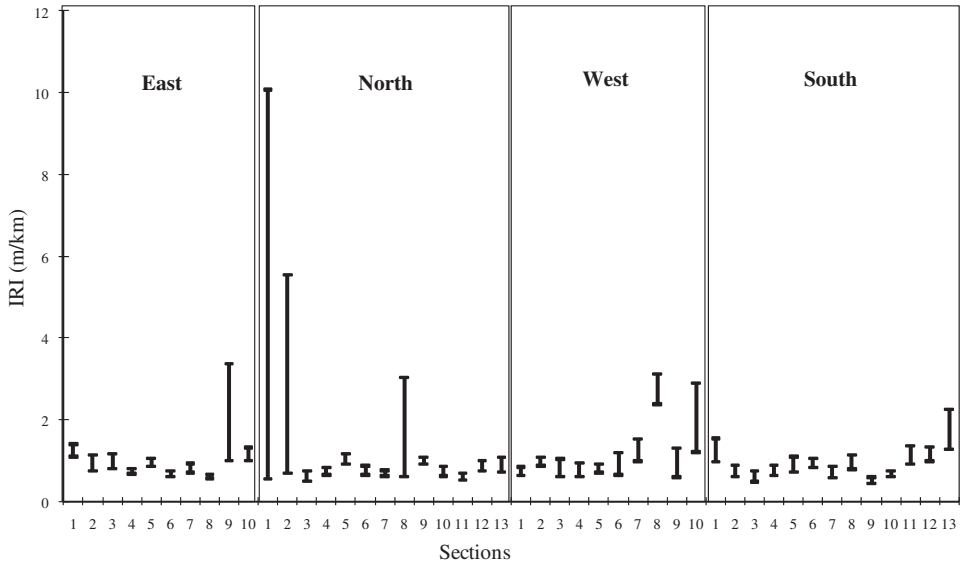

Source: Data provided by NCAT

Figure 4-3. NCAT track roughness data.

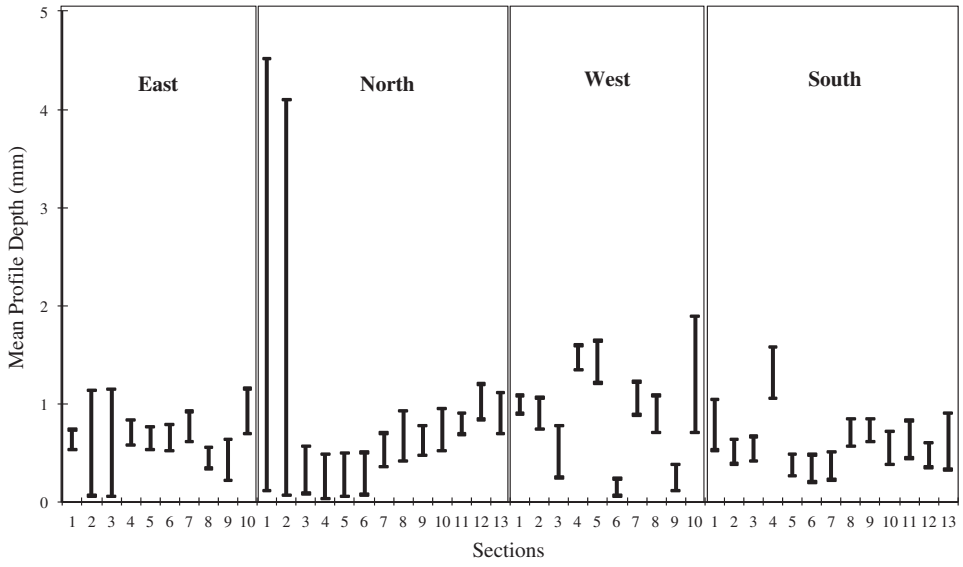

Source: Data provided by NCAT

Figure 4-4. NCAT track texture data.

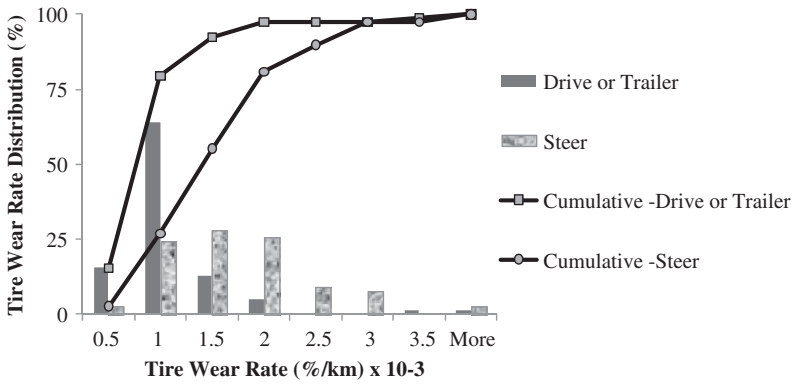

1%/km = 1.6%/mi

Figure 4-5. Cumulative distribution of tire wear data collected from NCAT.

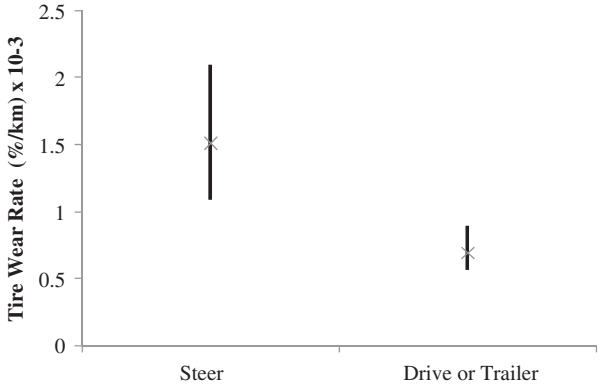

Figure 4-6. Tire wear data used for calibration.

Because tire wear data were collected only for articulated trucks and passenger cars, the calibration was only performed for these two vehicle classes. The passenger car tire wear data obtained on I-69 and the NCAT truck tire wear data were used to calibrate the HDM 4 passenger car and articulated truck tire wear models, respectively.

The calibration procedure was as follows:

1. The road surface calibration factor *Kcr*2 (Table 4-1) was assigned the same value obtained during the calibration of the HDM 4 fuel consumption model (Table 3-1).
2. The constant from Equation 4.2 (0.0027) was removed.
3. The optimal values for C_{0tc} was calculated using the data obtained from tire manufacturers for passenger cars and articulated trucks (Table 4-5).
4. The optimal values for C_{tcte} were estimated by minimizing the SSE between the observed field values and those predicted using the HDM 4 model.
5. The optimal values for C_{0tc} and C_{tcte} for the remaining vehicle classes were estimated using Equations 4.3 and 4.4 and assuming that the ratios between the values reported in the HDM 4 (Table 4-5) between vehicle categories are acceptable:
   - For small and large cars, vans, SUVs, light trucks, minibuses, and light buses:

$$C_{0tc}^{new} = \frac{C_{0tc}^{old}}{C_{0tc}^{old}(\text{Passenger Car})} \times C_{0tc}^{new}(\text{Passenger Car})$$
$$C_{tcte}^{new} = \frac{C_{tcte}^{old}}{C_{tcte}^{old}(\text{Passenger Car})} \times C_{tcte}^{new}(\text{Passenger Car}) \quad (4.3)$$

   - For medium and heavy trucks, medium and heavy buses, and coaches:

$$C_{0tc}^{new} = \frac{C_{0tc}^{old}}{C_{0tc}^{old}(\text{Articulated Truck})} \times C_{0tc}^{new}(\text{Articulated Truck})$$
$$C_{tcte}^{new} = \frac{C_{tcte}^{old}}{C_{tcte}^{old}(\text{Articulated Truck})} \times C_{tcte}^{new}(\text{Articulated Truck}) \quad (4.4)$$

Where:

C_{0tc}^{new} = Calibrated tread wear rate constant
C_{0tc}^{old} = Current HDM 4 tread wear rate constant
C_{tcte}^{new} = Calibrated tread wear rate coefficient
C_{tcte}^{old} = Current HDM 4 tread wear rate coefficient

Table 4-6 summarizes the new coefficients for the tire wear model. For example, the C_{0tc} and C_{tcte} values for heavy trucks are:

$$C_{0tc}^{new}(\text{HeavyTruck}) = 0.03529 \times 0.04328/0.03988 = 0.03829\ \text{dm}^3/1000\ \text{km}$$
$$C_{tcte}^{new}(\text{HeavyTruck}) = 0.00275 \times 0.00153/0.00311 = 0.00135\ \text{dm}^3/\text{MNm}$$

While, the I-69 tire wear data were used to calibrate the current HDM 4 tire wear model, the M-99 tire wear data were used to validate the newly calibrated HDM 4 model. Figure 4-11 presents the results of the calibration and validation processes.

Table 4-4. Tire wear field test matrix.

Road	Start	End	Pavement Type		Texture Depth (mm)	IRI Range (m/km)	Length (km)	Speed (km/h)
			AC	PCC				
M-99 S	Bishop Rd	Holt Hwy		X	0.25–2.7	0.8–4.8	3.6	80
M-99 S	Holt Hwy	Columbia Hwy		X			6.4	80
M-99 N	Columbia Hwy	Holt Hwy	X		0.23–1.85	0.5–4.1	6.4	80
M-99 N	Holt Hwy	Diamondale Rd	X				1.6	80
M-99 N	Diamondale Rd	Waverly Rd		X			0.8	80
M-99 N	Waverly Rd	Bishop Rd		X			2.1	80
I-69E	Airport Rd	Francis Rd		X	0.3–0.75	0.8–3.8	4.8	96
I-69W	Francis Rd	Airport Rd		X	0.2–1.25	1.1–3.1	4.8	96

1 in. = 25.4 mm; 1 m/km = 63.4 in./mi; 1 mi = 1.6 km; 1 mph = 1.6 km/h

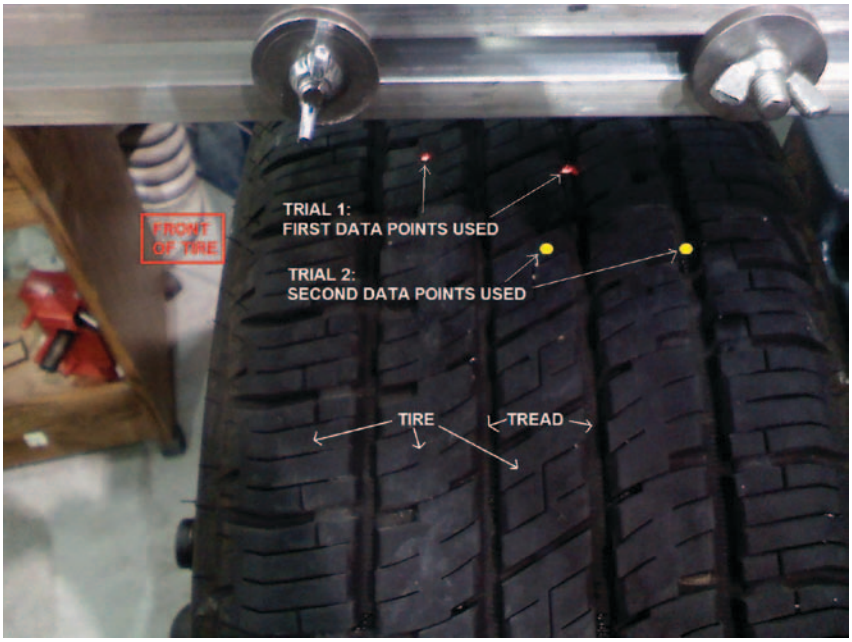

Figure 4-7. Locations of tread depth measurements of the tire cross section.

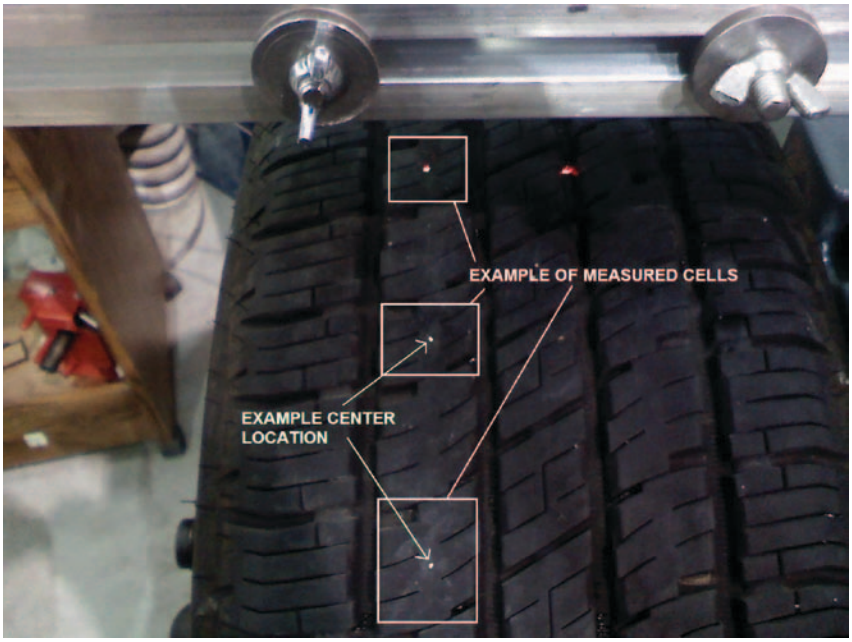

Figure 4-8. Locations of tread depth measurements in the longitudinal direction.

Table 4-5. Tire tread depth and life data.

Vehicle Class	Tire Information[a]			Tire Life		
	New Tire Tread Depth [mm (in.)]	Tire Tread Depth Limit [mm (in.)]	Tire Volume [dm^3 (ft^3)]	New Tire [km (mi)]	After First Recap [km (mi)]	After Second Recap [km (mi)]
Passenger cars	7.94 (10/32)	1.6 (2/32)	1.4 (0.049)	64,000[a] (40,000)	No recaps	
Heavy trucks	23.81 (30/32)	3.2 (4/32)	8 (0.283)	160,000[a] (100,000)	128,000[a,b,c] (80,000)	64,000[a,b,c] (40,000)

[a]Tire manufacturers
[b]Tire Retread and Repair Information Bureau (TRIB)
[c]These values are not considered in calculating the average tire wear rate
1 mi = 1.6 km

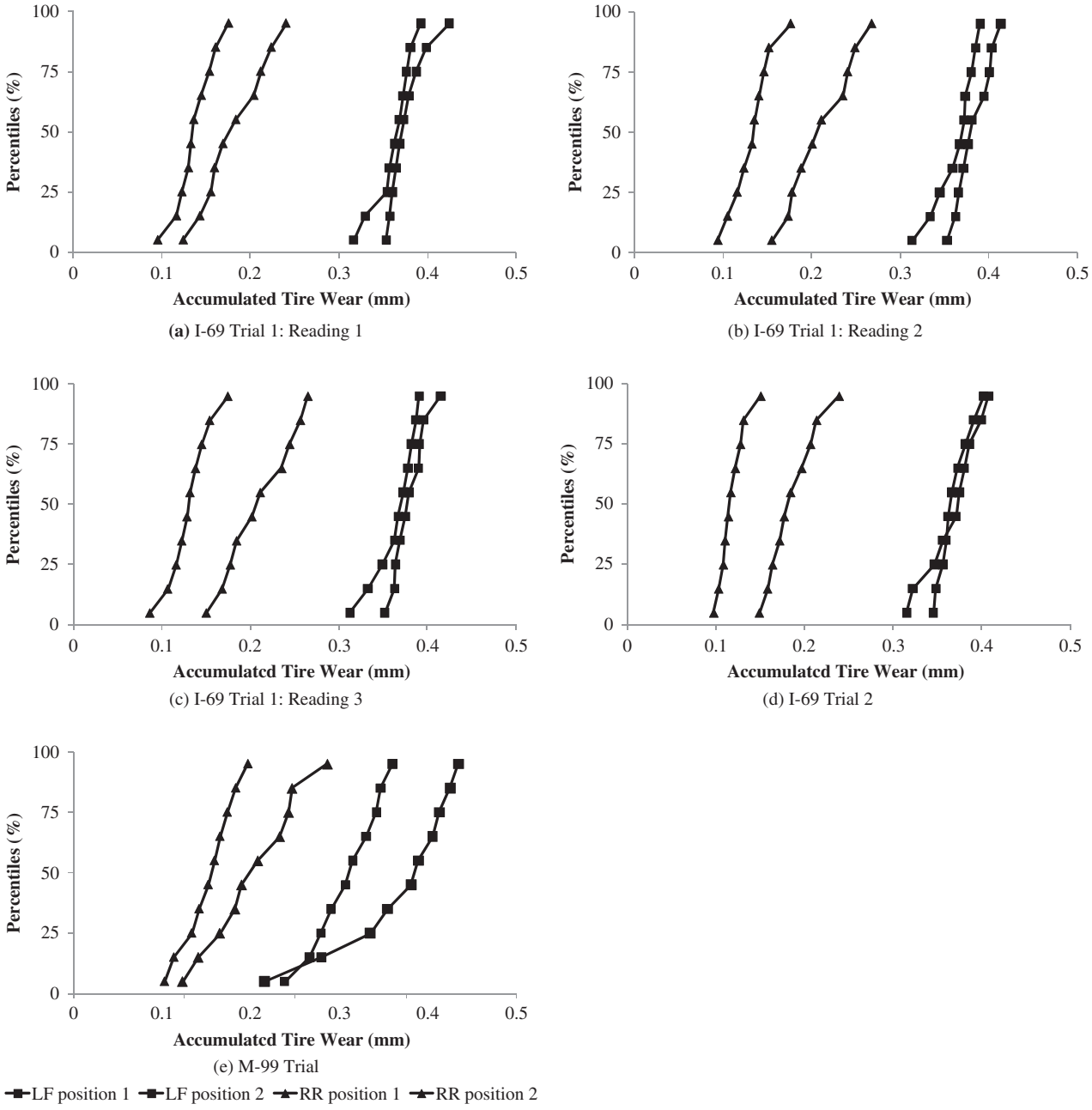

Figure 4-9. Cumulative distribution of tire wear data for a passenger car.

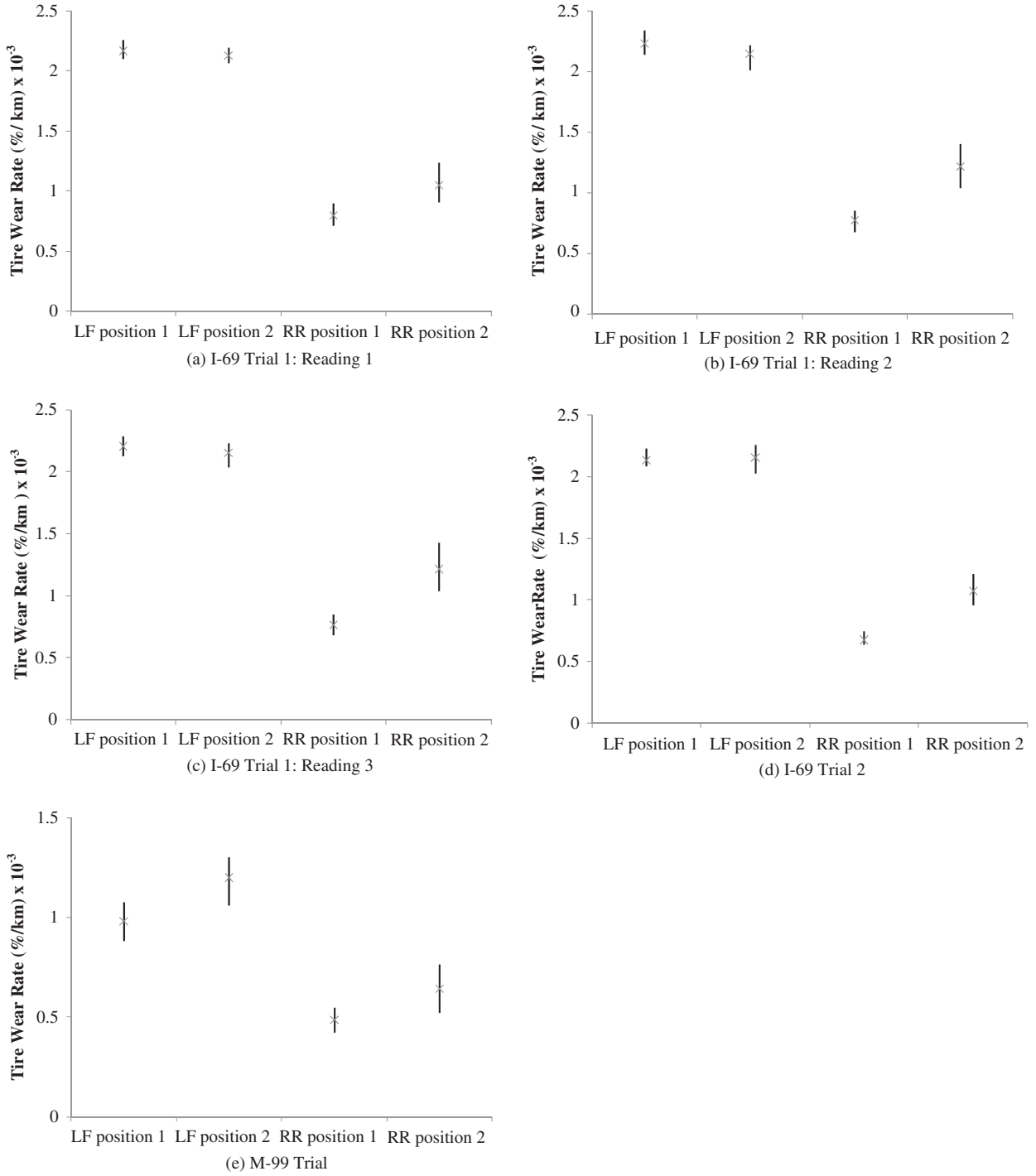

Figure 4-10. Tire wear data used for calibration for a passenger car.

Table 4-6. Calibrated tread wear rate constants and coefficients.

Vehicle Type	C_{0tc} (dm^3/1000 km)	C_{tcte} (dm^3/MNm)
Small car	0.01747	0.001
Medium car	0.01747	0.001
Large car	0.01747	0.001
Van	0.01602	0.00092
Four-wheel drive	0.01602	0.00092
Light truck	0.01602	0.00092
Medium truck	0.02999	0.00099
Heavy truck	0.03829	0.00135
Articulated truck	0.04328	0.00153
Mini bus	0.01747	0.00092
Light bus	0.01747	0.00092
Medium bus	0.02999	0.00099
Heavy bus	0.03829	0.00135
Coach	0.03829	0.00135

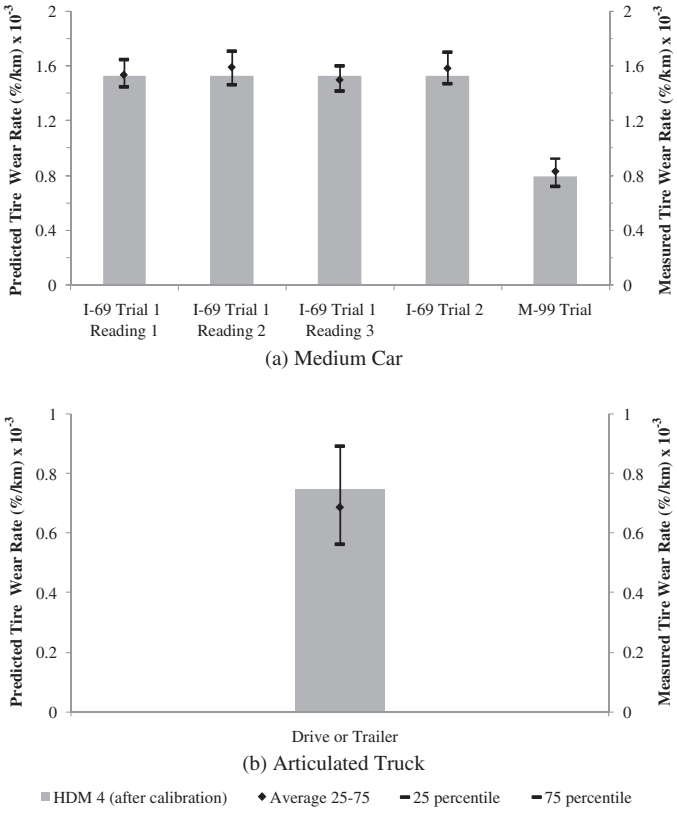

Figure 4-11. Comparison between the calibrated HDM 4 predictions and measurements.

Effect of Roughness on Tire Wear

The calibrated HDM 4 provides an accurate estimate of the roughness effect on rolling resistance and thus on tire wear, since it is a function of rolling resistance. The change in tire wear as a function of IRI for the different speeds shown in Figure 4-12, generated at 17°C (62.6°F) when the mean profile depth is 1 mm (0.04 in.) and grade is 0%, indicates the following:

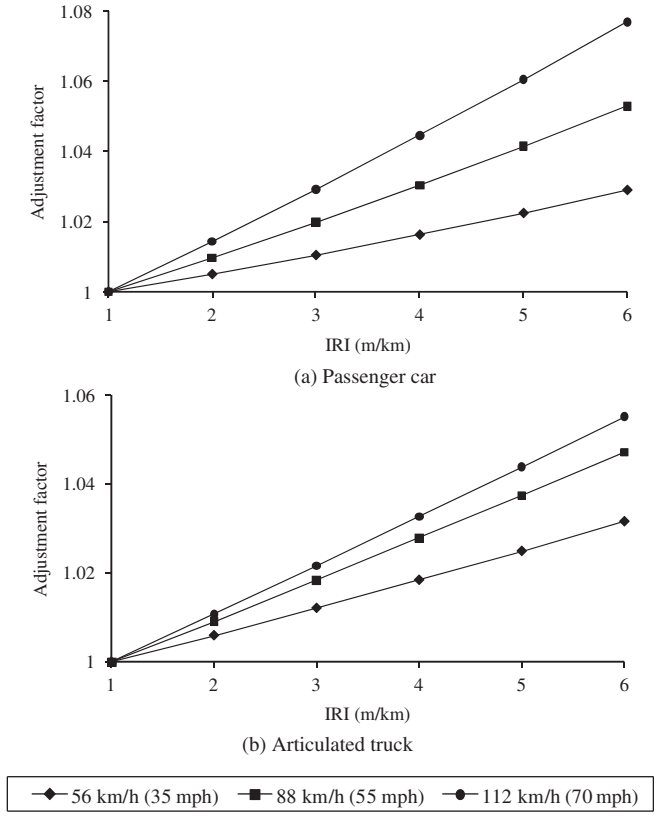

Figure 4-12. Effect of roughness on tire wear estimated using calibrated HDM 4.

- The effect of roughness on tire wear increases as speed increases. Table 4-7 lists the change in tire wear caused by change of IRI from the baseline condition of IRI = 1 m/km (63.4 in./mi) for all vehicle classes at 56, 88, and 112 km/h (35, 55, and 70 mph).
- Roughness will affect passenger car tires more than articulated truck tires. However, because trucks have more tires than passenger cars, the total effect of roughness per vehicle will be greater.

Summary

The information presented showed that the calibrated HDM 4 tire wear model adequately predicts tire wear of passenger cars and articulated trucks. The calibrated model is presented in Tables 4-8 through 4-11; the new default values for vehicle and tire characteristics are summarized in Table 4-12.

Table 4-7. Effect of roughness on tire wear.

Speed	Vehicle Class (Number of Wheels)	Baseline Conditions (%/km)[a]	Baseline Conditions (%/mi)[a]	Adjustment Factors from the Baseline (Fraction per Tire)				
		IRI (m/km)						
		1		2	3	4	5	6
56 km/h (35 mph)	Medium car (4)	0.0013	0.0021	1.01	1.01	1.02	1.02	1.03
	Van (4)	0.0011	0.0017	1.00	1.01	1.01	1.02	1.02
	SUV (4)	0.0011	0.0017	1.01	1.02	1.03	1.04	1.05
	Light truck (4)	0.0012	0.0020	1.01	1.02	1.03	1.04	1.05
	Articulated truck (18)	0.0006	0.0010	1.01	1.01	1.02	1.02	1.03
88 km/h (55 mph)	Medium car (4)	0.0014	0.0022	1.01	1.02	1.03	1.04	1.05
	Van (4)	0.0013	0.0021	1.01	1.01	1.02	1.03	1.04
	SUV (4)	0.0013	0.0021	1.01	1.03	1.05	1.06	1.08
	Light truck (4)	0.0018	0.0029	1.01	1.02	1.04	1.05	1.06
	Articulated truck (18)	0.0007	0.0012	1.01	1.02	1.03	1.04	1.05
112 km/h (70 mph)	Medium car (4)	0.0015	0.0025	1.01	1.03	1.04	1.06	1.08
	Van (4)	0.0018	0.0028	1.01	1.02	1.03	1.04	1.04
	SUV (4)	0.0017	0.0027	1.02	1.04	1.06	1.08	1.10
	Light truck (4)	0.0029	0.0046	1.01	1.02	1.04	1.05	1.06
	Articulated truck (18)	0.0009	0.0015	1.01	1.02	1.03	1.04	1.06

[a] percentage of new tire volume

Table 4-8. HDM 4 tire consumption model.

Name	Description	Unit
Number of equivalent new tires (*EQNT*)	$EQNT = \frac{TWT}{10 \times VOL}$	% new tire/km
VOL	= Tire volume	dm^3
Total change in tread wear (*TWT*)	$TWT = C_{0tc} + C_{tcte} \times \frac{CFT^2 + LFT^2}{NFT}$ $TWT = C_{0tc} + C_{tcte} \times TE$	dm^3/1000 km
C_{0tc}	= Tread wear rate constant (Table 4-12)	dm^3/1000 km
C_{tcte}	= Tread wear coefficient (Table 4-12)	dm^3/MNm
Tire energy (*TE*)	$TE = \frac{CFT^2 + LFT^2}{NFT}$	MNm/1000 km
Circumferential force on the tire (*CFT*)	$CFT = \frac{(1 + CTCON * dFUEL) * (Fa + Fr + Fg)}{NW}$	N
CTCON	= Incremental change of tire consumption related to congestion	ratio
dFUEL	= Incremental change of fuel consumption related to congestion	ratio
Fa	= Aerodynamic forces	N
Fr	= Rolling resistance forces	N
Fg	= Gradient forces	N
Lateral force on the tire (*LFT*)	$LFT = \frac{Fc}{NW}$	N
Fc	= Curvature forces	N
Nw	= Number of wheels	dimensionless
Normal force on the tire (*NFT*)	$NFT = \frac{M * g}{NW}$	N
M	= Vehicle mass	kg
g	= Gravity	m/s^2

Table 4-9. HDM 4 tractive forces model.

Name	Description	Unit
Aerodynamic forces (*Fa*)	$Fa = 0.5 * \rho * CD * AF * \upsilon^2$	N
CD	Drag coefficient (Table 4-12)	dimensionless
AF	Frontal area (Table 4-12)	m^2
ρ	Mass density of the air (default = 1.2)	kg/m^3
υ	Vehicle speed	m/s
Gradient forces (*Fg*)	$Fg = M * GR * g$	N
M	Vehicle weight (Table 4-12)	kg
GR	Gradient	radians
g	Gravity	m/s^2
Curvature forces (*Fc*)	$Fc = \max\left(0, \frac{\left(\frac{M * \upsilon^2}{R} - M * g * e\right)^2}{Nw * Cs} * 10^{-3}\right)$	N
R	Curvature radius (Default = 3000)	m
Superelevation (*e*)	$e = \max(,0.045 - 0.68 * Ln(R))$	m/m
Nw	Number of wheels (Table 4-12)	dimensionless
Tire stiffness (*Cs*)	$Cs = a0 + a1 * \frac{M}{Nw} + a2 * \left(\frac{M}{Nw}\right)^2$	kN/rad
*a*0 to *a*2	Model parameter (Table 4-10)	dimensionless
Rolling resistance (F_r)	$Fr = CR2 * (b11 * Nw + CR1 * (b12 * M + b13 * \upsilon^2))$	N
*CR*1	Rolling resistance tire factor (Table 4-12)	factor
Rolling resistance parameters (*b*11, *b*12, *b*13)	$b11 = 37 * Dw$ $b12 = 0.064 / Dw$ $b13 = 0.012 * Nw / Dw^2$	factors
Dw	Diameter of wheel	
Rolling resistance surface factor (*CR2*)	$= Kcr2[a0 + a1 * Tdsp + a2 * IRI + a3 * DEF]$	factor
*Kcr*2	Calibration factor (Table 4-12)	factor
*a*0 to *a*3	Model coefficient (Table 4-11)	dimensionless
Texture depth using sand patch method (*Tdsp*)	$Tdsp = 1.02 * MPD + 0.28$	mm
MPD	Mean Profile Depth	mm
IRI	International roughness index	m/km
DEF	Benkelman Beam rebound deflection	mm

Table 4-10. Final parameters for tire stiffness (*Cs*) model.

	≤ 2500 kg		> 2500 kg	
Coefficient	Bias	Radial	Bias	Radial
*a*0	30	43	8.8	0
*a*1	0	0	0.088	0.0913
*a*2	0	0	−0.0000225	−0.0000114

Source: Bennett and Greenwood (2003b)

Table 4-11. Final parameters for rolling resistance coefficient (*CR*2) model.

	≤ 2500 kg				> 2500 kg			
Surface Type	*a*0	*a*1	*a*2	*a*3	*a*0	*a*1	*a*2	*a*3
Asphalt	0.5	0.02	0.1	0	0.57	0.04	0.04	1.34
Concrete	0.5	0.02	0.1	0	0.57	0.04	0.04	0

Source: Bennett and Greenwood (2003b)

Table 4-12. HDM 4 new default values—vehicle and tire characteristics.

Vehicle Class	Number of Axles	*Nw*	M (tons)	*Kcr*2	CD	AF (m^2)	WD	Tire Type	*CR*1	*b*11	*b*12	*b*13	C_{0tc} (dm^3/1000 km)	C_{tcte} (dm^3/MNm)	VOL (dm^3)	VEHF AC
Small car	2	4	1.9	0.5	0.42	1.9	0.62	Radial	1	22.2	0.11	0.13	0.01747	0.001	1.4	2
Medium car	2	4	1.9	0.5	0.42	1.9	0.62	Radial	1	22.2	0.11	0.13	0.01747	0.001	1.4	2
Large car	2	4	1.9	0.5	0.42	1.9	0.62	Radial	1	22.2	0.11	0.13	0.01747	0.001	1.4	2
Van	2	4	2.54	0.67	0.5	2.9	0.7	Radial	1	25.9	0.09	0.10	0.01602	0.00092	1.6	2
Four-wheel drive	2	4	2.5	0.58	0.5	2.8	0.7	Radial	1	25.9	0.09	0.10	0.01602	0.00092	1.6	2
Light truck	2	4	4.5	0.99	0.6	5	0.8	Radial	1	29.6	0.08	0.08	0.01602	0.00092	1.6	2
Medium truck	2	6	6.5	0.99	0.6	5	0.8	Bias	1.3	29.6	0.08	0.11	0.02999	0.00099	6	1
Heavy truck	3	10	13	1.1	0.7	8.5	1.05	Bias	1.3	38.85	0.06	0.11	0.03829	0.00135	8	1
Articulated truck	5	18	13.6	1.1	0.8	9	1.05	Bias	1.3	38.85	0.06	0.20	0.04328	0.00153	8	1
Mini bus	2	4	2.16	0.67	0.5	2.9	0.7	Radial	1	25.9	0.09	0.10	0.01747	0.00092	1.6	2
Light bus	2	4	2.5	0.99	0.5	4	0.8	Radial	1	29.6	0.08	0.08	0.01747	0.00092	1.6	2
Medium bus	2	6	4.5	0.99	0.6	5	1.05	Bias	1.3	38.85	0.06	0.07	0.02999	0.00099	6	1
Heavy bus	3	10	13	1.1	0.7	6.5	1.05	Bias	1.3	38.85	0.06	0.11	0.03829	0.00135	8	1
Coach	3	10	13.6	1.1	0.7	6.5	1.05	Bias	1.3	38.85	0.06	0.11	0.03829	0.00135	8	1

CHAPTER 5

Repair and Maintenance Costs Model

This chapter presents the methodology for developing vehicle repair and maintenance cost models using the two most promising models identified in this project: HDM 4 model and the model identified in the Texas Research and Development Foundation (TRDF) study (Zaniewski et al., 1982). This chapter also presents a new mechanistic–empirical approach to estimate the effect of pavement roughness on repair and maintenance costs.

Repair and Maintenance Models

HDM 4 Model

HDM 3 allowed users to predict vehicle operating costs using relationships derived from road user cost studies in Brazil, India, Kenya, and the Caribbean (Watanatada et al., 1987). For HDM 4, the parts model was simplified over that used in HDM 3 (Bennett and Greenwood, 2003b). Equations 5.1 through 5.4 show the final model. The HDM 4 model suggested parameters for parts and labor for all the vehicle classes are listed in Table 5-1.

$$\text{PARTS} = \left(\text{K0}_{\text{pc}}\left[\text{CKM}^{\text{kp}}\left(\text{a}_0 + \text{a}_1\text{RI}\right)\right] + \text{K1}_{\text{pc}}\right)\left(1 + \text{CPCON} \times \text{dFUEL}\right) \quad (5.1)$$

$$RI = \max\left(IRI,\ \min\left(IRI0,\ a_2 + a_3 * IRI^{a_4}\right)\right) \quad (5.2)$$

$$a_2 = IRI0 - a_5$$

$$a_3 = \frac{a_5}{IRI0^{\frac{IRI0}{a_5}}} \quad (5.3)$$

$$a_4 = \frac{IRI0}{a_5}$$

$$a_5 = IRI0 - 3$$

$$\text{LH} = \text{K0}_{\text{lh}}\left(a_6 \times \text{PARTS}^{a_7}\right) + \text{K1}_{\text{lh}} \quad (5.4)$$

where:

- PARTS = Standardized parts consumption as a fraction of the replacement vehicle price per 1000 km
- K0_{pc} = Rotational calibration factor (default = 1.0)
- CKM = Vehicle cumulative kilometer (Table 5-1)
- a_0, a_1, kp = Model constants (Table 5-1)
- RI = Adjusted roughness
- IRI = Roughness in IRI (m/km)
- IRI0 = Limiting roughness for parts consumption in IRI (3 m/km)
- a_2 to a_5 = Model parameters
- K1_{pc} = Translational calibration factor (default = 0.0)
- CPCON = Congestion elasticity factor (default = 0.1)
- dFUEL = Additional fuel consumption due to congestion as a decimal
- LH = Number of labor hours per 1,000 km
- K0_{lh} = Rotation calibration factor (default = 1)
- K1_{lh} = Translation calibration factor (default = 0)
- a_6, a_7 = Model constants (Table 5-1)

The model suggests eliminating the effects of roughness on parts consumption at low IRI. This is achieved by using Equations 5.2 and 5.3.

TRDF Study

Winfrey (1969) presented repair and maintenance costs based on the results of surveys. These costs were updated by Claffey (1971). Zaniewski et al. (1982) further updated costs for maintenance and repair at constant speed at level terrain in good condition by multiplying Winfrey's costs by a factor to reflect the current overall repair and maintenance costs and listing the costs in tables. The results from the TRDF study were generated for a Pavement Serviceability Index (PSI) of 3.5 (IRI was not the accepted standard roughness index at that time). To include the effect of pavement condition, Zaniewski et al. (1982) compiled the two different rela-

Table 5-1. HDM 4 repair and maintenance model parameters and vehicle characteristics.

Vehicle Type	Parts Consumption Model				Labor Model	
	CKM (km)	*kp*	a_0*1E^{-6}	a_1*1E^{-6}	a_6	a_7
Motorcycle	50,000	0.308	9.23	6.2	1161.42	0.584
Small car	150,000	0.308	36.94	6.2	1161.42	0.584
Medium car	150,000	0.308	36.94	6.2	1161.42	0.584
Large car	150,000	0.308	36.94	6.2	1161.42	0.584
Light delivery car	200,000	0.308	36.94	6.2	611.75	0.445
Light goods vehicle	200,000	0.308	36.94	6.2	611.75	0.445
Four-wheel drive	200,000	0.371	7.29	2.96	611.75	0.445
Light truck	200,000	0.371	7.29	2.96	2462.22	0.654
Medium truck	240,000	0.371	11.58	2.96	2462.22	0.654
Heavy truck	602,000	0.371	11.58	2.96	2462.22	0.654
Articulated truck	602,000	0.371	13.58	2.96	2462.22	0.654
Mini bus	120,000	0.308	36.76	6.2	611.75	0.445
Light bus	136,000	0.371	10.14	1.97	637.12	0.473
Medium bus	245,000	0.483	0.57	0.49	637.12	0.473
Heavy bus	420,000	0.483	0.65	0.46	637.12	0.473
Coach	420,000	0.483	0.64	0.46	637.12	0.473

1 km = 0.62 mi

tionships that were established as part of the Brazilian study (Watanatada, 1987) to estimate parts and labor expenses as a function of surface roughness and calculated adjustment factors (Table 5-2).

Collection and Assessment of Data Applicability

Repair and maintenance costs data (i.e., parts and labor costs) and vehicle characteristics (i.e., vehicle type, odometer readings, model year, vehicle age, etc.) have been collected from different sources, including commercial truck fleet data collected as part of NCHRP Project 1-33 (Papagiannakis, 2000) and state DOT vehicle fleet data extracted from Texas DOT and Michigan DOT databases (these data are presented in Appendix C). To correlate pavement condition and repair and maintenance, roughness data from the pavement management systems of Texas and Michigan DOTs were used.

The content of the data obtained for all vehicle types appears adequate for making statistical inferences. Although the Michigan DOT fleet does not include heavy and articulated trucks (for normal operations), these data were available from the Texas DOT and the NCHRP 1-33 (Papagiannakis, 2000) data.

The quality of the data depends on whether repair and maintenance costs could be related to pavement conditions (i.e., roughness) and the availability of sufficient variance in roughness condition between different regions/districts.

Table 5-2. Repair and maintenance costs adjustment factors.

Pavement Serviceability Index	IRI (m/km)	Passenger Cars and Pickup Trucks	Single-Unit Trucks	2-S2 and 3-S2 Semi Trucks
1	8.94	2.3	1.73	2.35
1.5	6.69	1.98	1.48	1.82
2	5.09	1.71	1.30	1.5
2.5	3.85	1.37	1.17	1.27
3	2.84	1.15	1.07	1.11
3.5	1.98	1.00	1.00	1.00
4	1.24	0.90	0.94	0.92
4.5	0.59	0.83	0.90	0.86

1 m/km = 63.4 in./mi
Source: Zaniewski et al. (1982)

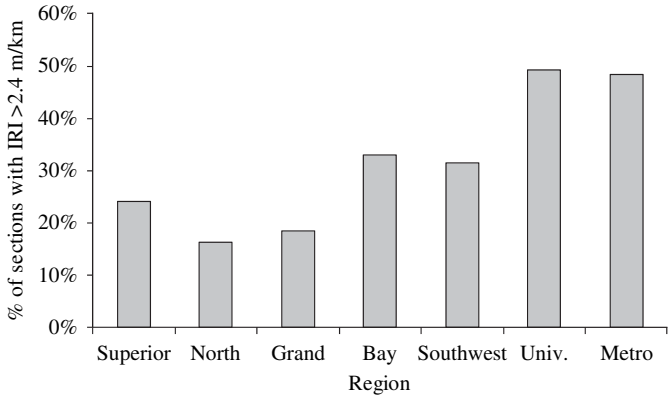

Source: Michigan DOT

Figure 5-1. Percentage of Michigan sections with IRI > 2.4 m/km by region.

Preliminary analysis of pavement roughness data in Michigan and Texas suggests that there is enough variability in roughness conditions among different regions, districts, and counties. The regions of Michigan were divided into three categories (Figure 5-1):

- University and metro regions (~50% of sections with IRI > 2.4 m/km)
- Bay and Southwest regions (~30% of sections with IRI > 2.4 m/km)
- Superior, North, and Grand regions (~20% of sections with IRI > 2.4 m/km)

Similarly, the road network for the state of Texas was divided into five groups (Figure 5-2):

- Group A: roughness > 2.1 m/km (133.1 in./mi)
- Group B: 1.9 m/km (120.5 in./mi) < roughness < 2.1 m/km (133.1 in./mi)
- Group C: 1.7 m/km (107.8 in./mi) < roughness < 1.9 m/km (120.5 in./mi)
- Group D: 1.5 m/km (95.1 in./mi) < roughness < 1.7 m/km (107.8 in./mi)
- Group E: roughness < 1.5 m/km (95.1 in./mi)

This classification was obtained using the average roughness of 1.9 m/km (120.5 in./mi) and a standard deviation of 0.2 m/km (12.7 in./mi).

Repair and maintenance data for vehicle fleets reported in NCHRP 1-33 (Papagiannakis, 2000) were correlated with pavement condition (IRI) and compared with HDM 4 predictions (Figure 5-3). Figure 5-3 indicates the following regarding the data reported in NCHRP 1-33:

- The range of IRI is limited.
- The parts costs are lower than those predicted by HDM 4.
- The labor costs are much lower than those predicted by HDM 4.

The HDM 4 model was calibrated using data from developing countries (e.g., Brazil, India) that tend to overestimate the labor hours expended for repair and maintenance compared to US conditions. Also, there is a difference between parts consumption in the United States and those predicted from HDM 4 because of the different market places and inflation in parts and vehicle prices. In light of this situation, the research team decided to update the results of the TRDF study and develop a new mechanistic–empirical model.

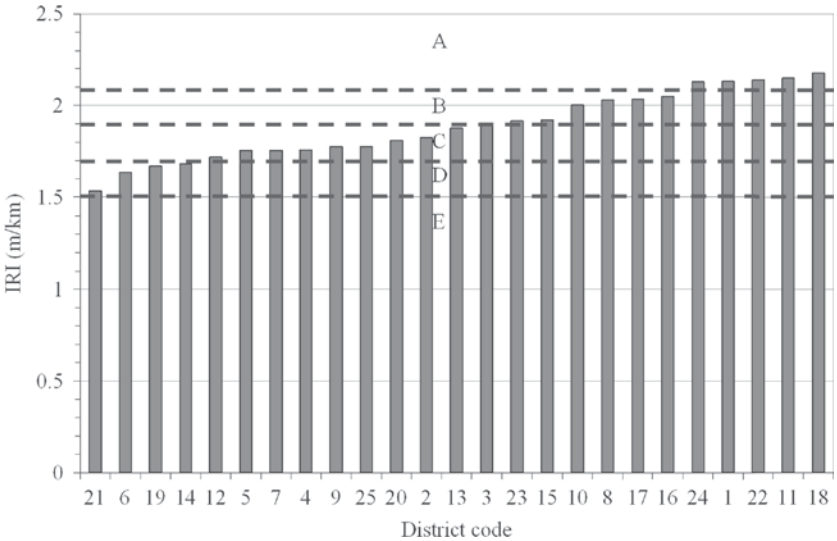

1 m/km = 63.4 in./mi
Source: Texas DOT

Figure 5-2. Categories of roughness for Texas DOT districts.

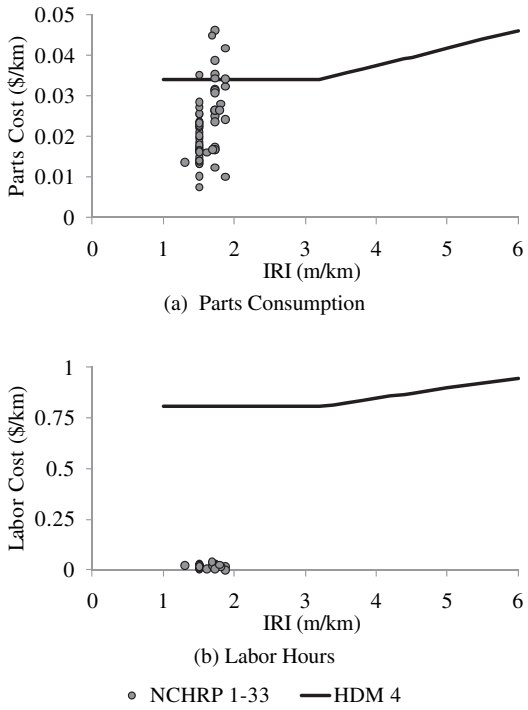

1 m/km = 63.4 in./mi

Figure 5-3. Parts consumption and labor hours estimates.

Updating Results of TRDF Study

Texas and Michigan DOT data were first sorted by car make, model, and year. Then, only repair costs related to damage from vibrations were extracted (e.g., underbody inspection, axle repair and replacement, and shock absorber replacement). In spite of the adequacy of data quality, it was not possible to fit a relationship between roughness and repair and maintenance cost for the following reasons:

- The data showed wide scatter and high variability.
- The range of roughness was narrow (IRI between 1.4 and 2.4 m/km) and does not cover the full range encountered in the United States (IRI ~ 1 to 5 m/km).
- The maximum roughness (IRI) was less than 3 m/km (190.2 in./mi); earlier studies (Bennett and Greenwood, 2003b; Poelman and Weir, 1992) reported no effect on repair and maintenance costs at such a low level of roughness.

To deal with these limitations, the latest comprehensive research conducted in the United States (Zaniewski et al., 1982) was used and updated to current conditions. The models were updated using macro-economic model corrections for overall (average) economic data (e.g., average labor hours for typical vehicles and average parts cost comparisons). This update was done by multiplying the costs from the TRDF study (which take into account all the relevant factors such as roughness, grade, and speed) by the ratio of current overall repair and maintenance costs to those used in the TRDF study. Current overall repair and maintenance costs were estimated using Michigan and Texas DOT databases. The inflation rate between 1982 and 2007 was calculated as the ratio of current overall average repair and maintenance costs to those reported in the TRDF study. Table 5-3 shows the costs from the TRDF study, current repair and maintenance costs, and the inflation rate for different vehicle classes.

The 1982 database collected by Zaniewski et al. (1982) does not include medium trucks (6.350 to 11.793 metric tons or

Table 5-3. Repair and maintenance costs.

Vehicle Class	Average Cost ($/km) x 10^{-3}		Average Cost ($/mi) x 10^{-3}		Inflation Ratio (1982 to 2007)	Average Vehicle Age† (years)	Average Vehicle Odometer Reading† (km)	Data Points†
	Zaniewski et al. (1982)	Current Cost† (2007)	Zaniewski et al. (1982)	Current Cost† (2007)				
Small car	21.44	40.23	34.3	64.37	1.56	9.23	96,215	680
Medium car	26		41.6					
Large car	30.03		48.05					
Pickup truck	33.01	51.78	52.82	82.85	1.57	7.31	92,038	2764
Light truck	61.88	92.13	99	147.4	1.49	7.80	86,963	1536
Medium truck	87.50*	118.6	140*	189.76	1.36	7.40	87,449	1831
Heavy truck	87.50	119.27	140	190.83	1.36	12.50	196,378	1735
Articulated truck	90.63	124.28	145	198.85	1.37	14.64	352,633	181
Buses	87.50*	119.12	140*	190.59	1.36	22.75	323,174	8

1 km = 0.62 mi

* Assumed equal to heavy truck cost

† Estimated using both Texas and Michigan DOT data

14,000 to 26,000 lb) based on the US DOT Vehicle Inventory and Use Survey classification. However, the data collected as part of this study (especially the data collected from Texas DOT) included all truck classes (light, medium, heavy, and articulated trucks) and buses. Therefore, the average repair and maintenance costs for medium trucks and buses were assumed to be equal to those for heavy trucks. Table 5-3 also presents the number of data points for the data collected from Michigan and Texas DOTs. Enough data points that are representative of current vehicle and commercial truck fleets in the United States were available for statistical inferences.

The effect of roughness was accounted for using an approach similar to that used in Zaniewski et al. (1982). First, the HDM 4 repair and maintenance equations were compiled for all vehicle classes for different roughness levels (from 1 to 6 m/km in increments of 0.5 m/km). Then, these values were compared to the baseline condition, which is assumed to be 2 m/km (PSI ≈ 3.5). The proportionate change from this baseline condition to the respective roughness level is the adjustment factor applied to the updated costs. Adjustment factors for each vehicle class and IRI value were calculated using Equations 5.5 and 5.6 and are summarized in Table 5-4. The HDM 4 model assumes no effect of roughness on parts consumption at low IRI (less than 3 m/km), which is achieved by using the smoothing relationship given in Equations 5.4 and 5.5. This assumption was also reported in others studies (Poelman and Weir, 1992) and was observed from the data collected as part of this study.

$$AF_i = \frac{COST(IRI_i)}{COST(2)} \tag{5.5}$$

$$COST(IRI_i) = PARTS(IRI_i) + LH(IRI_i) \tag{5.6}$$

where:

$AF_i(\%)$ = Adjustment factor (percentage)
$COST\ (IRI_i)$ = Total cost per 1,000 km evaluated at IRI_i
$PARTS\ (IRI_i)$ = Parts consumption per 1,000 km evaluated at IRI_i using Equation 5.1
$LH\ (IRI_i)$ = Labor cost per 1,000 km evaluated at IRI_i using Equation 5.4
IRI_i = International Roughness Index (m/km)

Mechanistic–Empirical Approach

A mechanistic–empirical methodology was developed in this study to estimate the effect of roughness on repair and maintenance costs. The approach consists of conducting fatigue damage analysis using numerical modeling of vehicle response. Its main assumption is that damage to vehicle suspension components follows a Miner's rule type of fatigue accumulation (Poelman and Weir, 1992; Hammarström and Henrikson, 1994). A sensitivity analysis was performed to quantify the relationship between roughness level and vehicle suspension damage. The analysis consists of the following steps:

1. Generate an artificial road surface profile for a given roughness (IRI);
2. Estimate the response of the vehicle using numerical modeling of the vehicle;
3. Compute the induced damage to the vehicle suspension using a rainflow counting algorithm and Miner's rule;
4. Repeat Steps 1 through 3 for different roughness levels.

Artificial Generation of Road Surface Profiles

The road roughness profiles can be represented as stochastic processes, depending on the spatial road coordinate x of the traveling vehicle (ISO-8608:1995, "Mechanical Vibration–Road Surface Profile"). The one-sided power spectral density (PSD) is a simple and often used road roughness representation approach. A detailed description of the models currently in use is included in Appendix C. These models were used to generate road profiles for roughness prediction purposes. In

Table 5-4. Repair and maintenance costs adjustment factors.

	Adjustment Factors										
	IRI (m/km)										
Vehicle Class	1.0	1.5	2	2.5	3	3.5	4	4.5	5	5.5	6
Small car	1.0	1.0	1.0	1.0	1.01	1.03	1.12	1.26	1.40	1.55	1.71
Medium car	1.0	1.0	1.0	1.0	1.01	1.03	1.12	1.26	1.40	1.55	1.71
Large car	1.0	1.0	1.0	1.0	1.01	1.03	1.12	1.26	1.40	1.55	1.71
Pickup trucks	1.0	1.0	1.0	1.0	1.01	1.03	1.12	1.26	1.40	1.55	1.71
Light truck	1.0	1.0	1.0	1.0	1.01	1.05	1.20	1.41	1.65	1.91	2.18
Medium truck	1.0	1.0	1.0	1.0	1.01	1.04	1.15	1.32	1.50	1.69	1.90
Heavy truck	1.0	1.0	1.0	1.0	1.01	1.04	1.15	1.32	1.50	1.69	1.90
Articulated truck	1.0	1.0	1.0	1.0	1.01	1.03	1.14	1.29	1.45	1.62	1.80
Buses	1.0	1.0	1.0	1.0	1.02	1.06	1.24	1.52	1.83	2.17	2.53

1 m/km = 63.4 in./mi

1979, Robson suggested the following model to generate the pavement surface roughness profiles, which was included in ISO 8608:1995:

$$S_u(k) = c|k|^{-n} \tag{5.7}$$

Where

$S_u(k)$ = Displacement spectral density (m^3/cycle)

$n = 2.5$

$K = \frac{n}{N\Delta}$ $n = 0,1, \ldots . (N-1)$ = Wavenumber

N = Number of samples in the profiles

Δ = Distance interval between successive ordinates of the surface profile

c = Characterizes the roughness level

The constant c in Equation 5.7 was found to be correlated with the IRI (Robson, 1979) and could be estimated using Equation 5.8:

$$c = 1.69 \times 10^{-8} (IRI)^2 \left(m^{1/2} cycle^{3/2}\right) \tag{5.8}$$

To generate a random road surface profile, a set of random phase angles uniformly distributed between 0 and 2π is applied to the desired spectral density. Then, the inverse discrete Fourier transform was applied to the spectral coefficients (Cebon, 1987).

Dynamic Vehicle Simulation

As reported by Prem (2000) and Cebon (1999), several numerical models have been developed to predict the behavior of vehicles when traveling on irregular pavement surfaces. The most basic models are based on quarter-vehicles represented by a second-order, two-degree-of-freedom, linear differential equation (Equation 5.9), whereby the vehicle response is computed for the vertical orientation with the pavement surface profile as the excitation function (Figure 5-4).

$$\begin{cases} m_u \ddot{x}_u - c_s(\dot{x}_s - \dot{x}_u) - k_s(x_s - x_u) + k_t(x_u - u(t)) = 0 \\ m_s \ddot{x}_s + c_s(\dot{x}_s - \dot{x}_u) + k_s(x_s - x_u) = 0 \end{cases} \tag{5.9}$$

Where,

$u(t)$ = Road profile (time)

x_u = Elevation of unsprung mass (axle)

x_s = Elevation of sprung mass (body)

k_t = Tire spring constant

k_s = Suspension spring constant

m_u = Unsprung mass

m_s = Sprung mass

c_s = Shock absorber constant

To account for the more complex behavior of road vehicles, more sophisticated vehicle models have been developed to describe the dynamic behavior of half-vehicles (complete axle) and even full-vehicle models (Gillespie, 1985). These have been aimed at predicting the roll and pitch response of vehicles, which have been found to be significant for some vehicle types. It was suggested, however, that in most cases, the vertical vibration remains the dominant component of vibration induced by irregular pavement surfaces (Gillespie, 1985). A half- or quarter-car model cannot be expected to predict loads on a physical vehicle exactly, but it will highlight the most important road characteristics as far as fatigue damage accumulation is concerned; it might be viewed as a "fatigue-load filter" (Cebon, 1999; Prem, 2000; Bogsjö, 2006; Kouta, 1994; Rouillard, 2008).

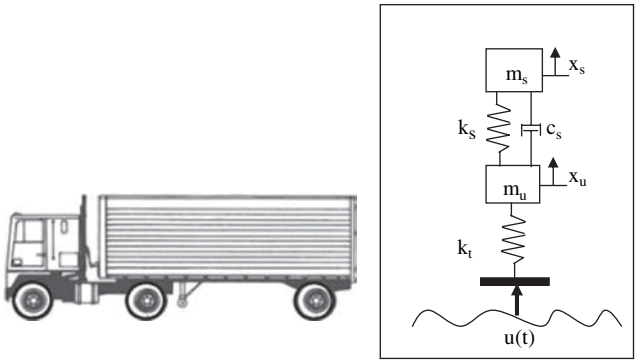

Figure 5-4. Schematic of two-degrees-of-freedom quarter-car vehicle model.

There have been several such models with various specific parameter values proposed to emulate the response of a wide variety of road vehicles ranging from small sedans to large trucks with air ride and more conventional steel suspension systems (Cebon, 1999). These models have also been used to predict the response of large vehicles with different axles in recognition of the differing suspension elements used for the driver's cabin and the trailer. Quarter-car parameters for a passenger car (Sayers and Karamihas, 1998) and a full truck with typical air and steel suspensions (Cebon, 1999) are given in Figure 5-5.

Model Parameters				
Constants		Truck		Car
Name	Unit	Steel	Air	-
m_s	kg	4500	4500	250
m_u	kg	500	500	40
k_s	MN/m	1	0.4	0.028
k_t	MN/m	2	2	0.125
c_s	KNs/m	20	20	2

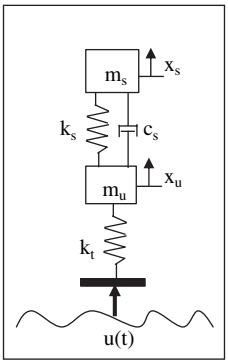

Figure 5-5. Parameters for quarter-car vehicle model.

A simple generic linear numerical quarter-vehicle model was developed to compute the vertical vibration level of typical vehicle types from different pavement profiles at constant speeds. This numerical model, developed with the Matlab/Simulink® programming environment, effectively computes the solution to the two-degrees-of-freedom system using the fixed-point method. The inputs to the model are the longitudinal pavement profile and the velocity of the vehicle.

Vehicle Fatigue Damage Analysis

Miner's linear accumulation hypothesis was used to estimate the total fatigue damage caused by a given load sequence:

$$D = \sum_i \frac{1}{N_i} \tag{5.10}$$

where N_i is the number of cycles to failure at a given load level *i*.

For a given sinusoidal load amplitude U_i, N_i can be obtained using Basquin's relation:

$$N_i = C^{-1} U_i^{-\beta} \tag{5.11}$$

Usually, for vehicle components, the fatigue exponent β takes values between 3 and 8 (Bogsjö, 2006). A typical β value for steel suspensions can be obtained using the "half-life" rule. This rule states that the half life of a steel component will be approximated by a 10% to 12% increase in cyclic load amplitude (Fuchs and Stephens, 1980). Applying this to Basquin's relation gives a β value for steel suspensions of 6.3 (Kouta, 1994; Bogsjö, 2006; and Abdullah et al., 2004).

Since loads caused by road roughness fluctuate randomly, it is necessary to extract cycles from the load sequence to assess the fatigue damage. The rainflow counting method introduced by Matsuishi and Endo (1968) was used for this purpose: The load sequence on the sprung mass of the vehicle model is rainflow counted to extract the load cycles U_i. The definition of the rainflow counting method was given by Rychlik (1987) and adopted in ASTM E 1049-85R05, "Standard Practices for Cycle Counting in Fatigue Analysis." Therefore, the total fatigue damage caused by the rainflow-counted load sequence is:

$$D = C \sum_i U_i^{\beta} \tag{5.12}$$

where $U_i = M_i - m_i^{RFC}$.

Suspension Failure Threshold

Vehicle owners tend to replace their suspensions at about 160,000 km (100,000 mi) for cars and 400,000 km (250,000 mi) for trucks (Repair Pal, 2009). This value was also reported as the lifetime warranty for suspensions given by vehicle manufacturers in the United States. Consequently, in this study, the average life of car and truck suspensions for typical driving conditions was assumed to be about 160,000 km (100,000 mi) and 400,000 km (250,000 mi), respectively. Vehicle suspensions are generally replaced when certain signs of wear become evident to compromise the safety and comfort of drivers. The amount of service life used up to that point was estimated using the following procedure:

1. Estimate the roughness (IRI) distribution of US roads (Figure 5-6), in the range of 1 m/km (63.4 in./mi) for a smooth road to 6 m/km for a very rough road. The probability density distribution presented in Figure 5-6 was generated using the data reported by the FHWA (2008);
2. Generate 30 road surface profiles for each of the IRI values;
3. Calculate the accumulated damage (D_{IRI}^{ij}) induced by each of the road profiles generated in Step 2 for a length of 1.6 km (1 mi) and assuming a value of 6.3 for β in Equation 5.12;
4. Take the average value of the accumulated damage calculated for each profile set having the same IRI level.
5. Estimate the number of kilometers per IRI (L_{IRI}^{i}) value using the distribution obtained in Step 1 and assuming that these vehicles are driven for 160,000 km (100,000 mi) and 400,000 km (250,000 mi) for cars and trucks respectively.
6. Compute the total accumulated damage using Equation 5.13:

$$D_{replace} = \sum_{i=1}^{N} \left(\frac{\sum_{j=1}^{30} D_{IRI}^{ij}}{30} \times L_{IRI}^{i} \right) \tag{5.13}$$

For example, using the above procedure, the value for $D_{replace}$ is about 87.3% at 112 km/h (70 mph) for cars and 62.2% at 96 km/h (60 mph) for trucks.

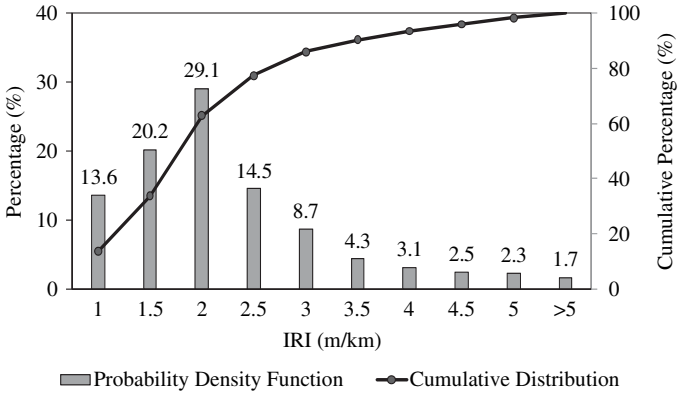

1 m/km = 63.4 in./mi
Source: FHWA (2008)

Figure 5-6. Road surface roughness distribution in the United States.

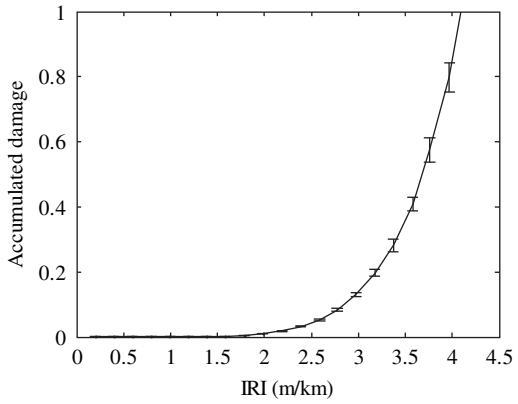

1 m/km = 63.4 in./mi

Figure 5-7. Accumulated damage in car suspensions after 160,000 km (100,000 mi) as a function of IRI at 112 km/h (70 mph) using the mechanistic–empirical approach.

Suspension Damage in Cars

Figure 5-7 shows the damage accumulated in car suspensions after 160,000 km (100,000 mi) on a road with a given (constant) IRI value. This damage is obtained by multiplying the damage calculated in Step 3 (for cars) by 160,000. The error bars show the error in accumulated damage caused by the variations in the profiles; i.e., different profiles will generate different suspension vibrations (even though they may have the same IRI).

Many car manufacturers design their vehicles for the 90th to 95th percentile road roughness (Poelman and Weir, 1992). Figure 5-6 shows that 3.9 m/km (247.3 in./mi) is the 93rd percentile of the roughness distribution in the United States. Figure 5-7 shows that a car driven for 160,000 km (100,000 mi) on a road with IRI = 3.9 m/km would accumulate suspension damage of about 84.5%, which is very close to the value obtained from Equation 5.13 (87.3%). This confirms the reasonableness of the value for β used in the analysis.

Road profiles from in-service pavements were used to check the accuracy of the approach for estimating car suspension damage. Table 5-5 summarizes the pavement conditions of the different sections used in this study. Figure 5-8 shows the accumulated suspension damage for cars induced by actual and artificially generated profiles at each roughness level. These data show that the results from actual profiles follow the general trend of the curve generated using artificial profiles (with limited scatter). This variance is caused by the actual content of the profiles. For example, the two profiles highlighted in Figure 5-8 (Profiles 3 and 6) have an IRI of 2.4 m/km (152 in./mi); however, Profile 3 causes more damage than Profile 6. According to Table 5-5, Profile 3 has deteriorated joints while Profile 6 has only low severity faulting and curling.

The additional cost induced by roughness features when the accumulated damage reaches $D_{replace}$ was assumed to be equal to the price of a new suspension and the labor hours for replacement. This value is equal to $1,000 according to Repair Pal (2009). The repair and maintenance cost for

Table 5-5. Summary surface conditions for in-service pavements used in the analysis.

Summary Information			Road										
			I-69	I-69	I-69	I-69	LTPP 20-0201	I-69	M-99S	M-99N	Creyts Rd	Waverly Rd	LTPP 20-0101
Pavement type			PCC	PCC	PCC	PCC	PCC	PCC	PCC	AC	AC	AC	AC
Length (km)			0.64	0.93	0.93	1.4	0.15	4.8	6.4	9.4	2.5	1.3	0.15
IRI range (m/km)			1.7-3.2	1.3-1.8	1.6-2.8	2.7-4.1	1.9	1.1-2.5	1.5-2.6	0.8-4.6	1.3-8.5	3.3-6	1.5
Faulting	Counts	Low	199	124	57	150	33	56	205	–	Not applicable		
		Medium	16	4	12	48	1	0	1	–			
		High	1	0	0	0	0	0	0	–			
	Highest magnitude (mm)		25.4	14.2	9.7	13.7	14	2.2	4.1	–			
	Lowest magnitude (mm)		–3.4	–2.8	–3.8	–10.9	1	–3.5	–6.8	–			
Deteriorated joints	Counts		–	–	1	2	–	–		–			
	Height differential (mm)		–	–	–5.3	–13.9	–	–		–			
	Width (m)		–	–	0.14	0.5	–	–		–			
Curling	Counts		57	57	–	–	–	260	–	–			
	Highest magnitude (mm)		4.5	2.3	–	–	–	4.5	–	–			
Potholes*	Counts		N/A	N/A	N/A	N/A	N/A	N/A	N/A	3	13	6	0
	Highest magnitude (mm)		N/A	N/A	N/A	N/A	N/A	N/A	N/A	–8.3	–22.4	–10.2	–

1 mi = 1.6km; 1 in./mi = 0.0157 m/km; 1 in = 25.4 mm; 1 ft = 0.3 m
* AC pavement distresses

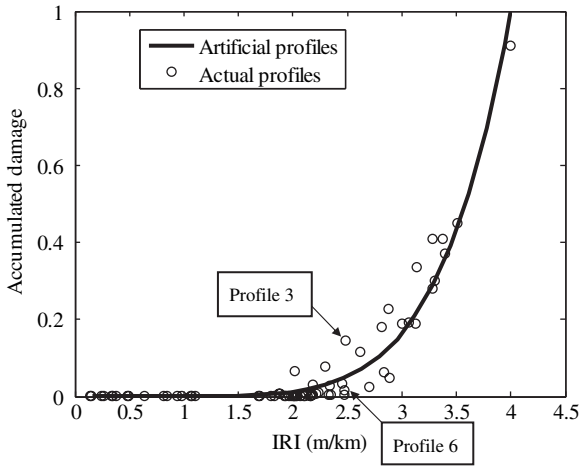

1 m/km = 63.4 in./mi

Figure 5-8. Accumulated car suspension damage from actual and artificial pavement surface profiles.

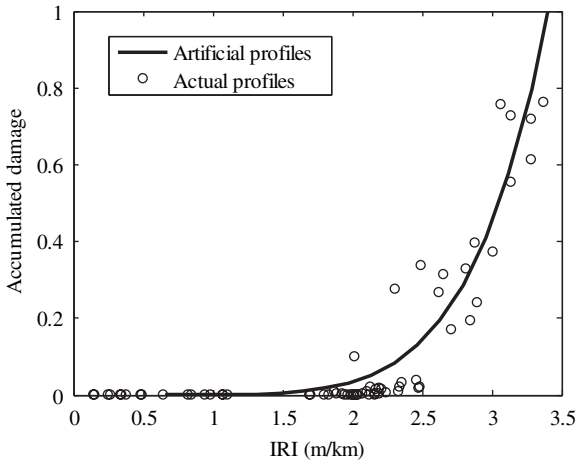

1 m/km = 63.4 in./mi

Figure 5-10. Accumulated truck suspension damage from actual pavement surface profiles.

a given IRI level is calculated by dividing the accumulated damage corresponding to that IRI value (see Figure 5-7) by $D_{replace}$ and multiplying the result by $1,000.

Suspension Damage in Trucks

Figure 5-9 shows the truck suspension damage resulting from driving 400,000 km (250,000 mi) on a road with a given (constant) IRI value. This damage is obtained by multiplying the damage induced by each of the road profiles generated for a given IRI value (for trucks) for a length of 1.6 km (1 mi) by 400,000. The error bars show the accumulated damage caused by the variations in the profiles (i.e., different profiles will generate different suspension vibrations although they may have the same IRI).

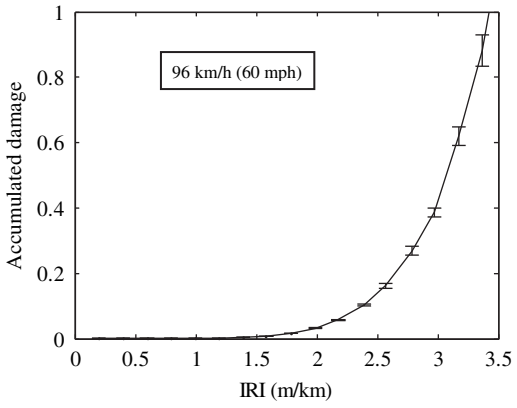

1 m/km = 63.4 in./mi

Figure 5-9. Effect of road surface roughness on truck suspension after 400,000 km (250,000 mi) using the mechanistic–empirical approach.

Trucks are generally designed for the 80th to 95th percentile road roughness. Figure 5-6 shows that 3.2 m/km (203 in./mi) is the 87th percentile of the roughness distribution in the United States. Figure 5-9 shows that a truck driven on 400,000 km (250,000 mi) of road with IRI = 3.2 m/km will accumulate suspension damage of about 66%. This value is very close to the value obtained from Equation 5.16 (62.2%) confirming the reasonableness of the value for β used in the analysis.

The additional cost caused by roughness features when the accumulated damage reaches $D_{replace}$ was assumed to be equal to the price of a new suspension plus the required labor hours for replacement. The total cost was estimated to be $3,000 and $1,800 for air and steel suspensions, respectively. The repair and maintenance cost for a given IRI level is calculated by dividing the accumulated damage corresponding to that IRI value (see Figure 5-9) by $D_{replace}$ and multiplying the result by the replacement cost.

Actual road profiles were also used to check the accuracy of the approach for estimating truck suspension damage. Figure 5-10 shows the accumulated suspension damage for trucks caused by actual and artificially generated profiles at each roughness level. Similar observations can be made (i.e., the results from actual profiles follow the general trend of the curve generated using artificial profiles with limited scatter).

Mechanistic versus Empirical Approach

Figures 5-11 and 5-12 show the results from (1) the mechanistic–empirical (M-E) approach using actual profiles from the Michigan road network and the Long Term Pavement Performance (LTPP) database, (2) the mechanistic–

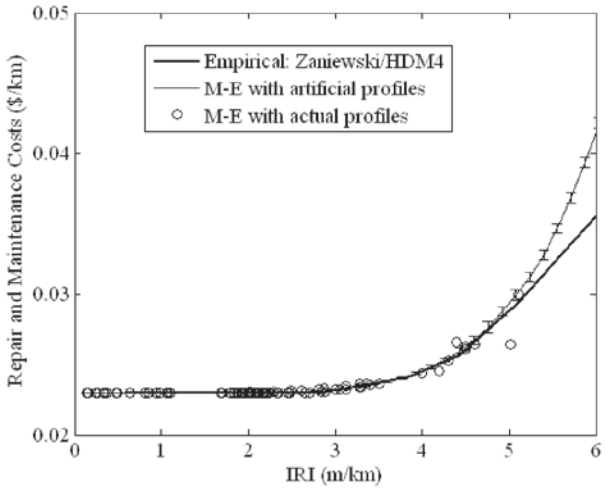

1 m/km = 63.4 in./mi; 1 mi = 1.6 km

Figure 5-11. Car repair and maintenance costs.

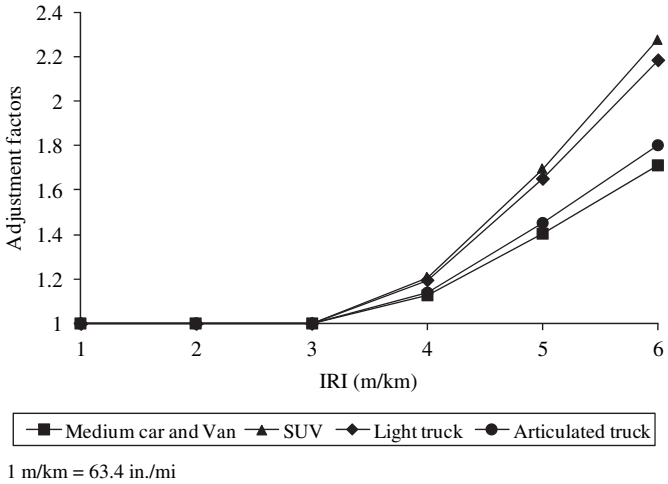

1 m/km = 63.4 in./mi

Figure 5-13. Effect of roughness on repair and maintenance costs.

empirical approach using artificially generated profiles, and (3) the empirical approach (i.e., updated TRDF study) for cars and trucks, respectively. The results show that the accumulated damage computed using actual profiles follows the curve generated for artificial profiles with limited scatter. The variance is caused by the difference in actual profile roughness contents. While roughness effects below 3 m/km are minimal, a constant repair and maintenance cost, which corresponds to other routine maintenance costs that are not related to roughness is still observed. Therefore, the curves were shifted upward from the mechanistic–empirical analysis to match the empirical curves in the IRI range below 3 m/km (190 in./mi). The results from the mechanistic–empirical approach compare very well with the empirical data up to an IRI of 5 m/km (317 in./mi), with a standard error of about 2%. Since the typical IRI range in the United States is 1 to 5 m/km, these results are appropriate for pavement management at the network level. However, at the project level, the effect of roughness features should be considered.

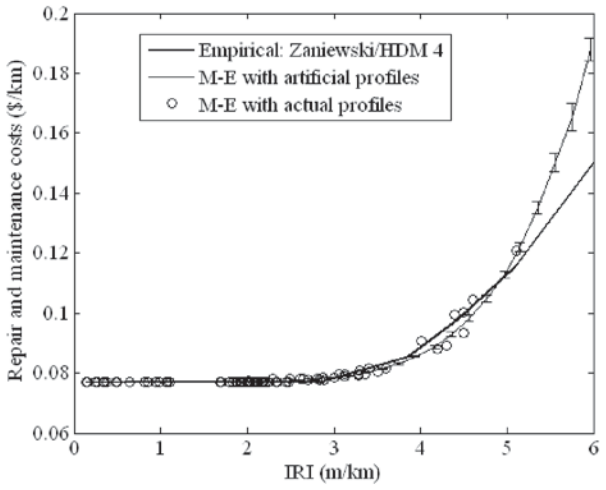

1 m/km = 63.4 in./mi

Figure 5-12. Truck repair and maintenance costs.

Effect of Roughness on Repair and Maintenance Costs

Figure 5-13 presents the change in repair and maintenance as a function of IRI. It should be noted that the mechanistic–empirical approach only estimates the effect of roughness on passenger cars and articulated trucks. The updated TRDF study was used to estimate the effect for the other vehicle classes (i.e., SUV, van, and light truck). The figure indicates the following:

- The effect of roughness on repair and maintenance costs increases as speed increases.
- Roughness affects light trucks and SUVs more than articulated trucks and passenger cars.

Summary

In this chapter, two different approaches for estimating repair and maintenance costs induced by pavement roughness were proposed: (1) An empirical approach that uses the updated TRDF study (Zaniewski et al., 1982) and adjustment factors (Table 5-4) and (2) a mechanistic–empirical approach to conduct fatigue damage analysis using numerical modeling of vehicle vibration response.

The results from the mechanistic–empirical approach and the empirical results (i.e., updated Zaniewski's tables) were found to be very similar for up to an IRI of 5 m/km, with a standard error of about 2%. Because the typical IRI range in the United States is between 1 and 5 m/km, this approach

Table 5-6. Effect of roughness on repair and maintenance costs.

Speed	Vehicle Class	Average Repair and Maintenance Cost * ($/km)	Average Repair and Maintenance Cost * ($/mi)	Baseline Conditions ($/km)	Baseline Conditions ($/mi)	Adjustment Factors from the Baseline Conditions				
				IRI (m/km)						
				1		2	3	4	5	6
56 km/h (35 mph)	Medium car	0.040	0.064	0.015	0.024	1.0	1.0	1.1	1.4	1.7
	Van	0.052	0.083	0.020	0.032	1.0	1.0	1.1	1.4	1.7
	SUV	0.052	0.083	0.020	0.032	1.0	1.0	1.2	1.7	2.3
	Light truck	0.058	0.092	0.021	0.034	1.0	1.0	1.2	1.7	2.2
	Articulated truck	0.124	0.199	0.046	0.074	1.0	1.0	1.1	1.5	1.8
88 km/h (55 mph)	Medium car	0.040	0.064	0.019	0.030	1.0	1.0	1.1	1.4	1.7
	Van	0.052	0.083	0.025	0.040	1.0	1.0	1.1	1.4	1.7
	SUV	0.052	0.083	0.025	0.040	1.0	1.0	1.2	1.7	2.3
	Light truck	0.058	0.092	0.029	0.046	1.0	1.0	1.2	1.7	2.2
	Articulated truck	0.124	0.199	0.063	0.101	1.0	1.0	1.1	1.5	1.8
112 km/h (70 mph)	Medium car	0.040	0.064	0.023	0.036	1.0	1.0	1.1	1.4	1.7
	Van	0.052	0.083	0.030	0.047	1.0	1.0	1.1	1.4	1.7
	SUV	0.052	0.083	0.030	0.047	1.0	1.0	1.2	1.7	2.3
	Light truck	0.058	0.092	0.035	0.057	1.0	1.0	1.2	1.7	2.2
	Articulated truck	0.124	0.199	0.077	0.123	1.0	1.0	1.1	1.5	1.8

1 m/km = 63.4 in./mi

* These costs were obtained by converting the average costs in Table 5-4 to $/km and $/mi and are unit repair costs related only to damage from vibrations.

seems applicable to US conditions. All the models currently in use are empirical in nature, except for the VETO model, which is reported to yield predictions that are much higher than the actual costs observed in Sweden. Table 5-6 summarizes the change in repair and maintenance costs per kilometer for all vehicle classes due to change in IRI from the baseline condition of IRI = 1 m/km (63.4 in./mi).

The developed model is a combination of the mechanistic–empirical approach and the updated TRDF study. The mechanistic–empirical approach to estimate the effect of pavement conditions on repair and maintenance costs only involves passenger cars and articulated trucks. Then, it uses the results from the 1982 TRDF study by Zaniewski et al. to estimate the costs for the other vehicle classes. The model is expected to provide better estimates of repair and maintenance costs at the project and network levels. For project-level analysis, the actual road profile should be used to take into account the effect of roughness features. To facilitate use of the developed model, a computer program (provided on the accompanying CD-ROM) has been prepared.

CHAPTER 6

Applicability to Emerging Technologies

In recent years, growing world population and the increased demand for road transportation (with its associated energy requirements that are primarily derived from fossil fuels) have led to the consideration, design, and development of energy-efficient vehicles and processes. To realize improvements in energy efficiency (with respect to road transportation), various engineering processes and/or technologies have been developed. Among these are drag-reducing vehicle designs, intelligent vehicle operating technologies (e.g., cruise control), use of alternative energy sources (e.g., electricity), and intelligent transportation systems that facilitate wireless communication between vehicles and transport infrastructure. These and other technological interventions help reduce vehicle operating costs and fossil energy consumption as well as carbon footprints. An overview of these technologies is provided in Appendix D. While emerging vehicle technologies can play a major role in reducing vehicle operating costs and mitigating negative environmental impacts, their impact on the effect of pavement conditions on vehicle operating costs may not be as substantial. This chapter discusses the potential impact of such emerging vehicle technologies on the effect of pavement conditions on vehicle operating costs. Few definitive conclusions could be reached about the effect of pavement conditions on vehicle operating costs for emerging technologies.

Mechanistic models are theoretically formulated to consider the main physical parameters and apply basic laws of physics/mechanics. By introducing a calibration factor in these models, the effect of emerging vehicle technologies on vehicle operating costs can be predicted. The following types of emerging technologies are discussed in this section:

- New engine and combustion technologies to improve the engine efficiency of vehicles, including engine friction reduction, gasoline direct injection, engine downsizing, variable valve actuation, cylinder deactivation, variable compression ratio, homogeneous charge compression ignition, integrated starter/generator systems, continuously variable transmission, automated manual transmission, and six+ speed gearboxes;
- Alternative fuels and technologies, including hybrid vehicles and vehicles powered by natural gas, vehicles powered by electricity, hydrogen, biodiesel, or ethanol;
- Vehicle design, including regenerative braking systems, electric motor drive/assist, lightweight materials, reduction of vehicle aerodynamics, and intelligent transportation systems;
- Automatic gear shift for heavy trucks; and
- Tire technologies, including tire pressure monitoring systems, tire inner liners, use of nitrogen for filling tires, and low rolling resistance tires.

New Engine and Alternative Fuel Technology

The change in fuel consumption as a function of change in roughness is calculated using Equations 6.1 and 6.2:

$$\%FC_{2-1} = \frac{FC_2 - FC_1}{FC_1} \tag{6.1}$$

$$FC_i = \xi \times P_i, i = 1 \text{ or } 2 \tag{6.2}$$

Where:

$\%FC_{2-1}$ = Percentage change in fuel consumption as a function of change in IRI
FC_i = Fuel consumption due to roughness IRI_i
ξ = Fuel-to-power efficiency
P_i = The total power required (tractive power caused by IRI_i, engine drag, and vehicle accessories)

Because new engine technology will have better engine efficiency, the same power will be delivered for lower fuel consumption. Therefore, percentage change in power is a constant for a given roughness change if the fuel-to-power

efficiency is assumed to not be affected by roughness. By substituting new and old efficiency in Equation 6.2, the following equation is obtained:

$$\%FC_{2-1}^{old} = \frac{\xi^{old} \times (P_2 - P_1)}{\xi^{old} \times P_1} = \frac{(P_2 - P_1)}{P_1} = \frac{\xi^{new} \times (P_2 - P_1)}{\xi^{new} \times P_1} = \%FC_{2-1}^{new} \quad (6.3)$$

Therefore, if the efficiency is not affected by roughness, the new technology will affect only the absolute value of fuel consumption, but not the contribution of roughness on fuel consumption. However, some of the hardware involved with new technologies might be sensitive to vehicle vibration that would require more maintenance under rougher roads than current technologies. In any case, it is likely that the effect of vibrations on the efficiency is secondary. The following savings in the fuel efficiency were reported:

1. Engine and combustion technologies (US Department of Energy, 2010):
   a. Gasoline direct injection will increase engine efficiency by up to 12%.
   b. Engine downsizing and cylinder deactivation will both increase engine efficiency by up to 7.5%.
   c. Variable valve actuation has the potential of increasing engine efficiency of up to 5%.
   d. Continuously variable and automated manual transmissions increase the engine efficiency by up to 6% and 7%, respectively.
2. Alternative fuels and technologies: Figure 6-1 shows the average fuel efficiency for passenger cars and light trucks in the United States with and without new technology (Bureau of Transportation Statistics, 2010; US Department of Transportation, 2010), and the projected fuel efficiency from 2010 through 2015 (NHTSA, 2009).

Vehicle Design

Vehicle manufacturers seek to minimize aerodynamics through vehicle design (smoothing vehicle shapes). In the United States, the drag coefficient has generally fallen in the

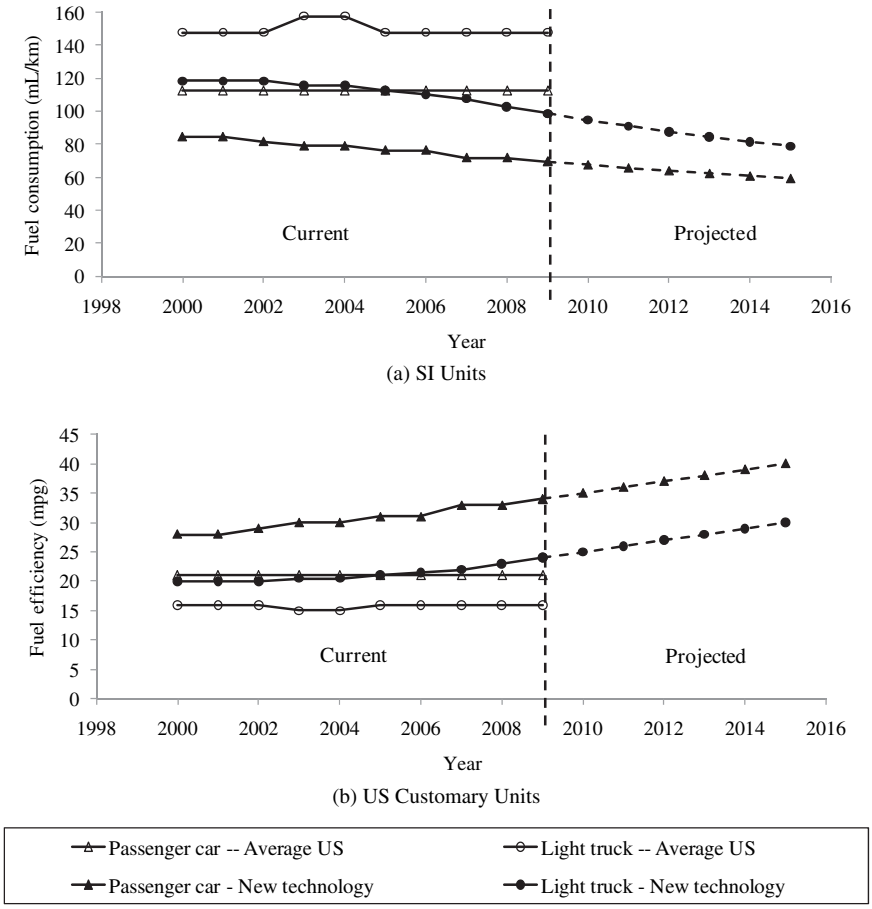

Source: Bureau of Transportation Statistics (2010)

Figure 6-1. Current and projected average fuel consumption.

current decade and vehicles have become smaller and more fuel efficient. Typical drag coefficients for current passenger cars range from 0.3 to 0.52 and is expected to range from 0.25 to 0.35 for future passenger cars (US Department of Energy, 2010).

Truck Manufacturers Association and the US Department of Energy conducted a 2-year collaborative study to investigate a variety of design improvements that would reduce aerodynamic drag and significantly improve fuel efficiency (US Department of Energy, 2006). The following technologies were identified:

- Gap enclosures that reduce aerodynamic drag in the gap between the tractor and trailer,
- Side skirts that improve aerodynamics and reduce airflow under the trailer in crosswinds, and
- Side mirror designs that reconfigure shape and support systems to reduce aerodynamic drag.

When introducing all aerodynamic improvements in one vehicle, the reduction in aerodynamic drag could be as much as 23%. Every 2% reduction in aerodynamic drag will result in a 1% improvement in fuel efficiency. However, these reductions in fuel consumption are believed to be slightly affected by pavement conditions.

Automatic Gear Shift for Heavy Trucks

A study by SCANIA Inc. reported that automatic gearshift for heavy trucks could save as much as 10% in fuel consumption (Lundstrom, 2010). However, these reductions in fuel consumption are believed to be slightly affected by pavement conditions.

New Tire Technology

Use of tires with lower rolling resistance coefficients than conventional tires will result in less fuel consumption. Equation 6.4 describes the rolling resistance model in the HDM 4 after calibration. The rolling resistance is a function of vehicle characteristics and pavement conditions.

$$Fr = CR2 \times \left(b11 \times Nw + CR1 \times \left(b12 \times M + b13 \times \upsilon^2\right)\right) \qquad (6.4)$$

where:

$b11$ to $b13$ = A function of the wheel diameter

$$\begin{cases} b11 = 37 * WD \\ b12 = 0.064 / WD \\ b13 = 0.012 * Nw / WD^2 \end{cases}$$

WD = Wheel diameter (mm)
Nw = Number of wheels
M = Mass of the vehicle (kg)

Table 6-1. Calibration factor for rolling resistance force.

Vehicle Class	$Kcr2$
Medium car	0.5
SUV	0.58
Light truck	0.99
Van	0.67
Articulated truck	1.1

υ = Vehicle velocity (m/s)
$CR1$ = Rolling resistance tire factor
1.3 for cross-ply bias
1.0 for radial
$CR2$ = Rolling resistance surface factor
$= Kcr2[a0 + a1 * Tdsp + a2 * IRI + a3 * DEF]$
$Kcr2$ = Calibration factor (Table 6-1)
$Tdsp$ = Texture depth from the sand patch method (mm)
$= 1.02 \times MPD + 0.28$
MDP = Mean profile depth
DEF = Benkelman Beam rebound deflection (mm)
IRI = International roughness index (m/km)
$a0$ to $a3$ = Model coefficient (function of the vehicle mass, surface class and type) (Table 6-2)

The effect of new tire technology on fuel and tire consumption could be accommodated by modifying some of the tire-related variables in HDM 4 such as $b11$ through $b13$ and $CR1$. Alternatively, limited field tests (e.g., coast down test) could be conducted to estimate the new parameters $a0$ to $a3$ for $CR2$. Sandberg (2007) reported the coefficients for the rolling resistance surface factor ($CR2$) listed in Table 6-3 for advanced tires.

Finally, the coefficients C_{0tc} and/or C_{tcte} could be affected by new tire technologies. If these coefficients were updated, a new calibration study would need to be conducted.

Summary

The growing demand for fuel-efficient vehicles has accelerated the research and development efforts dealing with the use of alternative fuels in vehicle propulsion, combustion and

Table 6-2. Parameters for rolling resistance surface factor (*CR2*) model with conventional tires.

	Vehicle Mass							
	≤ 2500 kg				> 2500 kg			
Surface Type	$a0$	$a1$	$a2$	$a3$	$a0$	$a1$	$a2$	$a3$
Asphalt	0.9	0.022	0.022	0	0.84	0.03	0.03	1.34
Concrete	0.9	0.022	0.022	0	0.84	0.03	0.03	0

Table 6-3. New parameters for rolling resistance surface factor (*CR*2) model with advanced tires.

	Vehicle Mass							
	≤ 2500 kg				> 2500 kg			
Surface Type	*a*0	*a*1	*a*2	*a*3	*a*0	*a*1	*a*2	*a*3
Asphalt	0.5	0.02	0.1	0	0.57	0.04	0.04	0
Concrete	0.5	0.02	0.1	0	0.57	0.04	0.04	0

Source: Sandberg (2007)

propulsion processes, environmental issues, aerodynamic/pavement friction efficiency, and congestion impacts. The technologies presented in this chapter (and Appendix D) have the potential of lowering vehicle operating costs. The majority of current research and development efforts that focus on engine and combustion technologies (including alternative fuels) have the potential for significantly reducing energy loss from vehicle operation. The cost of retrofitting existing fleets and the expected decreasing cost of these vehicles will determine the validity of the predicted VOC savings.

In summary, new technologies dealing with engines and combustion, alternative fuels, vehicle design and maintenance, and tires will affect vehicle operating costs. The effect of pavement conditions on vehicle operating costs will also be influenced by some of these technologies, specifically:

1. **New engine technology:** The HDM 4 model could be updated by changing the engine efficiency of vehicles to take into account these technologies. This study reports that new engine technologies will increase engine efficiency by 5% to 12% and concludes that the effect of roughness on fuel consumption would likely be unaffected by these technologies.
2. **Vehicle design:** The HDM 4 model could be updated by changing the aerodynamic characteristics of vehicles to take into account these technologies. This study reports that, when introducing all aerodynamic improvements in one vehicle, the reduction in aerodynamic drag could be as much as 23%. Every 2% reduction in aerodynamic drag will result in a 1% improvement in fuel efficiency. However, these reductions in fuel consumption are believed to be slightly affected by pavement conditions.
3. **Automatic gear shift for heavy trucks** could save as much as 10% in fuel consumption. However, these reductions in fuel consumption are believed to be slightly affected by pavement conditions.
4. **New tire technology:** The effect of new tire technology on fuel and tire consumption could be accommodated by modifying some of the tire-related variables in HDM 4 such as *b*11 through *b*13 and *CR*1. Alternatively, limited field tests (e.g., coast down test) could be conducted to estimate the new parameters *a*0 to *a*3 for *CR*2.

Although the new technologies will make vehicles more fuel efficient, the expenses of these technologies relative to current vehicles will be higher. Some of the hardware involved with new technologies might be sensitive to vehicle vibration such that more maintenance would be required under rougher roads than current technologies. On the other hand, newer technologies in suspension systems, axle designs, etc. could require less frequent maintenance. In either case, the mechanistic–empirical approach for repair and maintenance costs adopted in this study offers a methodology to further investigate this issue.

CHAPTER 7

Summary and Suggested Research

Summary

The objective of this research was to recommend models for estimating the effects of pavement conditions on vehicle operating costs. These effects are essential to sound planning and management of highway investments, especially under increasing infrastructure demands and declining budget resources. The recommended models reflect current vehicle technologies in the United States. The research focused on the cost components that are mostly affected by pavement conditions, namely, fuel consumption, repair and maintenance costs, and tire wear. The research does not include the effects of pavement conditions on changes in travel time, nor does it consider the safety-related or other implications of pavement conditions.

To accomplish the objective of this research, several tasks were performed. First, a large amount of data and information was collected, reviewed, and analyzed to identify the most relevant VOC models. The review was focused on research that has identified factors affecting vehicle operating costs including pavement conditions. Next, a large field investigation involving surveys to collect pavement condition data and field trials to collect fuel consumption and tire wear data were conducted. These data were used to calibrate and validate the HDM 4 fuel consumption and tire wear models for conditions in the United States and estimate the effects of pavement conditions on these components. The research also involved the collection of the repair and maintenance data of vehicle fleets from two departments of transportation (Michigan and Texas). The fleet data were used to update earlier research and develop mechanistic–empirical repair and maintenance models that consider the paved surface conditions encountered in the United States and address the full range of vehicle types. Finally, an effort was made to consider how all these models would be impacted by emerging vehicle technologies.

This study demonstrated that vehicle operating costs increase with pavement roughness for all classes of vehicles and types of pavements investigated. The most important cost components affected by roughness are fuel consumption followed by repair and maintenance, then tire wear.

For fuel consumption, the most important factor is surface roughness (measured using IRI). An increase in IRI of 1 m/km (63.4 in./mi) will increase the fuel consumption of passenger cars by about 2% irrespective of speed. For heavy trucks, this increase is about 1% at normal highway speed (96 km/h or 60 mph) and about 2% at low speed (56 km/h or 35 mph). Surface texture (measured by MPD) and pavement type do not affect the fuel consumption of any vehicle class except for heavy trucks. An increase in MPD of 1 mm will increase fuel consumption by about 1.5% at 88 km/h (55 mph) and about 2% at 56 km/h (35 mph).

For repair and maintenance, there is no effect of roughness up to IRI of 3 m/km. Beyond this range, an increase in IRI up to 4 m/km will increase repair and maintenance cost by 10% for passenger cars and heavy trucks. At IRI of 5 m/km, this increase is up to 40% for passenger cars and 50% for heavy trucks.

For tire wear, only the effect of roughness was considered. An increase in IRI of 1 m/km (63.4 in./mi) will increase the tire wear of passenger cars and heavy trucks by 1% at 88 km/h (55 mph).

Fuel Consumption

The effects of pavement conditions were investigated using five instrumented vehicles to measure fuel consumption over different pavement sections with different pavement conditions. These data were used to calibrate the HDM 4 fuel consumption model. The calibrated models were verified and were found to adequately predict the fuel consumption under different operating, weather, and pavement conditions. Table 7-1 presents the predictions by the calibrated HDM 4. The increase in fuel consumption was computed from the baseline IRI of 1 m/km (63.4 in./mi). The table was generated at 17°C (62.6°F) when the MPD is 1 mm (0.04 in) and grade is 0%.

Table 7-1. Effect of roughness on fuel consumption.

Speed	Vehicle Class	Fuel Consumption											
		Base (mL/km)	Adjustment Factors from the Base Value					Base (mpg)	Adjustment Factors from the Base Value				
		IRI (m/km)						IRI (m/km)					
		1	2	3	4	5	6	1	2	3	4	5	6
56 km/h (35 mph)	Medium car	70.14	1.03	1.05	1.08	1.10	1.13	33.53	0.97	0.95	0.93	0.91	0.88
	Van	76.99	1.01	1.02	1.03	1.04	1.05	30.55	0.99	0.98	0.97	0.96	0.95
	SUV	78.69	1.02	1.05	1.07	1.09	1.12	29.89	0.98	0.95	0.93	0.92	0.89
	Light truck	124.21	1.01	1.02	1.04	1.05	1.06	18.94	0.99	0.98	0.96	0.95	0.94
	Articulated truck	273.41	1.02	1.04	1.07	1.09	1.11	8.60	0.98	0.96	0.93	0.92	0.90
88 km/h (55 mph)	Medium car	83.38	1.03	1.05	1.08	1.10	1.13	28.21	0.97	0.95	0.93	0.91	0.88
	Van	96.98	1.01	1.02	1.03	1.04	1.05	24.25	0.99	0.98	0.97	0.96	0.95
	SUV	101.29	1.02	1.04	1.07	1.09	1.11	23.22	0.98	0.96	0.93	0.92	0.90
	Light truck	180.18	1.01	1.02	1.03	1.04	1.05	13.05	0.99	0.98	0.97	0.96	0.95
	Articulated truck	447.31	1.02	1.03	1.05	1.06	1.08	5.26	0.98	0.97	0.95	0.94	0.93
112 km/h (70 mph)	Medium car	107.85	1.02	1.05	1.07	1.09	1.12	21.81	0.98	0.95	0.93	0.92	0.89
	Van	128.96	1.01	1.02	1.03	1.03	1.04	18.24	0.99	0.98	0.97	0.97	0.96
	SUV	140.49	1.02	1.04	1.06	1.08	1.10	16.74	0.98	0.96	0.94	0.93	0.91
	Light truck	251.41	1.01	1.02	1.02	1.03	1.04	9.36	0.99	0.98	0.98	0.97	0.96
	Articulated truck	656.11	1.01	1.02	1.04	1.05	1.06	3.58	0.99	0.98	0.96	0.95	0.94

The analysis assumed that there is no interaction between the effect of roughness (unevenness) and surface texture given that their wavelength ranges are independent. The model showed pavement surface texture has an effect on fuel consumption only for heavier trucks. For example, a 1 mm decrease in MPD will result in a decrease in fuel consumption of 2.25% and 1.5% at 56 and 88 km/h (35 and 55 mph) speeds, respectively.

Considering the significance of vehicle fuel consumption, the reduction of it is one of the main benefits that should be considered in technical and economic evaluations of road improvements. This research showed that a decrease in pavement roughness by 1 m/km (63.4 in./mi) will result in a 3% decrease in the fuel consumption for passenger cars. This decrease would save about 6 billion gallons of fuel per year of the 200 billion gallons consumed annually by the 255 million vehicles in the United States. With today's gas prices, this fuel savings will amount to about $24 billion.

Tire Wear

The effects of pavement conditions on tire wear were investigated using field data. The HDM 4 tire wear model was calibrated to adequately predict the tire wear of passenger cars and articulated trucks.

Table 7-2 presents the increase in tire wear as a function of IRI for all vehicle classes at 56, 88, and 112 km/h (35, 55, and 70 mph) caused by a change in IRI from the baseline condition of 1 m/km (63.4 in./mi). The table was generated at 17°C (62.6°F) when the MPD is 1 mm (0.04 in) and the grade is 0%. These data show, for the same IRI value, that tire wear increases with increasing speed, and that the roughness effect is higher at higher speeds.

This research showed that a decrease in pavement roughness by 1 m/km (63.4 in./mi) will result in about a 1% decrease in the tire wear for passenger cars. Assuming that the average annual kilometrage (mileage) for a passenger car is 24,000 km (15,000 mi), the average tire life is 72,000 km (45,000 mi), and the average price of a tire is $100, the 255 million vehicles will consume about $34.0 billion per year in tire wear cost. Therefore, a decrease in IRI by 1 m/km (63.4 in./mi) will save $340 million per year.

Repair and Maintenance

Two different approaches for estimating repair and maintenance costs induced by pavement roughness were developed: (1) an empirical approach that introduced adjustment factors to update the tables reported in an earlier study and (2) a mechanistic–empirical approach that involves fatigue damage analysis using numerical modeling of vehicle vibration response. The results from the mechanistic–empirical approach were compared to the empirical results and were found to be very close up to an IRI of 5 m/km (typical IRI range in the United States), with a standard error of about 2%. Table 7-3 lists the increase in repair and maintenance costs per kilometer for all vehicle classes due to an IRI increase from the baseline condition IRI of 1 m/km (63.4 in./mi) for pavements with 0% grade.

A computer program was also developed to facilitate the use of the model. The program can be used to estimate repair and maintenance costs at the project and network levels. For project-level analysis, the actual road profile should be used to account for the effect of roughness features.

The results show that there is no effect of roughness on repair and maintenance costs up to an IRI of 3 m/km. Beyond

Table 7-2. Effect of roughness on tire wear rates.

Speed	Vehicle Class (number of wheels)	Tire Wear						
		Baseline Conditions (%/km)	Baseline Conditions (%/mi)	Adjustment Factors from the Baseline Conditions				
		IRI (m/km)						
		1		2	3	4	5	6
56 km/h (35 mph)	Medium car (4)	0.0013	0.0021	1.01	1.01	1.02	1.02	1.03
	Van (4)	0.0011	0.0017	1.00	1.01	1.01	1.02	1.02
	SUV (4)	0.0011	0.0017	1.01	1.02	1.03	1.04	1.05
	Light truck (4)	0.0012	0.0020	1.01	1.02	1.03	1.04	1.05
	Articulated truck (18)	0.0006	0.0010	1.01	1.01	1.02	1.02	1.03
88 km/h (55 mph)	Medium car (4)	0.0014	0.0022	1.01	1.02	1.03	1.04	1.05
	Van (4)	0.0013	0.0021	1.01	1.01	1.02	1.03	1.04
	SUV (4)	0.0013	0.0021	1.01	1.03	1.05	1.06	1.08
	Light truck (4)	0.0018	0.0029	1.01	1.02	1.04	1.05	1.06
	Articulated truck (18)	0.0007	0.0012	1.01	1.02	1.03	1.04	1.05
112 km/h (70 mph)	Medium car (4)	0.0015	0.0025	1.01	1.03	1.04	1.06	1.08
	Van (4)	0.0018	0.0028	1.01	1.02	1.03	1.04	1.04
	SUV (4)	0.0017	0.0027	1.02	1.04	1.06	1.08	1.10
	Light truck (4)	0.0029	0.0046	1.01	1.02	1.04	1.05	1.06
	Articulated truck (18)	0.0009	0.0015	1.01	1.02	1.03	1.04	1.06

this range, an increase in IRI up to 4 m/km will increase repair and maintenance costs by 10% for passenger cars and heavy trucks. At an IRI of 5 m/km, this increase is up to 40% for passenger cars and 50% for heavy trucks. Assuming that the average annual kilometrage (mileage) for a passenger car is 24,000 km (15,000 mi), the repair and maintenance of the 255 million US vehicles will cost about $244.8 billion per year. Therefore, a decrease in IRI by 1 m/km (63.4 in./mi) will save $24.5 billion to $73.5 billion per year in repair and maintenance cost.

As an example, assuming that about 14% of the US road network has an IRI higher than 3 m/km, the average annual

Table 7-3. Effect of roughness on repair and maintenance costs.

Speed	Vehicle Class	Repair and Maintenance Costs								
		Average* ($/km)	Average* ($/mi)	Baseline Conditions ($/km)	Baseline Conditions ($/mi)	Adjustment Factors from the Baseline Conditions				
				IRI (m/km)						
				1		2	3	4	5	6
56 km/h (35 mph)	Medium car	0.040	0.064	0.015	0.024	1.0	1.0	1.1	1.4	1.7
	Van	0.052	0.083	0.020	0.032	1.0	1.0	1.1	1.4	1.7
	SUV	0.052	0.083	0.020	0.032	1.0	1.0	1.2	1.7	2.3
	Light truck	0.058	0.092	0.021	0.034	1.0	1.0	1.2	1.7	2.2
	Articulated truck	0.124	0.199	0.046	0.074	1.0	1.0	1.1	1.5	1.8
88 km/h (55 mph)	Medium car	0.040	0.064	0.019	0.030	1.0	1.0	1.1	1.4	1.7
	Van	0.052	0.083	0.025	0.040	1.0	1.0	1.1	1.4	1.7
	SUV	0.052	0.083	0.025	0.040	1.0	1.0	1.2	1.7	2.3
	Light truck	0.058	0.092	0.029	0.046	1.0	1.0	1.2	1.7	2.2
	Articulated truck	0.124	0.199	0.063	0.101	1.0	1.0	1.1	1.5	1.8
112 km/h (70 mph)	Medium car	0.040	0.064	0.023	0.036	1.0	1.0	1.1	1.4	1.7
	Van	0.052	0.083	0.030	0.047	1.0	1.0	1.1	1.4	1.7
	SUV	0.052	0.083	0.030	0.047	1.0	1.0	1.2	1.7	2.3
	Light truck	0.058	0.092	0.035	0.057	1.0	1.0	1.2	1.7	2.2
	Articulated truck	0.124	0.199	0.077	0.123	1.0	1.0	1.1	1.5	1.8

1 m/km = 63.4 in./mi

*These costs are unit repair costs related only to damage from vibrations.

Table 7-4. Unit costs.

Vehicle Class	Unit Costs				
	Fuel Cost* ($/gal)	Fuel Cost* ($/L)	Tire Cost* ($/tire)	Repair and Maintenance Costs ($/mi)†	Repair and Maintenance Costs ($/km)†
Small car	$3.63	$0.96	$100	0.064	0.040
Medium car	$3.63	$0.96	$100	0.064	0.040
Large car	$3.63	$0.96	$100	0.064	0.040
Van	$3.63	$0.96	$150	0.083	0.052
Four-wheel drive	$3.63	$0.96	$150	0.083	0.052
Light truck	$3.63	$0.96	$175	0.083	0.052
Medium truck	$3.63	$0.96	$200	0.092	0.058
Heavy truck	$3.97	$1.05	$250	0.119	0.074
Articulated truck	$3.97	$1.05	$250	0.191	0.119
Mini bus	$3.63	$0.96	$150	0.199	0.124
Light bus	$3.63	$0.96	$175	0.083	0.052
Medium bus	$3.97	$1.05	$200	0.092	0.058
Heavy bus	$3.97	$1.05	$250	0.119	0.074
Coach	$3.97	$1.05	$250	0.191	0.119

*These costs are estimates for 2011.
†These costs are repair and maintenance costs caused by roughness only and are estimated based on data from 2007.

mileage for a passenger car is 24,000 km (15,000 mi), and a total of 255 million cars travel on the US road network, then the repair and maintenance cost for passenger cars in the United States would range from $15 billion to $25 billion per year [for vehicle speeds ranging from 56 to 112 km/h (35 to 70 mph), respectively].

Table 7-4 lists the unit costs used in this study. Table 7-5 summarizes the change in vehicle operating costs per kilometer (mile) for all vehicle classes due to IRI changes from the baseline condition of 1 m/km (63.4 in./mi). These costs were computed using the default values.

Applicability to Emerging Technologies

Growing demand for fuel-efficient vehicles accelerated the research and development (R&D) efforts to meet this demand. New engine and combustion technologies, alternative fuels, vehicle design and maintenance, and tire technologies will

Table 7-5. Effect of roughness on vehicle operating costs.

Speed	Vehicle Class	Vehicle Operating Costs						
		Baseline Conditions (¢/km)	Baseline Conditions (¢/mi)	Adjustment Factors from the Baseline Conditions				
		IRI (m/km)						
		1		2	3	4	5	6
56 km/h (35 mph)	Medium car	8.8	14.0	1.02	1.04	1.08	1.15	1.22
	Van	10.0	16.1	1.01	1.02	1.05	1.11	1.18
	SUV	10.2	16.3	1.02	1.03	1.09	1.20	1.34
	Light truck	14.9	23.9	1.01	1.02	1.06	1.13	1.22
	Articulated truck	36.1	57.7	1.02	1.03	1.07	1.13	1.19
88 km/h (55 mph)	Medium car	10.5	16.8	1.02	1.04	1.08	1.15	1.22
	Van	12.6	20.2	1.01	1.01	1.05	1.11	1.17
	SUV	13.0	20.8	1.02	1.03	1.09	1.20	1.32
	Light truck	21.6	34.6	1.01	1.02	1.05	1.12	1.20
	Articulated truck	56.7	90.7	1.01	1.02	1.05	1.10	1.15
112 km/h (70 mph)	Medium car	13.3	21.3	1.02	1.03	1.07	1.14	1.21
	Van	16.5	26.5	1.01	1.01	1.04	1.10	1.16
	SUV	17.6	28.2	1.01	1.03	1.08	1.18	1.29
	Light truck	30.1	48.1	1.01	1.01	1.04	1.10	1.17
	Articulated truck	81.2	130.0	1.01	1.02	1.04	1.08	1.13

1 m/km = 63.4 (in./mi)

affect vehicle operating costs. The effects of pavement conditions on vehicle operating costs will also be influenced by some of these technologies, specifically:

- **New engine technology:** The HDM 4 model could be updated by changing the engine efficiency of vehicles to take into account these technologies. This study reports that new engine technologies will increase the engine efficiency by 5% to 12% and concludes that the effect of roughness on fuel consumption would likely be unaffected by these technologies.
- **Vehicle design:** The HDM 4 model could be updated by changing the aerodynamic characteristics of vehicles to take into account these technologies. This study reports that, when introducing all aerodynamic improvements in one vehicle, the reduction in aerodynamic drag could be as much as 23%. Every 2% reduction in aerodynamic drag will result in a 1% improvement in fuel efficiency.
- **Automatic gear shift for heavy trucks** could save as much as 10% in fuel consumption.
- **New tire technology:** Use of the calibrated HDM 4 fuel and tire consumption model and the coefficients for new tires will help account for emerging tire technology.

In addition, even though the new technologies will make vehicles more fuel efficient, the expenses of these technologies relative to current vehicles will be higher. Some of the hardware involved with new technologies might be sensitive to vehicle vibration that would require more maintenance under rougher roads than current technologies. The work done in this study on repair and maintenance costs might offer a methodology to investigate this issue in the future.

Suggested Research

The results of this study lead to the following suggestions:

- The fuel consumption model suggests a constant (dFuel) to take into account the effect of congestion and speed change cycles, but it does not explicitly formulate the calculation of the constant. Further research is needed to incorporate the effect of congestion on fuel consumption.
- In this study, the effect of pavement deflection/stiffness on fuel consumption was not investigated. Further research is needed to investigate this effect.
- The mechanistic–empirical approach to estimate the effects of pavement conditions on repair and maintenance costs only involves passenger cars and articulated trucks. Then, it uses the results from an earlier study to estimate the costs for the other vehicle classes. Further research is needed to estimate quarter-car model parameters for other vehicle classes.
- Since the tire wear field tests were conducted only for passenger cars and articulated trucks with conventional tires, tire wear field tests for other vehicle classifications and for emerging low fuel-consumption tires are needed.
- The tire wear model could be improved by enhancing the modeling of tire–pavement interaction and loss of rubber due to friction.
- This study focused on the effects of pavement conditions on fuel consumption, tire wear, and repair and maintenance costs. However, the research did not include the effects of pavement conditions on changes in travel time, nor did it consider the safety-related, environmental, or other implications of pavement conditions. Therefore, research is needed to investigate these effects.
- The operation of trucks not only involves fuel, tire, and repair and maintenance costs but also the damage induced to the products during transportation. Further research will help estimate the effects of pavement conditions on damage to transported goods.
- The fuel consumption model uses an empirical relationship between rolling resistance and IRI. The model could be further improved by developing a mechanistic formulation for predicting the effect of roughness on fuel consumption. For example, the vehicle models could be used to predict the dynamic load, which can then be used to replace the static weight in the model.

References

Abdullah, S., Giacomin, J. A., and Yates, J. R. (2004). "Identification of Fatigue Damaging Events Using a Wavelet-Based Fatigue Data Editing Algorithm," *Proceeding of the Institution of Mechanical Engineers, Part D, Journal of Automobile Engineering,* Vol. 218, pp. 243–258.

American Association of State Highway and Transportation Officials (1977). "AASHTO Red Book—A Manual on User Benefit Analysis of Highway and Bus Transit Improvements."

Barnes, G., and Langworthy, P. (2004). "Per Mile Costs of Operating Automobiles and Trucks." *Transportation Research Record: Journal of the Transportation Research Board, No. 1864,* Transportation Research Board of the National Academies, pp. 71–77.

Becker, M. A. (1972). "Selection of Optimal Investment Strategies for Low Volume Roads," M.S. Dissertation: Department of Civil Engineering, Massachusetts Institute of Technology.

Bein, P. (1993). "VOC Model Needs of a Highways Department," *Road and Transport Research,* Vol. 2, pp. 40.

Bennett, C. R. (1989). "The New Zealand Vehicle Operating Cost Model," *RRU Bulletin B2,* Transit New Zealand, Willington.

Bennett, C. R., and Greenwood, I. D. (2003a). *Volume 5: HDM-4 Calibration Reference Manual, International Study of Highway Development and Management Tools (ISOHDM),* World Road Association (PIARC), ISBN 2-84060-103-6.

Bennett, C. R., and Greenwood, I. D., (2003b). *Volume 7: Modeling Road User and Environmental Effects in HDM-4, Version 3.0, International Study of Highway Development and Management Tools (ISOHDM),* World Road Association (PIARC), ISBN 2-84060-103-6.

Berthelot, C. F., Sparks, G. A., Blomme, T., Kajner, L., and Nickeson, M. (1996). "Mechanistic-Probabilistic Vehicle Operating Cost Model," *Journal of Transportation Engineering,* 122(5), pp. 337–341.

Biggs, D. C. (1987). "Estimating Fuel Consumption of Light to Heavy Vehicles," ARRB Internal Report AIR 454-1, Australian Road Research Board, Nunawading.

Biggs, D. C. (1988). "ARFCOM—Models for Estimating Light to Heavy Vehicle Fuel Consumption," Research Report ARR 152, Australian Road Research Board, Nunawading.

Bogsjö, K. (2006). "Development of Analysis Tools and Stochastic Models of Road Profiles Regarding Their Influence on Heavy Vehicle Fatigue," *Vehicle System Dynamics,* Vol. 44, Supplement, pp. 780–790.

British Department of Transportation (1993). *COBA User's Manual,* Department of Transport, UK.

Brown, E. R., Cooley, L. A., Jr., Hanson, D., Lynn, C., Powell, B., Prowell, B., and Watson, D. (2002). "NCAT Test Track Design, Construction and Performance," National Transportation Symposium, Auburn, Alabama, November 13–14.

Bureau of Transportation Statistics (2010). "Highway Statistics," Washington, DC: Annual issues, Table VM-1.

Carpenter, P., and Cenek, P. (2000). "Tyre Wear Modelling for HDM-4," Report prepared by Opus International Consultants Limited, Central Laboratories, Lower Hutt, Central Laboratories Report, 98-529474, Prepared for ISOHDM.

Cebon, D. (1999). *Handbook of Vehicle-Road Interaction,* Swets & Zeitlinger, Lisse, Netherlands.

Chesher, A., and Harrison, R. (1987). *Vehicle Operating Cost: Evidence from Developing Countries,* World Bank Publications. Washington, DC.

Claffey, P. J. (1971). *NCHRP Report 111: Running Costs of Motor Vehicles as Affected by Road Design and Traffic,* Transportation Research Board, Washington, DC.

de Weille, J. (1966). "Quantification of Road User Savings." World Bank Staff Occasional Paper No. 2, Washington, DC.

du Plessis, H. W. (1989). "An Investigation of Vehicle Operating Cost Relationships for Use in South Africa," *Road Roughness Effects on Vehicle Operating Costs: Southern Africa Relations for Use in Economic Analyses and in Road Management Systems.* CSIR, Pretoria.

Federal Highway Administration (2008). Highway Statistics, US Department of Transportation. www.fhwa.dot.gov/policy/ohpi/hss/index.htm

Fuchs, H. O., and Stephens, R. I. (1980). *Metal Fatigue in Engineering,* John Wiley & Sons, pp. 155–156.

Gillespie, T. D. (1985). Heavy Truck Ride, SP-607, Society of Automotive Engineers, Warrendale, PA.

Gillespie, T. D., and Sayers, M. (1981). "Role of Road Roughness in Vehicle Ride," *Transportation Research Record 836,* Transportation Research Board, National Research Council, Washington, DC, pp. 15–20.

Governors Highway Safety Association (Accessed May 2011). www.motorists.org/speed-limits/state-chart

Hammarström, U. (1994). "Description of VETO, EVA and HDM III with Regard to Vehicle Effects and Proposals for HDM-4." English translation of VTI internal report, Linköping.

Hammarström, U., and Henriksson, P. (1994). "Reparationskostnader för bilar Kalibrering av Varldsbankens HDM-3-samband för svenska förhallanden." VTI Meddelande Nr. 743, Swedish Road and Traffic Institute, Linköping.

Hammarström, U., and Karlsson, B. (1991). "VETO: A Computer Program for Calculating Transport Costs as a Function of Road Standard." English translation of VTI Report 501, Swedish Road and Traffic Institute, Linkoping.

Henry, J. J. (2000). *NCHRP Synthesis of Highway Practice 291: Evaluation of Pavement Friction Characteristics,* Transportation Research Board, National Research Council, Washington, DC.

Kennedy, P., Gadd, J., and Moncrieff, I. (2002). *Emission Factors for Contaminants Released by Motor Vehicles in New Zealand,* prepared for Ministry of Transport, New Zealand.

Kilareski, W. P., Mason, J. M., Gittings, G. L., Antle, C. E., Wambold, J. C., Folmar, D. J., and Brydia, R. E. (1990). USA Road Surface and Use Characteristics Catalog, Prepared for Chrysler Motors Corporation, The Chrysler Challenge Fund, Pennsylvania Transportation Institute, PTI 9018.

Klaubert, E. C. (2001). Highway Effects on Vehicle Performance, FHWA-RD-00-164, US Department of Transportation, Federal Highway Administration, Washington, DC.

Kouta, R. (1994). "Methods of Correlation by Solicitations for Tracks of Vehicle Tests," Ph.D. Dissertation: Mechanical Engineering, Ecole doctorale des sciences pour l'ingénieur de Lyon, France.

Legret, M., and Pagotto, C. (1999). "Evaluation of Pollutant Loadings in the Runoff Waters from a Major Rural Highway," *The Science of the Total Environment,* 235: 143–150.

Lundstrom, A. (2010). "The Challenges for Heavy Vehicles," Presentation at the 11th International Symposium on Heavy Vehicle Weights and Dimensions, Melbourne, Australia, 14–17 March.

Marcondes, J. A., Synder, M. B., and Singh, S. P. (1992). "Predicting Vertical Acceleration in Vehicle Through Road Roughness," *Journal of Transportation Engineering,* Vol. 118, No.1, pp. 33–49.

Matsuishi, M., and Endo, T. (1968). "Fatigue of Metals Subjected to Varying Stress," Japan Society of Mechanical Engineering.

McFarland, W. F., Memmott, J. L., and Chui, M. L. (1993). "Microcomputer Evaluation of Highway User Benefits," NCHRP Project 7-12, Texas Transportation Institute, College Station, TX.

Michelin (2003). "The Tyre Encyclopedia Volume 3," France.

Muschack, W. (1990). "Pollution of Street Run-off by Traffic and Local Conditions," Science of the Total Environment, 93, 419–431.

National Association of Australian State Road Authorities (1978). *A Study of the Operation of Large Combination Vehicles (Road Trains),* Working Party Report No. I, National Association of Australian State Road Authorities.

National Center for Asphalt Technology (2010). www.pavetrack.com, Official website of the NCAT Test Track.

National Highway Traffic Safety Administration (2010). Average Fuel Economy Standards, Passenger Cars and Light Trucks, MY 2011–2015.

Papagiannakis, A. T. (2000). *NCHRP Research Results Digest 246: Methodology to Improve Pavement-Investment Decisions.* Transportation Research Board, National Research Council, Washington, DC.

Poelman, M. A., and Weir, R. P. (1992). "Vehicle Damage Induced by Road Surface Roughness," *Vehicle, Tire, Pavement Interface,* ASTM STP 1164, J. J. Henry and J. C. Wambold, eds., American Society for Testing and Materials, Philadelphia, pp. 97–111.

Prem, H. (2000). "A Road Profile-Based Truck Ride Index," Austroads Publication No. AP-R177/00, Austroads: Sydney, New South Wales, Australia.

Repair Pal (Accessed September 2009). repairpal.com

Robson, J. D. (1979). "Road Surface Description and Vehicle Response," *International Journal of Vehicle Design,* 1(1), pp. 25–35.

Rouillard, V. (2008). "Generating Road Vibration Test Schedules from Pavement Profiles for Packaging Optimization," *Packaging Technology and Science,* Vol. 21, pp. 501–514.

Rychlik, I. (1987). "A New Definition of the Rainflow Cycle Counting Method," *International Journal of Fatigue,* Vol. 9, pp. 119–121.

Sandberg, U., and Ejsmont, J. A. (2002). *Tyre/Road Noise Reference Book,* ISBN 91-631-2610-9, Informex, Kisa, Sweden.

Sandberg, U. S. I. (1990). "Road Macro- and Megatexture Influence on Fuel Consumption," ASTM STP 1031, pp. 460–479.

Sandberg, U. S. I. (2007). "Vägytans inverkan på trafikbulleremission och rullmotstånd. Slutrapport för projektet: Kunskapsinsamling om lågbullerbeläggningar" (Vägverket nr BY 20A 2006:6862/VTI projekt nr 50588). Statens väg- och transportforskningsinstitut. Linköping.

Sayers, M. W., and Karamihas, S. M. (1998). *The Little Book of Profiling,* UMTRI.

UK Environment Agency (1998). Tyres and the Environment, United Kingdom Environment Agency.

Ullidtz, P. (1987). *Pavement Analysis,* Developments in Civil Engineers, Vol. 19, Elsevier Science Publishing Company Inc., pp. 257–259.

US Department of Energy (2006). "Road Map and Technical White Papers," 21st Century Truck Partnership, December.

US Department of Energy (Accessed September 2010). "Energy Efficient Technologies—Engine Technologies," Energy Efficiency and Renewal Energy, Washington, DC. www.fueleconomy.gov/feg/tech_engine_more.shtml

US Department of Energy (2006). Basic Research Needs for Clean and Efficient Combustion of 21st Century Transportation Fuels, science.energy.gov/~/media/bes/pdf/reports/files/ctf_rpt.pdf

VTRIS (2005). "Vehicle Travel Information System," fhwapap07.fhwa.dot.gov/vtris/

Watanatada, T. (1987). *Highway Design and Maintenance Standards Model (HDM) Model Description and User's Manual—Release II,* Transportation, Water and Telecommunications Department Report, the World Bank, Washington, DC.

Watanatada, T., Harral, C. G., Paterson, W. D. O., Dhareshwar, A. M., Bhandari, A., and Tsunokawa, K. (1987). *The Highway Design and Maintenance Standards Model, Volume 1: Description,* The World Bank, John Hopkins University Press.

Winfrey, R. (1969). *Economic Analysis for Highways,* International Textbook Company, Scranton, PA.

Zaniewski, J. P., Butler, B. C., Cunningham, G., Elkins, G. E., Paggi, M. S., and Machemehl, R. (1982). "Vehicle Operating Costs, Fuel Consumption, and Pavement Type and Condition Factors," FHWA-PL-82-001, Texas Research and Development Foundation.

ATTACHMENT

User Guide for Vehicle Operating Cost Model

The vehicle operating cost (VOC) model is an engineering software application that allows you to calculate vehicle operating costs at the network and project levels. For network analysis, data for traffic, environmental, and pavement conditions [e.g., international reference index (IRI), mean profile depth (MPD), and pavement type) are the input to the model. For project analysis, profiles can be imported in text format and the model will calculate the IRI. Entire analysis projects can be saved, which preserves user information and analysis inputs. After analyses have been performed, you can export a report of the results of any analyses. The purpose of this document is to describe all software operations.

Software Installation

Hardware

While the VOC model should run on any system from the past several years, the following systems are recommended, at a minimum:

- 2 GHz processor,
- 2 GB RAM, and
- 1024 × 768 display resolution.

Software

Supported operating systems are Microsoft® Windows™ XP Professional Service Pack 3+, Windows Vista, and Windows 7.

The VOC model is a Microsoft Excel file with macros. Macros are written in Visual Basic. Microsoft Excel 2003 or more recent is required.

Installation

Once the installation kit is launched, the installation wizard will run automatically. To complete the process, click first on the "*MATLAB Component Runtime Installer*" link (Figure 1). A new window will open. Follow the steps to copy the files necessary for the software to work. Then, to install the software, click on the "*VOC Module Setup*" link in the installation wizard (Figure 1). You will need to unzip the file to a preferred location on the hard drive. Once the file is unzipped, click on the "*VOC Module*" Excel spreadsheet to launch the program. You will also be able to see an example of project-level analysis data and the data collected as part of NCHRP Project 1-45.

Figure 1. Installation wizard.

Getting Started

To make sure that the software is running, the security level for Excel must be set to "Medium" or "Low." Figure 2a shows the path to follow to change the security level in Excel 2003. For Excel 2007, you should go to the Developer tab and select "Macro security." Figure 2b shows how to change the security level in Excel 2007 and up.

Home Screen

Figure 3 shows the home screen of the VOC model. This is the starting screen when no project is currently open. It consists of two main sections: analysis levels (i.e., project or network levels) and unit system (i.e., US customary units or International System of units). You should choose an option from each section and click on the "*Run*" button, which will open the main spreadsheet.

The VOC model calculates vehicle operating costs based on traffic and highway conditions. Three components are included in cost calculations (fuel consumption, tire wear, and repair and maintenance cost).

The variables used to predict consumption rates of each VOC component include:

- IRI,
- Texture,
- Grade,
- Superelevation,
- Pavement type,
- Speed, and
- Temperature.

Network-Level Analysis

The general algorithm for estimating vehicle operating costs at the network level is:

$$VOC = VMT \times \sum_{i=1}^{3} (\text{Rate} \times \text{Price})_i \quad (1)$$

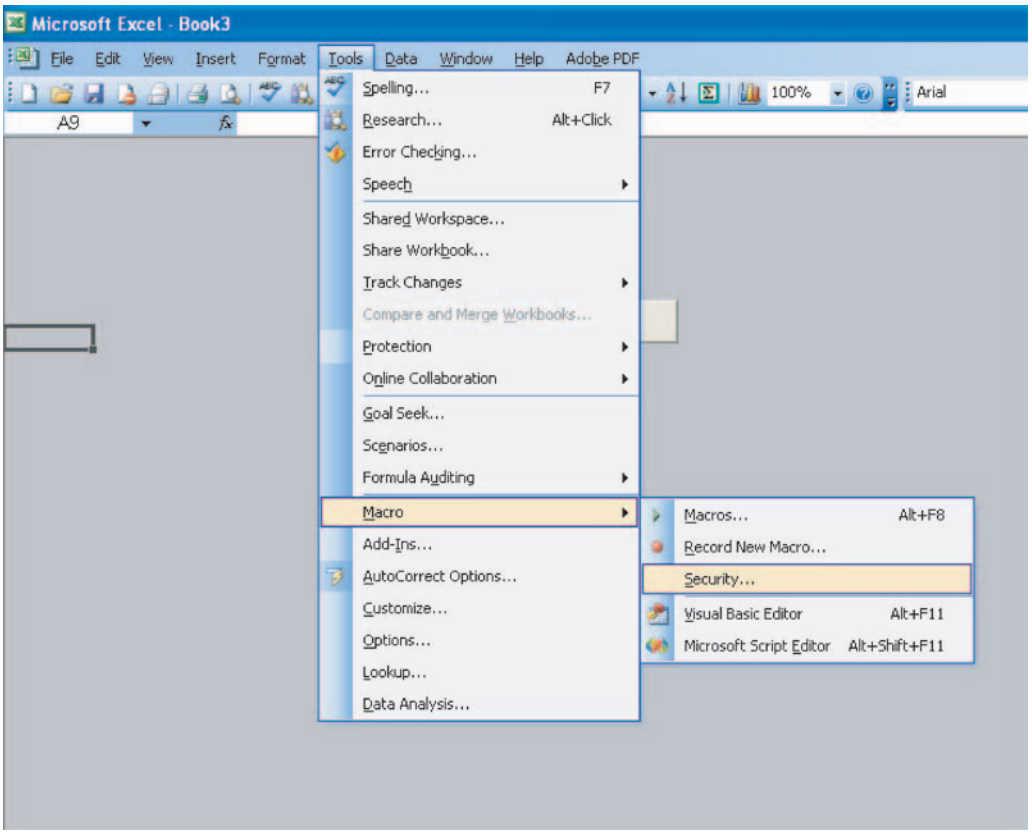

(a) For Microsoft Excel 2003

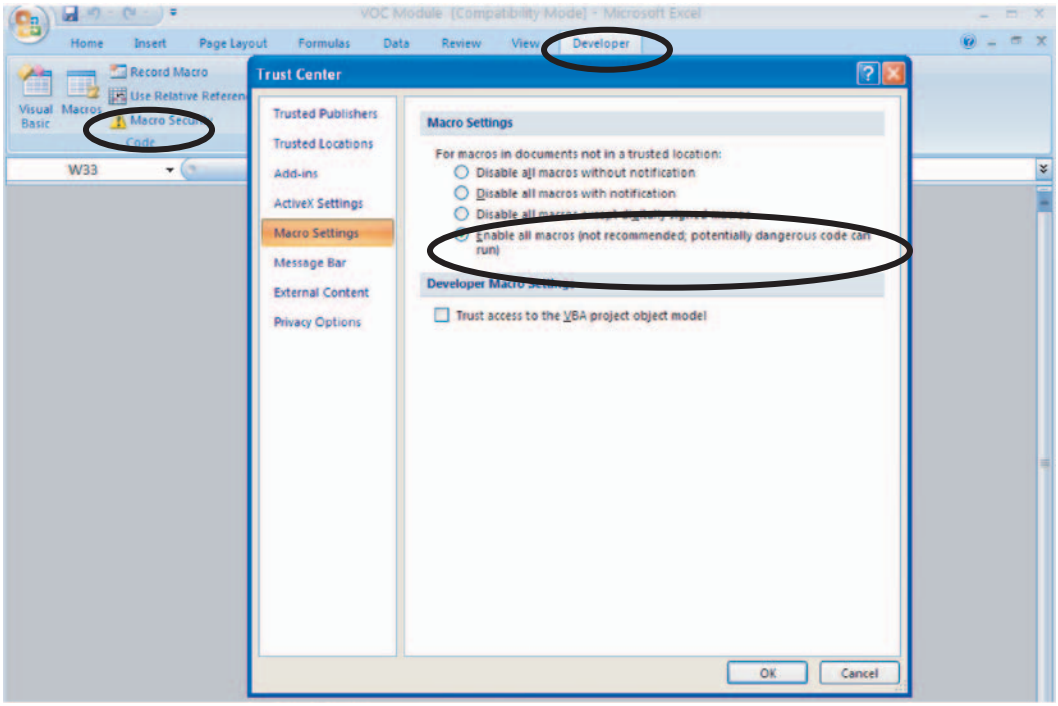

(b) For Microsoft Excel 2007 and up

Figure 2. Set up of the security level.

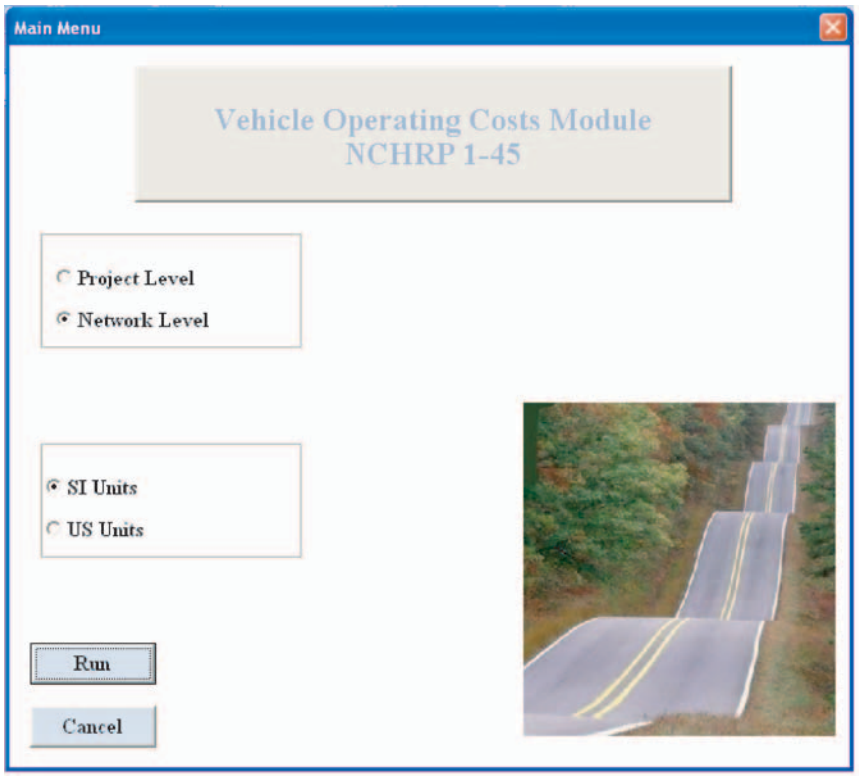

Figure 3. Home screen.

where:

VOC = Vehicle operating cost
VMT = Vehicle miles traveled (mi)
$Rate$ = Consumption rate
$Price$ = Unit price
i = Index for VOC components (fuel consumption, tire wear, and repair and maintenance costs)

At the network level, a grade of 0% and a superelevation of 0% are reasonable assumptions to calculate VOC savings unless there is a change in the radius of curves or grades.

To take into account traffic, input the total vehicle miles traveled (VMT) and the traffic distribution. If the traffic distribution is different for each scenario, click on the "*Traffic Distributions*" button to open a new spreadsheet and provide the distributions in each row. Then, click on the "*Return*" button. Delete any value in the "*Percentage*" column.

To calculate vehicle operating costs, click on the "Run" button. Two new spreadsheets will be created: "*Partial Costs*" and "*Total Costs.*" To save the results, click on the "Export" button, which opens a new screen asking the user to choose a file name and its path. Then, results can be exported to Excel using the "Save" button. Enter a file name followed by the extension ".xls" to export to an Excel file (Figure 4).

Project-Level Analysis

The general algorithm for estimating vehicle operating costs at the project level is:

$$VOC = 365 * \text{Distance} \times \text{AADT} \times \sum_{i=1}^{3} (\text{Rate} \times \text{Price})_i \quad (2)$$

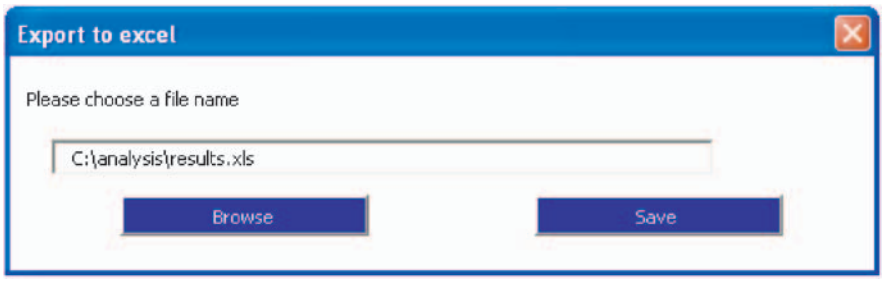

Figure 4. Export screen.

where:

VOC = Vehicle operating cost
$AADT$ = Average annual daily traffic
$Distance$ = Project length
$Rate$ = Consumption rate
$Price$ = Unit price
i = Index for VOC components (fuel consumption, tire wear, and repair and maintenance costs)

You will have two options:

1. Import the raw profile of the project so that the software will calculate the IRI every 0.16 km (0.1 mi), or
2. Input the IRI and section length.

For option 1, click on the "Import" button. A new screen will open asking you to choose a file name and its path (Figure 5). To look for the file, click on the "Browse" button (Figure 6). After locating the raw profile file (which should have the extension ".txt"), click on the "Open" button. The software will calculate IRI every 0.16 km (0.1 mi) and copy it to the input column. It should be noted that the profile elevation should be in inches. For option 2, you will have to input the IRI and the length of the section.

At the project level, a grade of 0% and a superelevation of 0% are reasonable assumptions to calculate VOC savings unless there is a change in the radius of curves or grades. To take into account traffic, input the AADT and the traffic distribution.

To calculate vehicle operating cost, click on the "Run" button. Two new spreadsheets will be created: "*Partial Costs*" and "*Total Costs.*" To save the results, the user should click on the "Export" button, which opens a new screen asking the user to choose a file name and its path. Then, results can be exported to Excel using the "Save" button. Enter a file name followed by the extension ".xls" to export to Excel file (Figure 7).

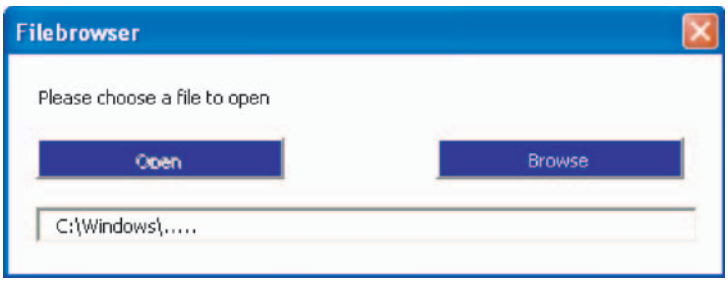

Figure 5. Import screen.

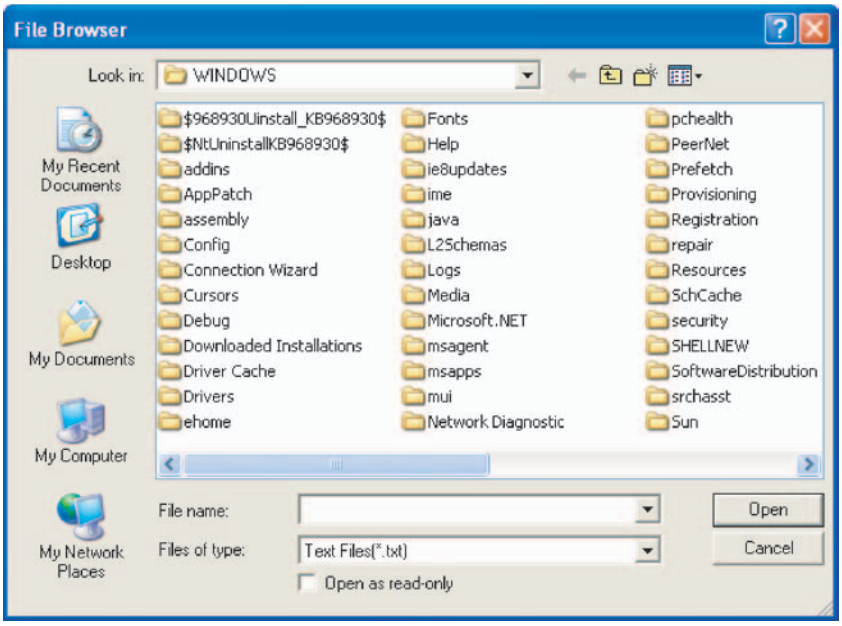

Figure 6. File browsing screen.

Examples

This section shows examples of how the VOC models will be used in practice. Three different examples are presented for (1) deterministic analysis, (2) project-level analysis, and (3) network-level analysis. The default values for vehicle characteristics used in these examples are presented in Chapters 3 through 5 of *NCHRP Report 720.* The unit costs are presented in Table 7-4. The software developed in this study was used to generate the results presented below.

Example 1: Deterministic Analysis

In this example, the sensitivity of the total vehicle operating cost to pavement conditions at 56, 88, and 112 km/h (35, 55 and 70 mph) is investigated. The pavement conditions considered are IRI and texture. IRI is a measurement of "roughness" that has a wavelength of 0.5 m (1.65 ft) and more. Texture refers to the categories of microtexture, macrotexture, and megatexture.

Effect of Roughness on Vehicle Operating Cost

The effect of pavement roughness (IRI) on vehicle operating cost is estimated for all vehicle classes using the models developed in this study. Figures 8 through 10 show examples of fuel, tire, and repair and maintenance costs expressed in cents per kilometer. Table 1 presents examples

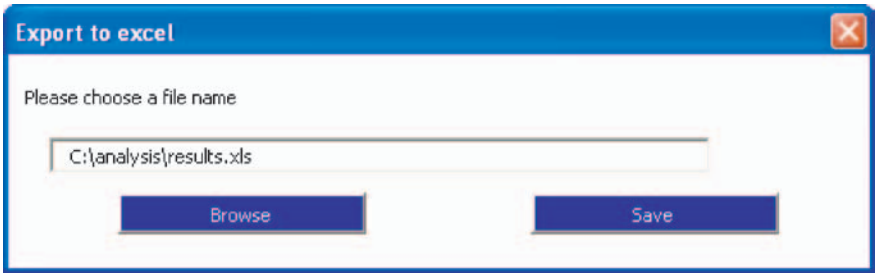

Figure 7. Export screen.

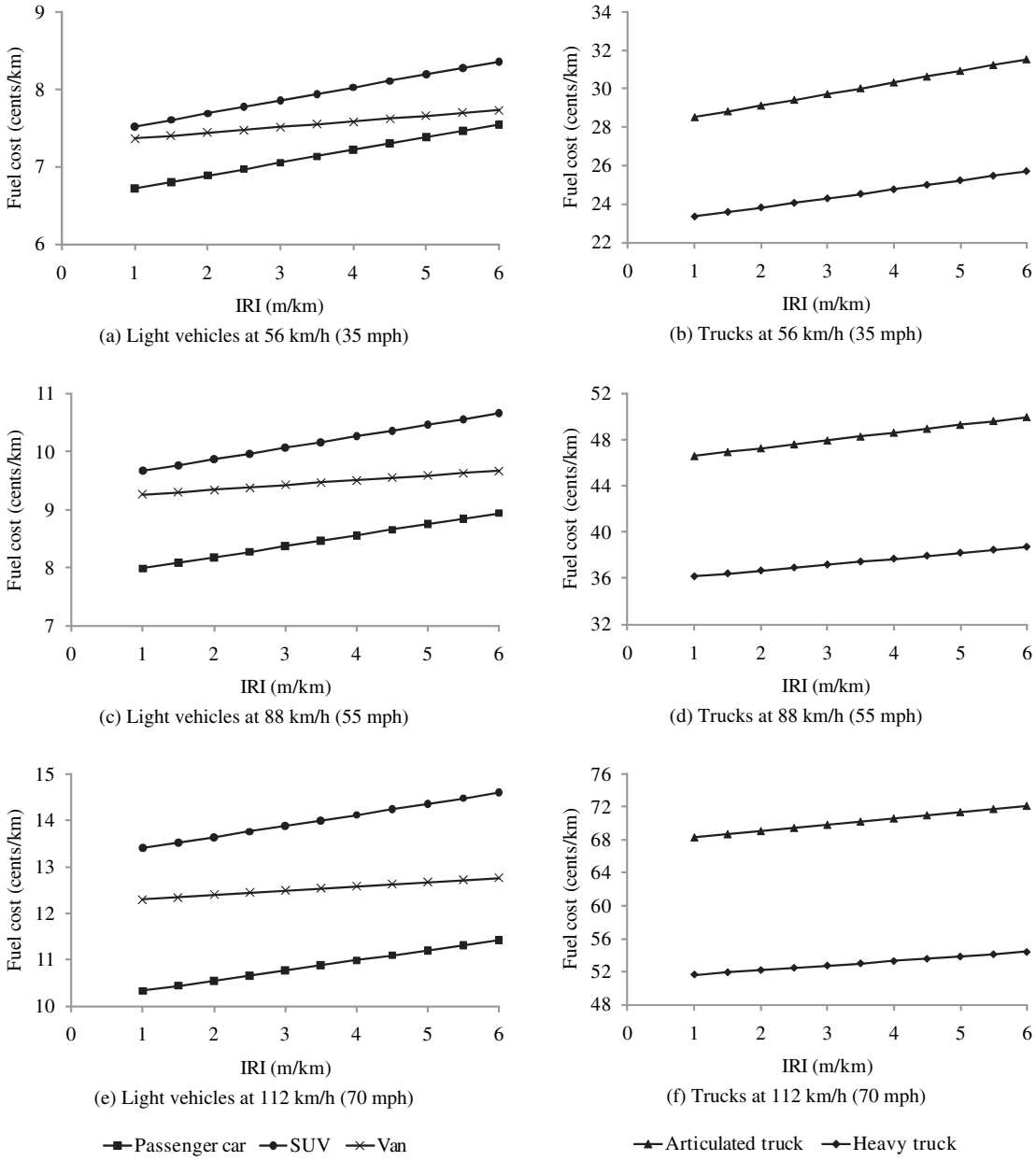

Figure 8. Effect of roughness on fuel costs.

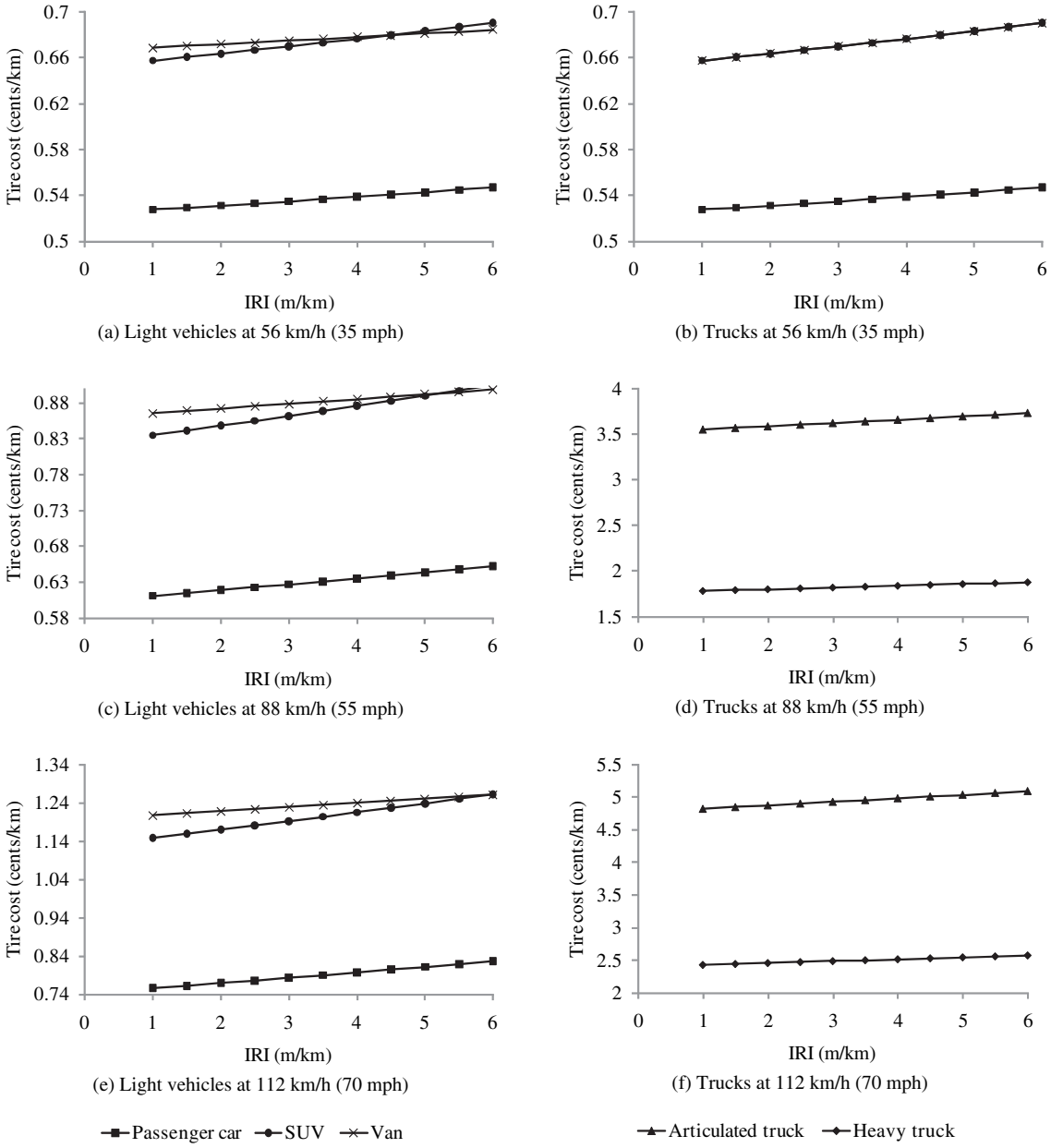

Figure 9. Effect of roughness on tire costs.

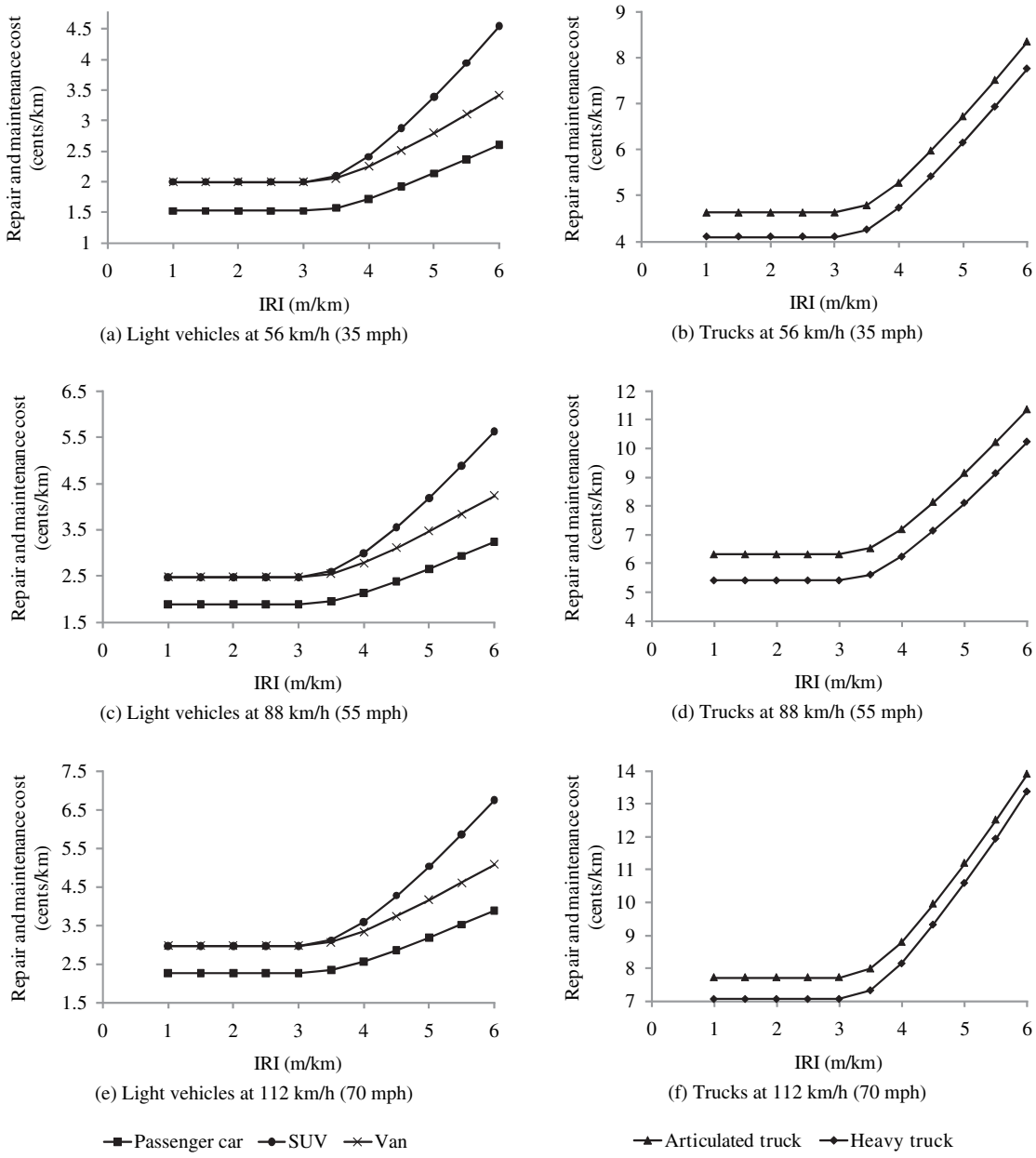

Figure 10. Effect of roughness on repair and maintenance costs.

of total cost expressed in cents per kilometer. The figures and the table were generated at 17°C (62.6°F), with mean profile depth of 1 mm (0.04 in.) and grade of 0%.

Effect of Texture on Vehicle Operating Cost

The effect of pavement surface texture (MPD) on vehicle operating cost is investigated for all vehicle classes using the models developed in this study. Table 2 presents examples of total cost expressed in cents per kilometer.

Discussion

The combined effect of MPD and IRI can be predicted by multiplying the roughness and texture factors. For example, if you would like to estimate the total vehicle operating cost for IRI = 3 m/km (190 in./mi) and MPD = 2 mm, for an articulated truck at 88 km/h (55 mph),

Table 1. Effect of roughness on vehicle operating cost.

Speed	Vehicle Class	Total Vehicle Operating Costs per Vehicle (¢/km) IRI (m/km) 1	1.5	2	2.5	3	3.5	4	4.5	5	5.5	6
56 km/h (35 mph)	Passenger Car	8.8	8.9	8.9	9.0	9.1	9.2	9.5	9.8	10.1	10.4	10.7
	Van	10.0	10.1	10.1	10.1	10.2	10.3	10.5	10.8	11.1	11.5	11.8
	SUV	10.2	10.3	10.3	10.4	10.5	10.7	11.1	11.7	12.3	12.9	13.6
	LT	15.0	15.1	15.1	15.2	15.3	15.5	15.9	16.4	17.0	17.6	18.2
	HT	28.8	29.1	29.3	29.6	29.8	30.2	30.9	31.8	32.8	33.8	34.9
	AT	35.9	36.2	36.5	36.9	37.2	37.6	38.4	39.5	40.5	41.6	42.8
88 km/h (55 mph)	Passenger Car	10.5	10.6	10.7	10.8	10.9	11.0	11.3	11.7	12.0	12.4	12.8
	Van	12.6	12.6	12.7	12.7	12.8	12.9	13.2	13.5	13.9	14.4	14.8
	SUV	13.0	13.1	13.2	13.3	13.4	13.6	14.1	14.8	15.5	16.3	17.2
	LT	21.8	21.9	22.0	22.0	22.1	22.3	22.9	23.6	24.4	25.2	26.1
	HT	43.3	43.6	43.8	44.1	44.4	44.8	45.7	46.9	48.1	49.4	50.8
	AT	56.5	56.8	57.2	57.5	57.9	58.4	59.5	60.8	62.1	63.6	65.1
112 km/h (70 mph)	Passenger Car	13.4	13.5	13.6	13.7	13.8	14.0	14.3	14.8	15.2	15.6	16.1
	Van	16.5	16.5	16.6	16.6	16.7	16.8	17.2	17.6	18.1	18.6	19.1
	SUV	17.5	17.6	17.8	17.9	18.0	18.3	18.9	19.7	20.6	21.6	22.6
	LT	30.3	30.4	30.5	30.6	30.7	31.0	31.6	32.5	33.4	34.4	35.5
	HT	61.1	61.4	61.7	62.0	62.3	62.9	64.0	65.4	67.0	68.7	70.4
	AT	80.9	81.3	81.7	82.1	82.5	83.2	84.4	85.9	87.6	89.3	91.1

1 km = 0.62 mi; 1 mm = 0.039 in.; 1 m/km = 63.4 in./mi; MPD = 1 mm, grade = 0%; temperature = 17°C (62.6°F).

Table 2. Effect of texture on vehicle operating cost.

Speed	Vehicle Class	Total Vehicle Operating Cost per Vehicle (¢/km) Mean Profile Depth (mm) 1	1.5	2	2.5	3	3.5	4	4.5	5	5.5	6
56 km/h (35 Mph)	Passenger Car	8.8	8.8	8.8	8.8	8.8	8.9	8.9	8.9	8.9	8.9	8.9
	Van	10.0	10.1	10.1	10.1	10.2	10.2	10.3	10.3	10.3	10.4	10.4
	SUV	10.2	10.2	10.2	10.2	10.2	10.3	10.3	10.3	10.3	10.3	10.3
	LT	15.0	15.1	15.1	15.2	15.3	15.4	15.4	15.5	15.6	15.7	15.7
	HT	28.8	29.1	29.3	29.6	29.8	30.0	30.3	30.5	30.8	31.0	31.2
	AT	35.9	36.2	36.5	36.9	37.2	37.5	37.8	38.1	38.4	38.7	39.0
88 km/h (55 mph)	Passenger Car	10.5	10.5	10.5	10.5	10.6	10.6	10.6	10.6	10.6	10.7	10.7
	Van	12.6	12.6	12.7	12.7	12.8	12.8	12.9	12.9	13.0	13.0	13.0
	SUV	13.0	13.0	13.0	13.0	13.1	13.1	13.1	13.1	13.1	13.2	13.2
	LT	21.8	21.9	22.0	22.0	22.1	22.2	22.3	22.4	22.5	22.6	22.6
	HT	43.3	43.6	43.8	44.1	44.4	44.6	44.9	45.2	45.4	45.7	46.0
	AT	56.5	56.8	57.2	57.5	57.9	58.2	58.6	58.9	59.3	59.6	60.0
112 km/h (70 mph)	Passenger Car	13.4	13.4	13.4	13.4	13.4	13.5	13.5	13.5	13.5	13.6	13.6
	Van	16.5	16.5	16.6	16.6	16.7	16.7	16.8	16.8	16.9	16.9	17.0
	SUV	17.5	17.5	17.6	17.6	17.6	17.6	17.7	17.7	17.7	17.8	17.8
	LT	30.3	30.4	30.5	30.6	30.7	30.8	30.9	31.0	31.1	31.2	31.3
	HT	61.1	61.4	61.7	62.0	62.3	62.6	62.9	63.2	63.5	63.8	64.1
	AT	80.9	81.3	81.7	82.1	82.5	82.9	83.3	83.7	84.1	84.5	84.9

1 km = 0.62 mi; 1 mm = 0.039 in.; 1 m/km = 63.4 in./mi; IRI = 1 m/km, grade = 0%; temperature = 17°C (62.6°F).

divide 57.2 by 56.5 from Table 2 (i.e., the table describes the effect of changing texture, holding IRI constant at 1 m/km), then multiply this ratio by 57.9 from Table 1 (i.e., the table describes the effect of changing IRI, holding MPD constant at 1 mm). The cost obtained for these conditions is 58.6 ¢/km (94 ¢/mi).

Example 2: Project-Level Analysis

This example uses the mechanistic-based approach developed in this study to calculate the vehicle operating costs (fuel consumption, tire wear, and repair and maintenance) for a 7.2 km long rigid pavement section on I-69 near Lansing, Michigan.

The average daily traffic (ADT) for this section is 29,145 in both directions, with 60% passenger cars, 15% commercial trucks, 10% heavy trucks, 7% SUV, 4% vans, 2% light trucks, and 2% buses. The pavement condition data (raw profile and texture depth) were collected by Michigan Department of Transportation using a Rapid Travel Profilometer and a Pavement Friction Tester. The grade was measured using a high-precision GPS. Figure 11 shows the raw profile of the section. Figure 12 summarizes the distributions of its pavement conditions.

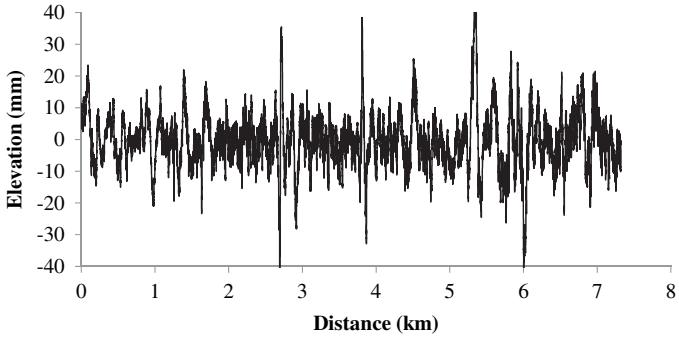

1 mm = 0.039 in.; 1 km = 0.62 mi

Figure 11. Raw profile of the analysis section.

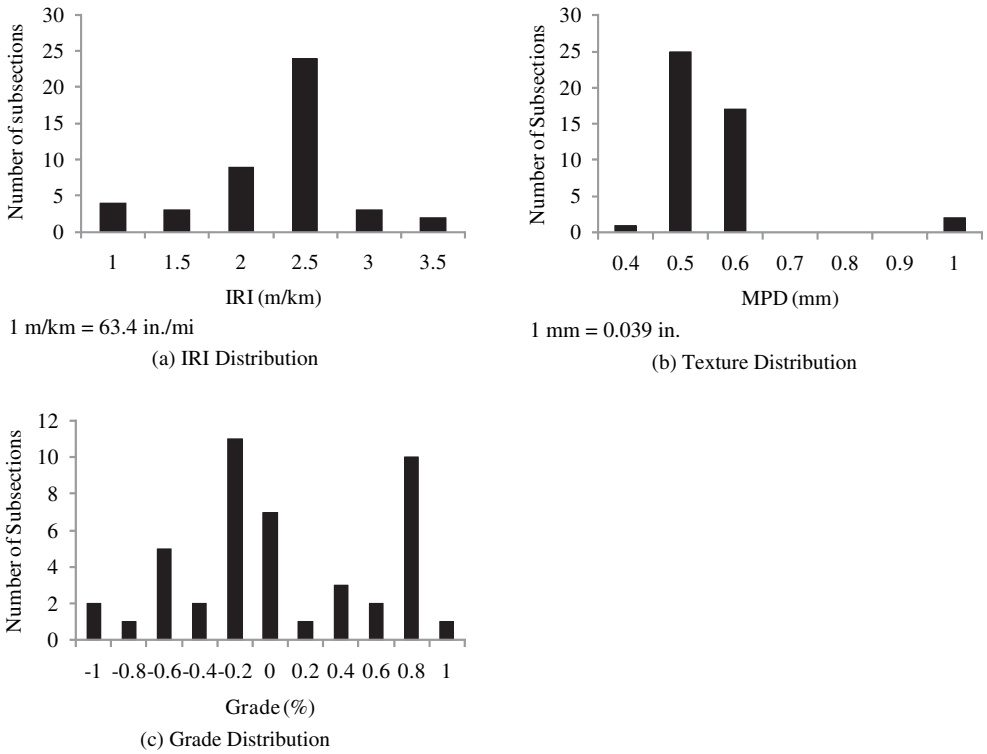

Figure 12. Pavement conditions of the analysis section.

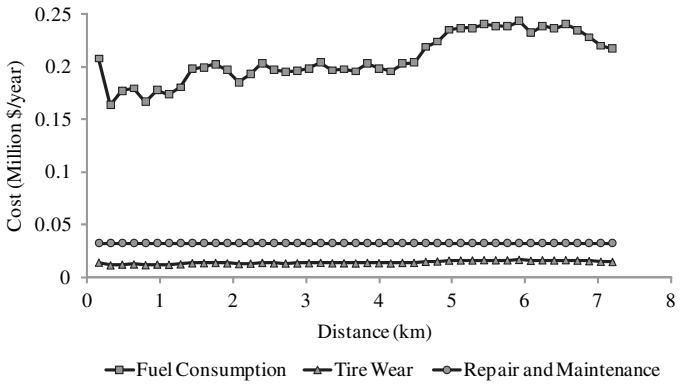

1 subsection = 0.16 km; 1 km = 0.62 mi

Figure 13. Costs per year induced by subsection.

The following procedure was followed to calculate vehicle operating cost:

- For repair and maintenance costs, the profile was input to the VOC model. The software calculated the accumulated damage in the suspension system, which was translated into repair and maintenance costs.
- For fuel consumption and tire wear, the raw profile was divided into 0.16 km long (0.1 mi) subsections, and the IRI values were computed for each subsection. The other pavement conditions (grade, texture depth, and curvature) were input to the calibrated HDM 4 models (described in Chapters 3 and 4 of *NCHRP Report 720*) to estimate fuel consumption and tire wear.
- The total costs were calculated according to the proportion of vehicle class mentioned above, and assuming average environmental conditions [temperature = 17°C (62.6°F)].

Figure 13 shows the costs for each subsection (0.16 km or 0.1 mi) for the traffic distribution generated at 96 km/h (60 mph) for trucks and buses and at 112 km/h (70 mph) for passenger cars, vans, and SUVs. Each point represents a subsection.

To estimate the reduction in vehicle operating cost from rehabilitating the I-69 project, a raw profile of a newly overlayed pavement with an average IRI of 1 m/km (63.4 in./mi) was simulated. The generated road profile is shown in Figure 14. It was assumed that the grade and texture distribution were not affected by the rehabilitation.

Figure 15 shows the reduction in vehicle operating cost for each subsection. The total reduction in vehicle operating cost from rehabilitating this project will be about $2.46 million per year.

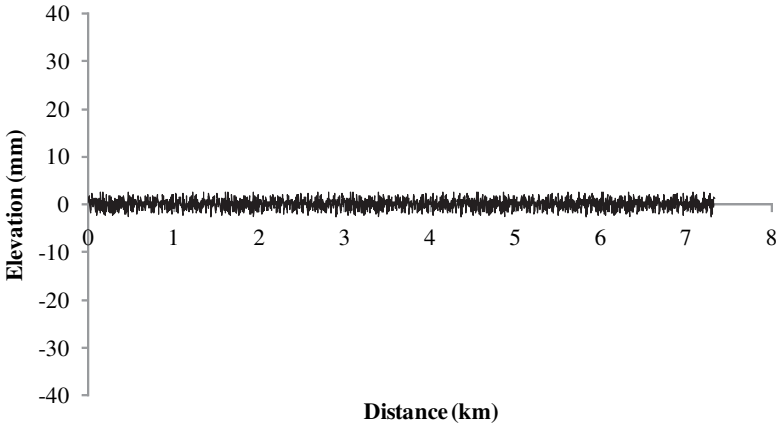

1 mm = 0.039 in.; 1 km = 0.62 mi

Figure 14. Simulated raw profile with an average IRI of 1 m/km (63.4 in./mi).

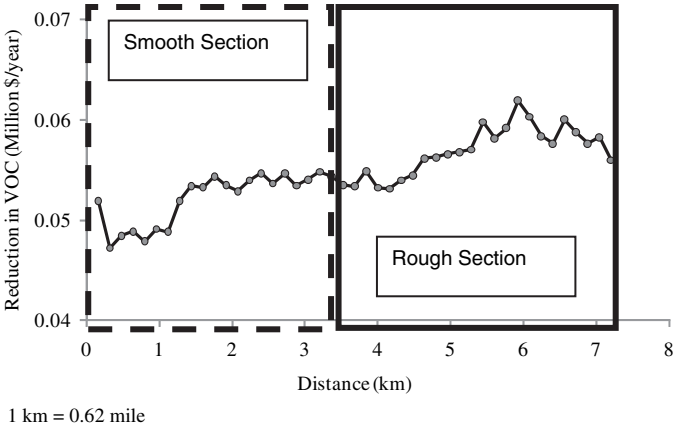

Figure 15. Reduction in vehicle operating cost from rehabilitating each section of the I-69 project.

These costs could be considered in a life cycle cost analysis. This detailed analysis would help identify the segments of the pavement section that would result in higher operating costs. These segments would be considered for early maintenance.

Example 3: Network-Level Analysis

In this example the developed models are used to compare the influence of maintaining the entire network versus maintaining a proportion of it (e.g., 50% or 90%) for simulated pavement networks of urban interstate highways in different states. A roughness range of 1 to 5 m/km was assumed. Figure 16 shows the assumed roughness distributions before and after rehabilitation. The distribution before rehabilitation was obtained by specifying a normal distribution with the desired IRI range. For the other two distributions, an IRI value of 1 m/km was assigned to rehabilitated sections. The remaining sections were then randomly assigned an IRI value from the original distribution. The vehicle kilometers traveled (VKT) for each state was estimated using Tables VM-3 and VM-1 from Highway Statistics (FHWA, 2008). Table 3 shows the speed limit for trucks and cars by state used in this example (Governors Highway Safety Association, 2011). Table 4 presents the estimated reduction in vehicle operating cost resulting from rehabilitating 50% versus 90% of the network for each state.

According to a study conducted by the Pennsylvania Transportation Institute (Kilareski et al., 1990), 95% of the road network in the United States is flat and straight (grade is 0% and superelevation is 0%). Therefore, at the network level, a grade of 0% and a superelevation of 0% are reasonable assumptions to calculate VOC savings.

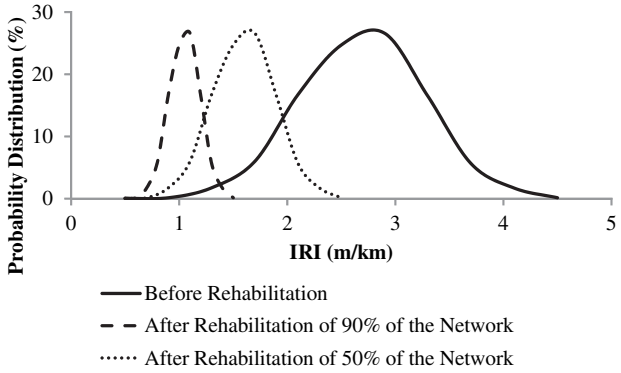

Figure 16. Assumed roughness distribution for network pavement.

Table 3. Speed limits used in Example 3.

STATE	URBAN INTERSTATES			
	Cars (km/h)	Trucks (km/h)	Cars (mph)	Trucks (mph)
Alabama	104	104	65	65
Alaska	88	88	55	55
Arizona	104	104	65	65
Arkansas	88	88	55	55
California	104	88	65	55
Colorado	104	104	65	65
Connecticut	88	88	55	55
Delaware	88	88	55	55
Dist. of Columbia	88	88	55	55
Florida	104	104	65	65
Georgia	104	104	65	65
Hawaii	80	80	50	50
Idaho	120	120	75	75
Illinois	88	88	55	55
Indiana	88	88	55	55
Iowa	88	88	55	55
Kansas	112	112	70	70
Kentucky	104	104	65	65
Louisiana	112	112	70	70
Maine	104	104	65	65
Maryland	104	104	65	65
Massachusetts	104	104	65	65
Michigan	112	96	70	60
Minnesota	104	104	65	65
Mississippi	112	112	70	70
Missouri	96	96	60	60
Montana	104	104	65	65
Nebraska	104	104	65	65
Nevada	104	104	65	65
New Hampshire	104	104	65	65
New Jersey	88	88	55	55
New Mexico	104	104	65	65
New York	88	88	55	55
North Carolina	112	112	70	70
North Dakota	120	120	75	75
Ohio	104	104	65	65
Oklahoma	112	112	70	70
Oregon	88	88	55	55
Pennsylvania	88	88	55	55
Rhode Island	88	88	55	55
South Carolina	112	112	70	70
South Dakota	120	120	75	75
Tennessee	112	112	70	70
Texas	112	112	70	70
Utah	104	104	65	65
Vermont	88	88	55	55
Virginia	112	112	70	70
Washington	96	96	60	60
West Virginia	88	88	55	55
Wisconsin	104	104	65	65
Wyoming	96	96	60	60
US Total	104	104	65	65

Table 4. Estimated vehicle operating costs for different scenarios.

STATE	Vehicle Operating Costs per Year ($ Billions)			Reduction in VOC per Year ($ Millions)	
	Original	50%	90%	50%	90%
Alabama	2.49	2.47	2.46	25.0	34.9
Alaska	0.23	0.22	0.22	2.3	3.2
Arizona	2.02	2.00	1.99	20.2	28.3
Arkansas	1.33	1.31	1.31	13.3	18.6
California	23.42	23.18	23.09	234.3	327.5
Colorado	2.50	2.47	2.46	25.0	34.9
Connecticut	3.27	3.24	3.23	32.7	45.8
Delaware	0.43	0.42	0.42	4.3	6.0
Dist. of Columbia	0.14	0.14	0.14	1.4	2.0
Florida	8.41	8.32	8.29	84.1	117.6
Georgia	6.52	6.46	6.43	65.3	91.2
Hawaii	0.64	0.63	0.63	6.4	8.9
Idaho	0.43	0.42	0.42	4.3	6.0
Illinois	7.66	7.58	7.55	76.6	107.1
Indiana	3.25	3.22	3.21	32.5	45.5
Iowa	0.87	0.86	0.85	8.7	12.1
Kansas	1.26	1.25	1.24	12.6	17.6
Kentucky	2.06	2.04	2.03	20.6	28.9
Louisiana	2.45	2.43	2.42	24.5	34.3
Maine	0.27	0.27	0.27	2.7	3.8
Maryland	4.51	4.47	4.45	45.2	63.1
Massachusetts	5.14	5.09	5.07	51.4	71.9
Michigan	5.24	5.19	5.16	52.4	73.2
Minnesota	2.90	2.87	2.86	29.0	40.6
Mississippi	1.19	1.18	1.17	11.9	16.6
Missouri	4.17	4.13	4.11	41.7	58.3

STATE	Vehicle Operating Costs per Year ($ Billions)			Reduction in VOC per Year ($ Millions)	
	Original	50%	90%	50%	90%
Montana	0.12	0.12	0.12	1.2	1.6
Nebraska	0.46	0.46	0.46	4.6	6.5
Nevada	1.19	1.17	1.17	11.9	16.6
New Hampshire	0.53	0.53	0.52	5.3	7.4
New Jersey	4.67	4.63	4.61	46.8	65.3
New Mexico	0.91	0.90	0.90	9.1	12.7
New York	7.00	6.93	6.90	70.1	97.9
North Carolina	4.77	4.72	4.70	47.7	66.7
North Dakota	0.13	0.13	0.13	1.3	1.8
Ohio	7.66	7.58	7.55	76.6	107.1
Oklahoma	1.59	1.57	1.56	15.9	22.2
Oregon	1.50	1.48	1.48	15.0	21.0
Pennsylvania	5.05	5.00	4.98	50.5	70.7
Rhode Island	0.59	0.59	0.58	5.9	8.3
South Carolina	2.06	2.04	2.03	20.6	28.8
South Dakota	0.21	0.21	0.21	2.1	2.9
Tennessee	3.90	3.86	3.84	39.0	54.5
Texas	13.48	13.34	13.29	134.9	188.5
Utah	2.00	1.98	1.97	20.0	27.9
Vermont	0.13	0.13	0.12	1.3	1.8
Virginia	5.13	5.08	5.06	51.4	71.8
Washington	3.65	3.61	3.59	36.5	51.0
West Virginia	1.06	1.05	1.04	10.6	14.8
Wisconsin	1.76	1.74	1.74	17.6	24.6
Wyoming	0.16	0.16	0.16	1.6	2.2
U.S. Total	162.47	160.85	160.20	1625.6	2272.1

Appendixes

Appendixes A through D are not published herein, but are available online at http://www.trb.org/Main/Blurbs/166904.aspx. These appendixes are titled as follows:

- Appendix A: Fuel Consumption Models,
- Appendix B: Tire Wear Models,
- Appendix C: Repair and Maintenance Models, and
- Appendix D: An Overview of Emerging Technologies.

Abbreviations and acronyms used without definitions in TRB publications:

AAAE	American Association of Airport Executives
AASHO	American Association of State Highway Officials
AASHTO	American Association of State Highway and Transportation Officials
ACI–NA	Airports Council International–North America
ACRP	Airport Cooperative Research Program
ADA	Americans with Disabilities Act
APTA	American Public Transportation Association
ASCE	American Society of Civil Engineers
ASME	American Society of Mechanical Engineers
ASTM	American Society for Testing and Materials
ATA	American Trucking Associations
CTAA	Community Transportation Association of America
CTBSSP	Commercial Truck and Bus Safety Synthesis Program
DHS	Department of Homeland Security
DOE	Department of Energy
EPA	Environmental Protection Agency
FAA	Federal Aviation Administration
FHWA	Federal Highway Administration
FMCSA	Federal Motor Carrier Safety Administration
FRA	Federal Railroad Administration
FTA	Federal Transit Administration
HMCRP	Hazardous Materials Cooperative Research Program
IEEE	Institute of Electrical and Electronics Engineers
ISTEA	Intermodal Surface Transportation Efficiency Act of 1991
ITE	Institute of Transportation Engineers
NASA	National Aeronautics and Space Administration
NASAO	National Association of State Aviation Officials
NCFRP	National Cooperative Freight Research Program
NCHRP	National Cooperative Highway Research Program
NHTSA	National Highway Traffic Safety Administration
NTSB	National Transportation Safety Board
PHMSA	Pipeline and Hazardous Materials Safety Administration
RITA	Research and Innovative Technology Administration
SAE	Society of Automotive Engineers
SAFETEA-LU	Safe, Accountable, Flexible, Efficient Transportation Equity Act: A Legacy for Users (2005)
TCRP	Transit Cooperative Research Program
TEA-21	Transportation Equity Act for the 21st Century (1998)
TRB	Transportation Research Board
TSA	Transportation Security Administration
U.S.DOT	United States Department of Transportation